ANTAGONIZING THE ANDROGEN RECEPTOR WITH A BIOMIMETIC ACYLTRANSFERASE

by

Yuchen Zhang

A dissertation submitted to the Faculty of the University of Delaware in partial fulfillment of the requirements for the degree of Doctor of Philosophy in Chemistry and Biochemistry

Fall 2016

ANTAGONIZING THE ANDROGEN RECEPTOR WITH A BIOMIMETIC ACYLTRANSFERASE

by

Yuchen Zhang

Approved: _____
Murray V. Johnston, Ph.D.
Chair of the Department of Chemistry and Biochemistry

Approved: _____
George H. Watson, Ph.D.
Dean of the College of Arts and Sciences

Approved: _____
Ann L. Ardis, Ph.D.
Senior Vice Provost for Graduate and Professional Education

I certify that I have read this dissertation and that in my opinion it meets the academic and professional standard required by the University as a dissertation for the degree of Doctor of Philosophy.

Signed: _____

John T. Koh, Ph.D.
Professor in charge of dissertation

I certify that I have read this dissertation and that in my opinion it meets the academic and professional standard required by the University as a dissertation for the degree of Doctor of Philosophy.

Signed: _____

Catherine Grimes, Ph.D.
Member of dissertation committee

I certify that I have read this dissertation and that in my opinion it meets the academic and professional standard required by the University as a dissertation for the degree of Doctor of Philosophy.

Signed: _____

Colin Thorpe, Ph.D.
Member of dissertation committee

I certify that I have read this dissertation and that in my opinion it meets the academic and professional standard required by the University as a dissertation for the degree of Doctor of Philosophy.

Signed: _____

Erin Bernberg, Ph.D.
Member of dissertation committee

ACKNOWLEDGMENTS

I would like to thank my research advisor Prof. John Koh, for his insightful and inspiring guidance and supervision over my graduate study and career. I am grateful for so many nurturing scientific discussion and encouragement during my science-pursuing trek. I would also like to thank him for caring and helpful suggestion for my life here in United States as a foreign student. I would like to thank my doctoral committee members Dr. Catherine Grimes, Dr. Colin Thorpe, Dr. Robert Sikes and Dr. Erin Bernberg for sharing their valuable suggestions and providing support over the years.

I would like to thank current and former members of the Koh group for their support, help and company. It would be so much harder for me to make it through without them. My special thanks to Dr. Pavan Mantravadi for his earnest help training me to get started in an entirely new laboratory environment.

I would like to thank all my friends, including but not limited to, Dr. Jun Liu, Dr. Kun Yang, Dr. Yuan Hu, Ping Gong, Fang Tan for their support and encouragement through the ups and downs of graduate school years as well as making the graduate school life enjoyable.

Most of all I would like to thank my parents, Changyin Zhang and Wen Chen and my wife, Kehui Zhang for their unconditional and utmost support throughout the years.

TABLE OF CONTENTS

LIST OF FIGURES

ABSTRACT

The androgen receptor (AR) remains the leading target of advanced prostate cancer therapies. Thiosalicylamide analogs have previously been shown to act in cells as acyltransfer catalysts that are capable of transferring cellular acetate, presumably from Acetyl-CoA, to HIV NCP. Here we explore if the cellular acetyl-transfer activity of thiosalicylamides can be redirected to other cellular targets guided by ligands for AR. We constructed conjugates of thiosalicylamides and the AR-binding small molecule tolfenamic acid, which binds the BF3 site of AR, proximal to the coactivator "FXXLF" binding surface. The thiosalicylamide-tolfenamic acid conjugate, YZ03, but not the separate thiosalicylamide and tolfenamic acid, significantly enhanced acetylation of endogenous AR in CWR22 cells. Further analysis confirms that Lys720, a residue critical to FXXLF coactivator peptide binding, is a primary site of YZ03 acetylation. Acyl-transfer conditions significantly enhance YZ03's ability to inhibit AR-coactivator association. These data suggest that biomimetic acyltransferases can enhance protein-protein interaction inhibitors through covalent modification of critical interfacial residues.

INTRODUCTION

1.1 Acetylation is an Important Post-Translational Modification

Lysine acetylation is a reversible post-translational modification (PTM) first discovered half a century ago on histones[1] in which ε-amino group of lysine residue is acetylated by the transfer of acetate from acetyl-CoA. Upon acetylation, the positive charge on lysine is neutralized, which can alter the protein function in various ways.

Due to the small size of the acetate group, protein acetylation as PTM was not easy to study with canonical biochemical methods such as gel electrophoresis. However, with the advancement of modern analytical technologies especially in high-resolution mass spectrometry based proteomics, thousands of acetylation sites have been identified, and the number of protein acetylations is considered to rival that of protein phosphorylation.[2]

Protein acetylation was initially thought to occur only in the nucleus, and only 20 years after the discovery of histone acetylation was tubulin identified as the first cytoplasmic acetylated protein.[3] Recent proteomics studies show that there are more proteins acetylated in cytoplasm, especially in the mitochondria.[4] This suggests that acetylations play important regulatory roles in the cytoplasm.

Biochemical lysine acetylation is catalyzed by a class of enzymes, lysine acetyltransferases (KAT), formerly know as histone acetyltransferases (HATs). Even though the KAT family is categorized into different subclasses based on their alignment and substrate specificity, they all share similarities consisting of a central

core domain for binding the acetyl-CoA and a cleft flanking the core domain for substrate binding. Often found at the core domain is a glutamate residue serving as a general base to extract the proton on the positively charged lysine residue to facilitate the acyl transfer. In addition, proximity of the two binding substrates significantly lowers the entropy of the acyl transfer reaction.[5]

Acetyl-CoA is the only known co-substrate for protein acetylation. It is 100-fold more reactive than oxoesters toward amines,[6] and the thiolate is also nucleophilic, making the acetyl-CoA an excellent intermediate for catalyzing protein acetylation. Due to its unique property, thioester has been an interesting subject to study and utilize in biochemistry, such as native chemical ligation.

1.2 Proximity Directed Reaction in Chemical Biology

1.2.1 Enzyme or Peptide Directed Protein Labelling

Protein (surface) modification has long been an interest since it provides valuable information for elucidating protein function and localization. However, due to the complex environment in cells, it is always difficult to achieve specificity. There are currently several strategies for specific protein surface modification: 1. biorthogonal reactions of co-translationally incorporated unnatural amino acid. 2. creation of protein chimeras with enzymes for labeling by an enzyme-probe pairs. 3. proximity-directed reactions with ligands bind specifically to a protein of interest (POI). Here we will focus on strategies 2 and 3, as they can be implanted with endogenous or expressed proteins.

The obvious limitation of biorthogonal labeling is often the requirement of special preparation of the POI, such as genetic incorporation of unnatural amino acids.

To overcome this, a number of enzyme based protein labeling methods have been developed taking advantage of specific enzyme-substrate recognition. Tsien *et al*. pioneered work on demonstrating that a peptide containing a tetracystein motif (CCXXCC) is able to bind to a fluorophore with two arsenic groups with picomolar binding affinity.[7] Another work was pioneered by Johnsson *et al*. where they employed a mutant human O^6-alkyguanine-DNA alkytransferase (hAGT) as an enzymatic fusion tag, which binds and reacts with O^6-alkyguanine derivatives to covalently label chimeric POIs. This is known as SNAP-tag and is been widely used to specifically label POIs.[8,9]

Another method developed by Promega used mutant haloalkane dehalogenase to covalently bind to a synthetic halo-tagged ligand conjugate.[10] Alternatively, another approach is to conjugate a peptide to the POI. Ting *et al*. developed the Probe Incorporation Mediated by Enzyme (PRIME) protein labelling system catalyzed by lipoic acid ligase (LplA). The mutant LplA recognizes a 13 amino acid LplA acceptor peptide and catalyzes the amide bond formation to the peptide with a functional group that can be further modified such as an azide. The Ting tag proved to be very efficient and highly specific within the cells.[11] The aforementioned method all requires co-expression of a large enzyme, to recognize and catalyze the covalent coupling, which is not ideal since they may have unwanted effect when heterogeneously expressed.

Related to enzyme based protein labeling is Activity-Based Protein profiling, which has proven to be a very powerful method for profiling enzyme activities. In general, an activity-based probe (ABP) consists of three components: 1) a reactive group that can both bind and covalently modify the active site of the enzyme, 2) a linker, and 3) a reporter tag, such as fluorescent group or biotin for detection or

isolation. Cravatt was an early pioneer of the field and demonstrated that with the help of the advanced mass spectrometry methods, discovery of hundreds of enzymes with similar active sites is achievable.[12]

1.2.2 Proximity-Directed Selective Labelling of Proteins

The aforementioned methods, except the activity-based protein profiling, all suffer the disadvantage of requiring the POI to be expressed as a chimera which could potentially change the protein function, making monitoring the native state of the protein difficult.

Cornish *et al*., Hamachi *et al*. and I independently explored the possibility of labeling POIs using ligands other than substrates to achieve specificity. Here, Cornish et al. developed the (Trimethylprim) TMP- conjugated fluorescent dye, the TMP will bind specifically to the dihydrofolate reductase (DHFR), with a mutation of K28C. The engineered mutant cysteine is proximal to the "warhead", an acrylamide on the dye that reacts with the cysteine by Michael addition. Although this method did not exploit the strong interactions between the enzyme active site and the corresponding substrate, it still requires mutation on the DHFR to achieve the desired reactivity.[13]

Hamachi *et al*. developed several approaches that use native ligands to direct native protein labelling. Recently, they developed the ligand-directed tosyl (LDT) chemistry, in which a phenylsulfonate is the reactive group directed by ligands for the POI. It brings the tosyl reactive group in proximity, and a simple S_N2 reaction occurs between a nucleophilic amino acid residue on the surface of the POI, and leaves the directing ligand free to disassociate from the POI.[14] Other reactive groups include acyl imidazole and acyl phenol.[15,16]

Pavan Mantravadi and I, from the Koh group, instead of choosing a strong binding ligand, developed a tolfenamic acid based ligand to target lysine on the surface of the androgen receptor. We used an artificial acetyltransfer domain to transfer acetate from the cellular milieu to lysine residues.[17]

1.2.3 Ligand-Tethered Catalyst for Protein Labelling

Whereas all these methods prove to be useful for protein surface modification, one cannot omit the fact that in order to achieve quantitative modification, a stoichiometric excess of reactive reagents are always needed.

4-Dimethylaminopyridine (DMAP) was widely used as organocatalyst for acyltransfer reactions, and based on this concept, Hamachi et al. designed and synthesized a series of affinity-guided DMAP catalysts consisting of a DMAP group conjugated to an affinity ligand. In the presence of excess added labeling reagent, these ligand-tethered catalysts can selectively label cell surface proteins.[18] They have also showed the feasibility of using the ligand-DMAP conjugates to target intracellular proteins but with partial selectivity.[19]

Appella *et al*. discovered the molecule MT-1 from screening for small molecule inhibitors the HIV virus. It was proposed that MT-1 acts as a nucleophilic acyl- transfer catalyst, which is acetylated by acetyl-CoA *in vivo* and can subsequently transfer the thiophenolester to the NCp7 domain of the HIV Gag protein.[20,21] This is the first evidence of an acetyltransfer catalyst functioning within cells using a cellular metabolite for protein modification. This work will describe applications of acyltransfer catalyst to selective acylate nuclear receptors. The following sections will outline the basic properties of nuclear receptor and specifically the androgen receptor.

1.3 Nuclear Hormone Receptor and the Androgen Receptor

Nuclear receptors (NRs) are intracellular transcription factors activated by ligands such as steroid hormones, thyroid/retinoic hormones or the fatty acids, to modulate gene expression.[22] The nuclear receptor superfamily is categorized into three classes: the steroid receptor family (SHR) (class I), the thyroid/retinoid family (class II), and the orphan receptor family, based on the types of ligands that activate the receptors.

The SHR family includes androgen receptor (AR), estrogen receptor (ER), progesterone receptor (PR), glucocorticoid receptor (GR) and mineralocorticoid receptor (MR).[23] The ligands that activate the SHR family are all derived from cholesterol, containing cyclopentanophenanthrene, and they share structural and mechanistic similarities. Almost all the SHR family members can be found in the cytoplasm and are bound to molecular chaperones such as heat shock proteins (HSPs) in the absence of activating ligands. Upon binding ligand, the receptors release the HSPs, translocate into the nucleus, and bind to specific DNA sequence as a homodimer to recruit coactivator proteins and trigger transcription of the down-stream genes.[22]

Unlike the SHR family members, the class II receptors typically function as heterodimers with retinoic X receptor (RXR). They tend to stay bound to DNA response elements regardless of the presence of agonists. In the absence of the ligand, transactivation is suppressed by bound corepressors. Upon agonist binding, corepressors are released and coactivators are recruited, triggering down-stream gene activation.

The orphan receptors can either dimerize with RXR or bind to response elements as monomers. The related ligands are unknown for the orphan receptors,

however, there is evidence suggesting that orphan receptors are involved in a number of lipid metabolic processes. Some other receptors fall into this category may simply not have a ligand.[24]

1.3.1 Structure of Nuclear Receptors

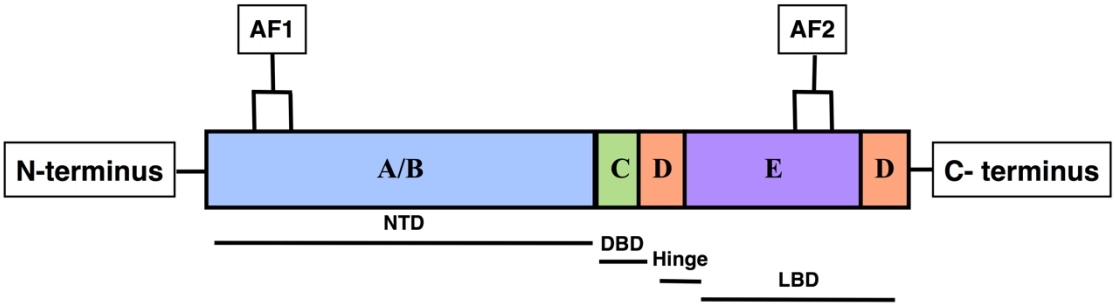

Figure 1.1. Domain structure of nuclear receptors. (NTD: N-terminal Domain)

All nuclear receptors share some structural similarities including the relatively conserved C-terminal ligand-binding domain (LBD) and a more conserved N-terminal DNA-binding domain (DBD) (See Figure 1.1).

The DBD is responsible for docking the receptor to the hexanucleotide response elements within the promoter region of genes regulated by nuclear receptors.[22] The LBD and the DBD are connected with a short hinge region whose function is not clear but evidence shows that phosphorylation of the hinge region increases transcriptional activation.[25] It binds to the importin protein for nuclear translocalizaition.[26]

The poorly defined N-terminal A/B domain, contains a transcriptional activation function 1 (AF-1) that can act in a ligand-independent manner. In addition,

A/B domain binds to heat-shock protein which serves as chaperone to stabilize the complex in the absence of the ligand.[27]

The LBD contains an interior binding pocket for cognate hormone or ligand and a transcriptional activation function domain (AF2) for recruiting coactivator proteins. The crystal structures of ligand-bound and unliganded NRs reveals a common mechanism of which AF-2 functions. Within the LBD, there are 12 α-helices (numbered from 1-12), and upon ligand binding, a "mousetrap" mechanism invokes the repositioning of helices 3, 6,11, 10 and 12[28,29] creating a hydrophobic binding site for coactivators with a peptide motif of LXXLL or FXXLF known as an NR box (Figure 1.2).

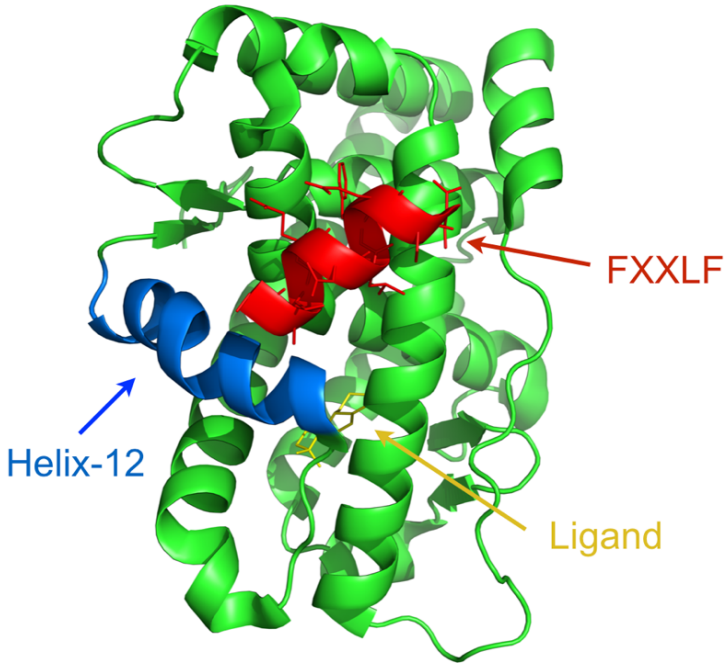

Figure 1.2. Liganded AR(LBD) with coactivator peptide.

Noting that within the coactivator binding groove, there are two charged amino acid residues Lys720 and Glu897, termed “charge clamp” that make direct interactions with the FXXLF motif. (Figure 1.3) Mutation studies have shown the importance of the two amino acid residues, especially Lys720. The Lys720->Ala mutation alone is able to severely reduce binding of most FXXLF peptides.[30]

From the co-crystallographic study of coactivator peptides and the AR(LBD), hydrogen bonding interactions were observed between the charge clamp lysine residue and the backbone carbonyl of the coactivator peptide. No other hydrogen bonding interactions from other residues within the charge clamp cluster were observed.[31]

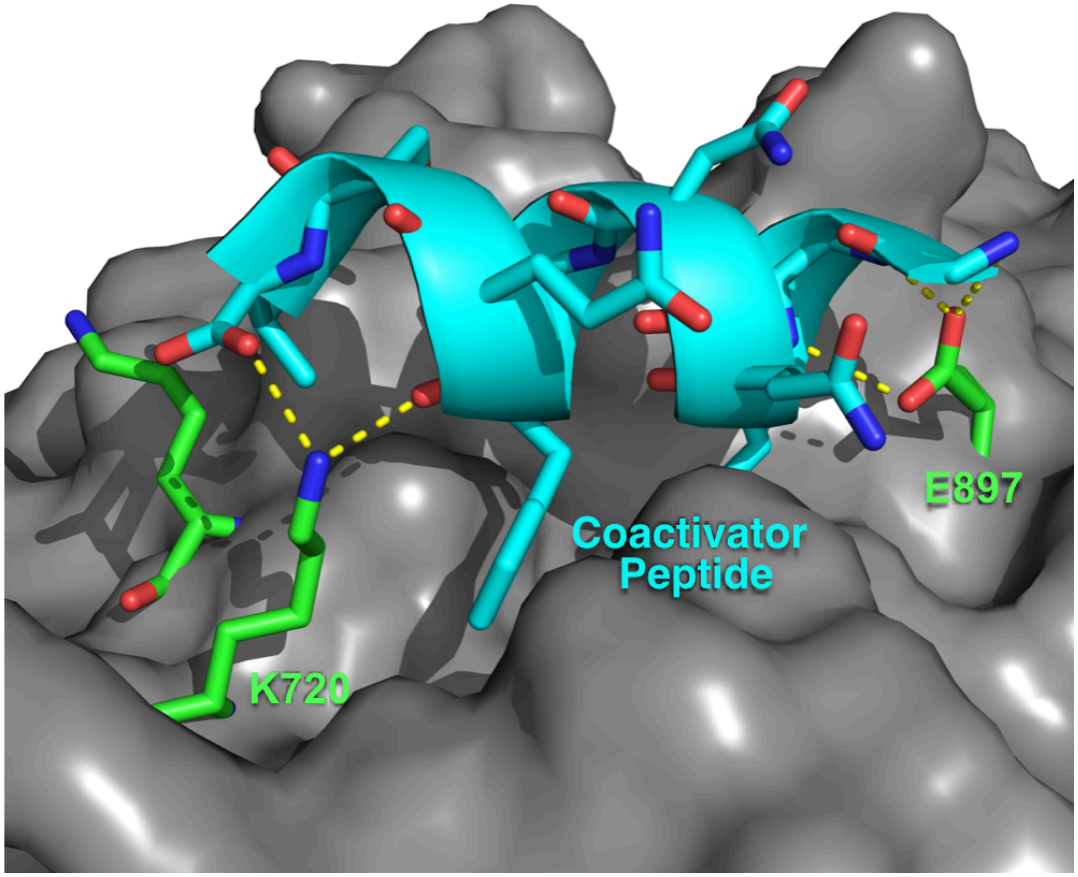

Figure 1.3. Charge clamp interaction with the coactivator peptide.

1.3.2 Androgen Receptor Antagonist

Prostate cancer is the second leading cause of male cancer deaths in Western countries.[32] The androgen receptor is the principal target of antiandrogens used for the treatment of advanced prostate cancer.[33] Antiandrogens are grouped into two classes, the first class are small molecules that compete with the natural AR ligand, such as testosterone and dihydrotestosterone (DHT), to bind the LBD of AR and inhibit AR signaling and the second class are DHT biosynthesis inhibitors. The current antiandrogens are divided into two groups based on their structures, steroidal and non-steroidal. (Figure 1.4)

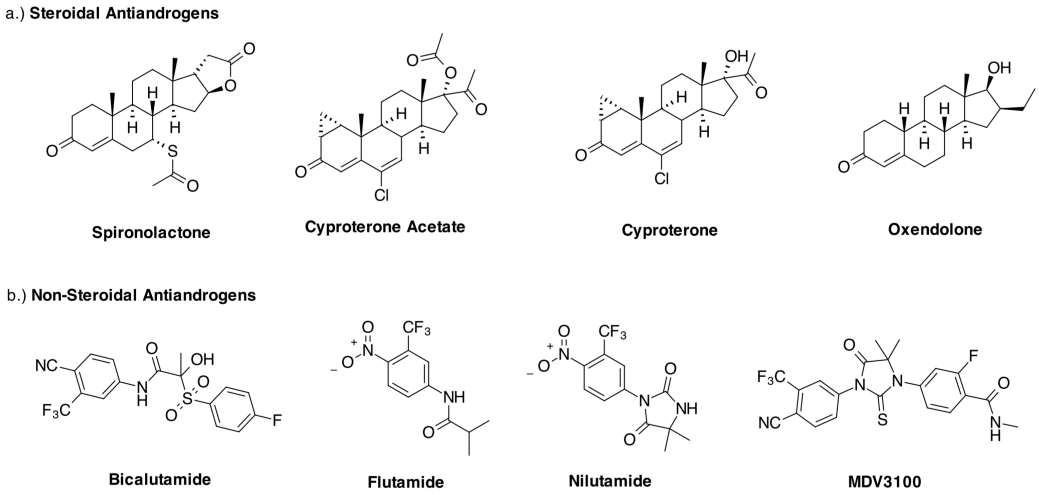

Figure 1.4. Steroidal and Nonsteroidal Antiandrogens.

The steroidal antagonists often show off-target effects towards other nuclear receptors and poor oral bioavailability. There is only one steroidal antiandrogen currently approved as a commercial antiandrogen, cyproterone acetate.[34]

Among all the nonsteroidal antiandrogens, bicalutamide is the most studied one.[35] Compared to flutamide and nilutamide, bicalutamide has lower toxicity and longer half life of 6 days. All of these nonsteroidal antiandrogens are very effective initially, however 20-30% of patients develop drug resistance over a prolonged course of treatment.[36] Recently, MDV3100 (Enzalutamide), was developed as a second generation antiandrogen and was approved for treatment of advanced prostate cancer.[35] MDV3100 binds to AR five to eight times tighter than bicalutamide and is effective against not only AR (wt) but also AR (T877A) and AR (W741C), which are mutants to which bicalutamide acts as an agonist instead of antagonist.[37,38] Although MDV3100 shows effectiveness against many known drug resistant prostate cancers, there have been reports of resistance to MDV3100 including a mutant AR(F876L) to which MDV3100 serves as an agonist.[39]

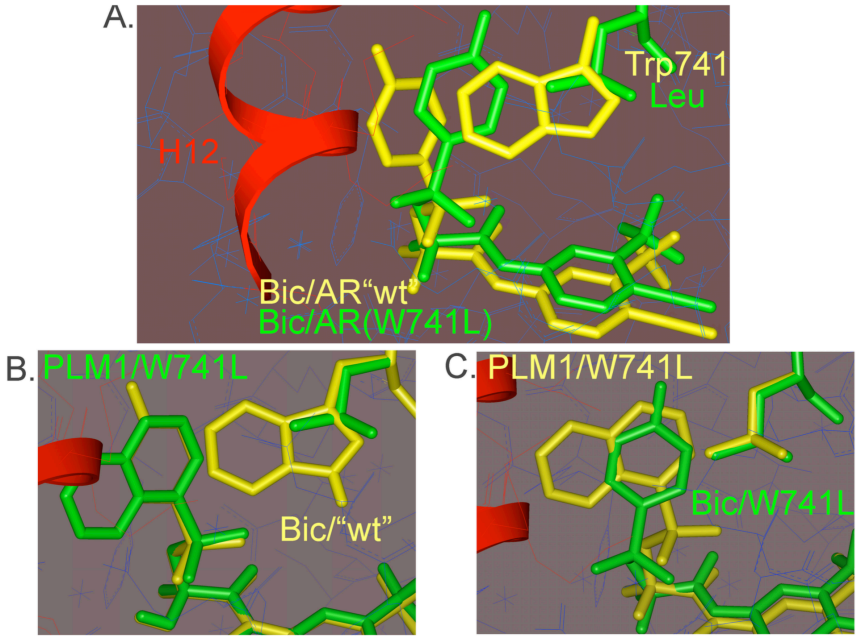

Figure 1.5. Position of Bicalutamide and AR. A. Position of bicalutamide in AR (wt) and AR (W741L). B. PLM1 with AR (W741L) and bicalutamide with AR (wt). C. PLM1 and bicalutamide with AR (W741L). *McGinley, P. L. et al. J. Am. Chem. Soc. 129, 3822–3823.*

Mutations associated drug resistance are believed to be the cause of antiandrogen withdrawal syndrome, wherein the antiandrogens act as agonists instead of antagonists. The crystal structure of bicalutamide resistant mutant AR(W741L) with bicalutamide was solved.[40] When Trp741 is mutated to a Leu, bicalutamide is able to fit in the larger space, failing to block Helix 12 from forming coactivator binding pocket (Figure 1.5).

One strategy to overcome antiandrogen withdrawal is to develop new antiandrogens that have bulky groups to compensate for the space created by mutations such that helix-12 would not be in a position to accommodate the coactivator. Paula McGinley a former graduate student from the Koh group developed several derivatives of bicalutamide with expanded groups off the aryl sulfone core. Among these compounds, PLM1,2 and 6 showed antagonistic activity against mutant AR(T877A), AR(W741L) and AR(W741C), to which bicalutamide showed agonistic activity.[41]

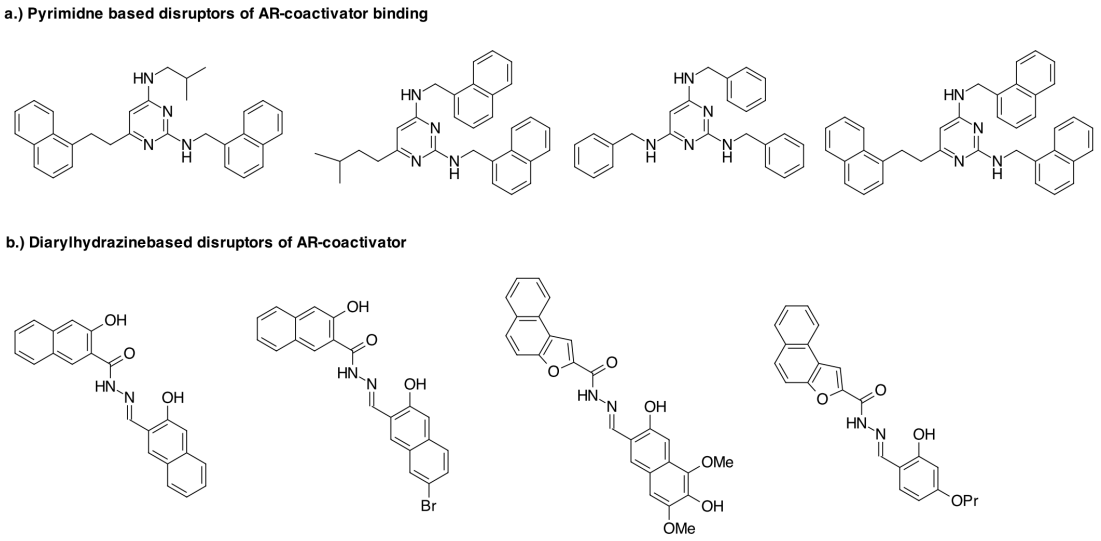

Figure 1.6. Compounds that disrupts AR-coactivator binding.

There have also been considerable efforts put into developing other nonconventional antiandrogens targeting sites on AR other than the ligand-binding pocket, including the coactivator binding site and allosteric binding site termed binding function 3 (BF-3).

Pyrimidine based tripeptide mimics of the FXXLF/LXXLX peptide motif were initially developed as ERα coactivator binding inhibitors, and later modified to inhibit AR specifically (Figure 1.6a).[42] Another set of compounds with a diarylhydrazine core were identified from screens designed to find disrupters of binding between AR and AR coactivators (Figure 1.6b).

Recently, binding function-3 (BF-3), a surface site on the AR(LBD), was discovered from a high throughput screen against a known compound library.[43] Small molecules, such as tolfenamic acid (TOF) and flufenamic acid (FLF) bind to this site and are believed to allosterically inhibit coactivator binding. The BF-3 is located near but distinct froms both the coactivator-binding pocket and the ligand-binding pocket that are normally targeted by general antiandrogens.(Figure 1.7) The major driving force for binding is believed to be hydrophobic effect where FLF aromatic rings interact with BF-3 to bury large solvent-exposed surface.[43]

1.3.3 Acetylation of Androgen Receptor

Androgen receptor was first discovered to be acetylated *in vitro* and *in vivo* by Pestell *et al*.[44] As mentioned above, AR recruits many cofactors for proper function, including KATs and HDACs.[45] Pestell et al. found that in vitro, an AR sequence within the hinge region was acetylated by p300/cAMP and successfully identified the ^{630}KLKK^{633} as the only naturally acetylated site on AR. Later it was discovered that AR's activity is governed by its acetylation state and acetylation promotes the binding of coactivators.[46] [47]

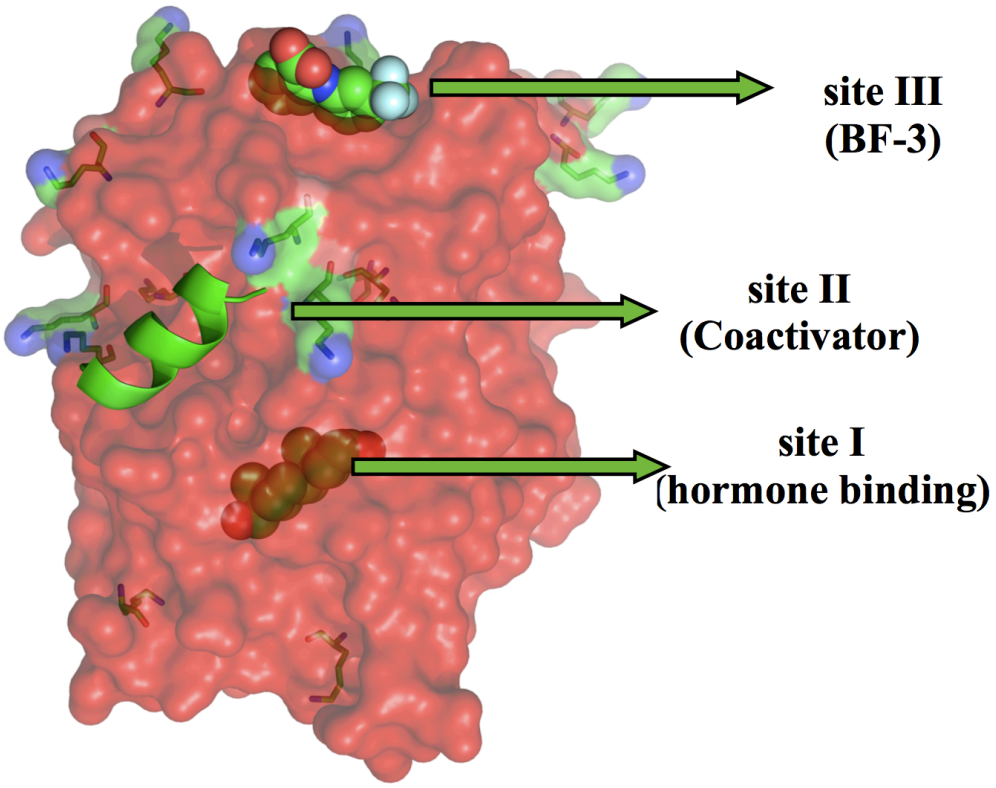

Figure 1.7. Ligand binding sites that could be used for proximity directed AR acylation. (PDB: 2PIX)

There are many lysine residues on the surface of AR which play important roles, such as the ones in the hinge region that affect nuclear import and the one in the coactivator binding pocket for FXXLF/LXXLF motif binding, so it was envisioned that by modifying these lysine residues we would be able to tune AR's function. Pavan Mantravadi, a former graduate student in the Koh group explored the possibility of using proximity directed acylation to specifically modify lysine residues on the surface of AR. There are three different ligand binding sites in the AR LBD that could be used to direct acylation: the hormone binding site, the coactivator binding site and the BF-3 binding site.

The BF-3 site seems ideal, since the site is on the surface instead of being sequestered inside of the protein, as is the hormone binding site. In addition, the BF-3 site is close to the lysine of the coactivator binding site and there are several known small molecule that bind at BF-3, making the design of the acyltransferring agent straightforward.

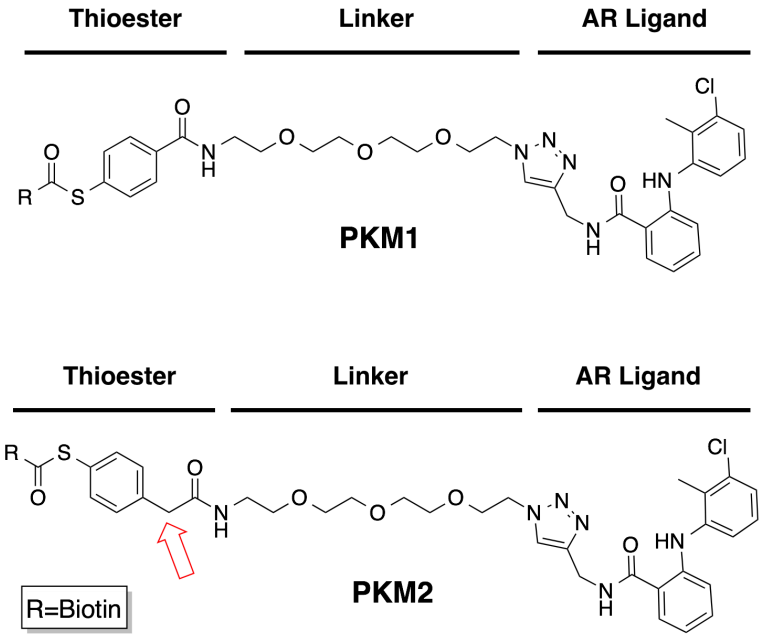

Figure 1.8. AR targeting acyltransferring agents PKM1 and PKM2.

Based on these hypotheses, two thioesters PKM1 and PKM2 were designed and synthesized (Figure 1.8). The thioester part consists of the highly reactive thiophenolester with a biotin tag for easy detection, the linker part is necessary so the bulky tag does not interfere with the binding of the AR ligand and the ligand is specific for binding to the AR BF-3 site. Noting that PKM2 has an extra methylene

group breaking the conjugation of the carbonyl with the thiophenol such that PKM2 is a less reactive thioester than PKM1.

In studies by Pavan Mantravadi, biotin transfer was initially conducted at 37°C using AR over expressing CWR22Rv1 cells lysates. Surprisingly, biotinylation was observed for PKM2 treatment but not PKM1 treatment (Figure 1.9). Significantly no biotinylation was observed from the treatment of the lysate with separate thioester and ligand. This demonstrates that the acylation is truly proximity directed. With 100 nM DHT to stabilize the AR added, a higher signal of biotinylation was observed.

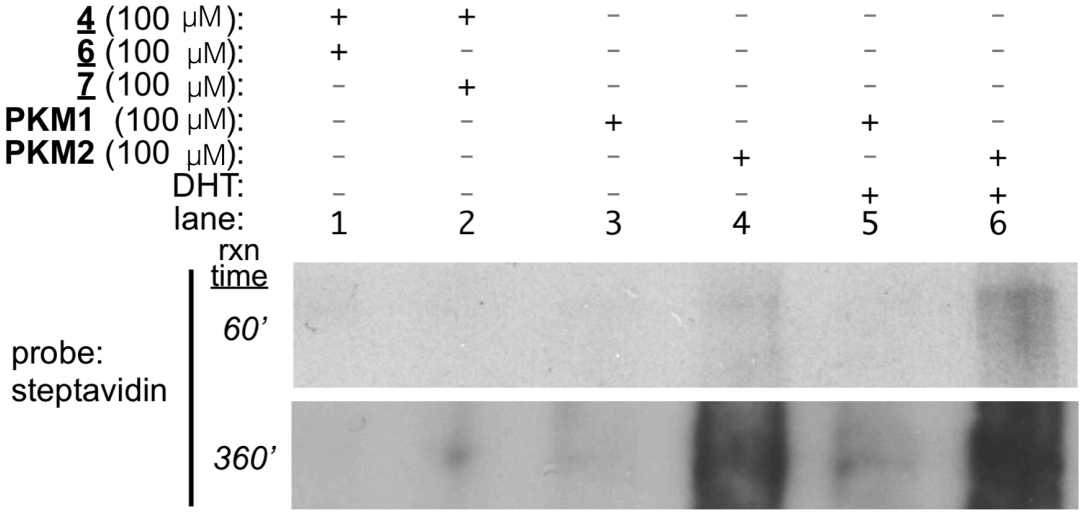

Figure 1.9. Biotin transfer by PKM1 and PKM2 to AR in CWR22Rv1 lysate. Mantravadi, P. K. (2014). New tools for controlling nuclear receptor function.

The observation that the more reactive PKM1 gave less signal seemed counterintuitive, however given the fact that the lysate contains numerous competing nucleophiles, it is reasonable to argue that the more reactive PKM1 was largely consumed before it reached AR. To confirm this supposition, Dr. Mantravadi examined the biotinylation of the supernatant after immunoprecipitation of the lysates treated with PKM1 and PKM2 and found that there was more non-specific

biotinylation by PKM1 than PKM2. This suggests that the less reactive PKM2 is more selective than the PKM1.

Another identical biotinylation experiment was conducted at 30°C. In 1h of treatment of PKM1 and PKM2, a significant amount of biotinylation was observed for PKM1 treatment (Figure 1.12). No detectable biotinylation by the less reactive PKM2 was observed. This confirms that PKM1 is indeed more reactive than PKM2, but in a complex milieu of competing nucleophiles, the reactivity must be tuned down to achieve higher selectivity and proximity directed acylation can be achieved with proper small molecule design.

REFERENCES

(1) Allfrey, V. G., Faulkner, R., and Mirsky, A. E. (1964) Acetylation and Methylation of Histones and Their Possible Role in the Regulation of RNA synthesis. *Proc Natl Acad Sci U S A 51*, 786–794.
(2) Choudhary, C., Kumar, C., Gnad, F., Nielsen, M. L., Rehman, M., Walther, T. C., Olsen, J. V., and Mann, M. (2009) Lysine Acetylation Targets Protein Complexes and Co-Regulates Major Cellular Functions. *Science 325*, 834–840.
(3) L'Hernault, S. W., and Rosenbaum, J. L. (1985) Chlamydomonas. alpha.-tubulin is posttranslationally modified by acetylation on the. epsilon.-amino group of a lysine. *Annu Rev Biochem 24*, 473–478.
(4) Smith, K. T., and Workman, J. L. (2009) Introducing the acetylome. *Nat. Biotechnol. 27*, 917–919.
(5) Marmorstein, R. (2001) Structure of histone acetyltransferases. *J. Mol. Biol. 311*, 433–444.
(6) Yang, W., and Drueckhammer, D. G. (2001) Understanding the Relative Acyl-Transfer Reactivity of Oxoesters and Thioesters: Computational Analysis of Transition State Delocalization Effects. *J. Am. Chem. Soc. 123*, 11004–11009.
(7) Griffin, B. A., Adams, S. R., and Tsien, R. Y. (1998) Specific covalent labeling of recombinant protein molecules inside live cells. *Science 281*, 269–272.
(8) Juillerat, A., Gronemeyer, T., Keppler, A., Gendreizig, S., Pick, H., Vogel, H., and Johnsson, K. (2003) Directed Evolution of O6-Alkylguanine-DNA Alkyltransferase for Efficient Labeling of Fusion Proteins with Small Molecules In Vivo. *Chem Biol 10*, 313–317.
(9) Xue, L., Karpenko, I. A., Hiblot, J., and Johnsson, K. (2015) Imaging and manipulating proteins in live cells through covalent labeling. *Nature Chemical Biology* 1–7.
(10) Los, G. V., Encell, L. P., McDougall, M. G., Hartzell, D. D., Karassina, N., Zimprich, C., Wood, M. G., Learish, R., Ohana, R. F., Urh, M., Simpson, D., Mendez, J., Zimmerman, K., Otto, P., Vidugiris, G., Zhu, J., Darzins, A., Klaubert, D. H., Bulleit, R. F., and Wood, K. V. (2008) HaloTag: A Novel Protein Labeling Technology for Cell Imaging and Protein Analysis. *ACS Chem. Biol. 3*, 373–382.
(11) Uttamapinant, C., White, K. A., Baruah, H., Thompson, S., Fernandez-Suarez, M., Puthenveetil, S., and Ting, A. Y. (2010) A fluorophore ligase for site-specific protein labeling inside living cells. *Proc Natl Acad Sci U S A 107*, 10914–10919.
(12) Evans, M. J., and Cravatt, B. F. (2006) Mechanism-Based Profiling of Enzyme Families. *Chem. Rev. 106*, 3279–3301.
(13) Chen, Z., Jing, C., Gallagher, S. S., Sheetz, M. P., and Cornish, V. W. (2012)

Second-Generation Covalent TMP-Tag for Live Cell Imaging. *J. Am. Chem. Soc. 134*, 13692–13699.
(14) Tsukiji, S., Miyagawa, M., Takaoka, Y., Tamura, T., and Hamachi, I. (2009) Ligand-directed tosyl chemistry for protein labeling in vivo. *Nature Chemical Biology 5*, 341–343.
(15) Fujishima, S.-H., Yasui, R., Miki, T., Ojida, A., and Hamachi, I. (2012) Ligand-Directed Acyl Imidazole Chemistry for Labeling of Membrane-Bound Proteins on Live Cells. *J. Am. Chem. Soc. 134*, 3961–3964.
(16) Hughes, C. C., Yang, Y.-L., Liu, W.-T., Dorrestein, P. C., Clair, J. J. L., and Fenical, W. (2009) Marinopyrrole A Target Elucidation by Acyl Dye Transfer. *J. Am. Chem. Soc. 131*, 12094–12096.
(17) Zhang, Y., Mantravadi, P. K., Jobbagy, S., Bao, W., and Koh, J. T. (2016) Antagonizing the Androgen Receptor with a Biomimetic Acyltransferase. *ACS Chem. Biol.* acschembio.6b00659–6.
(18) Hayashi, T., Sun, Y., Tamura, T., Kuwata, K., Song, Z., Takaoka, Y., and Hamachi, I. (2013) Semisynthetic Lectin–4-Dimethylaminopyridine Conjugates for Labeling and Profiling Glycoproteins on Live Cell Surfaces. *J. Am. Chem. Soc.* 130812075816005.
(19) Song, Z., Takaoka, Y., Kioi, Y., Komatsu, K., Tamura, T., Miki, T., and Hamachi, I. (2015) Extended Affinity-guided DMAP Chemistry with a Finely Tuned Acyl Donor for Intracellular FKBP12 Labeling. *Chemistry Letters 44*, 333–335.
(20) Miller Jenkins, L. M., Byrd, J. C., Hara, T., Srivastava, P., Mazur, S. J., Stahl, S. J., Inman, J. K., Appella, E., Omichinski, J. G., and Legault, P. (2005) Studies on the Mechanism of Inactivation of the HIV-1 Nucleocapsid Protein NCp7 with 2-Mercaptobenzamide Thioesters. *J. Med. Chem. 48*, 2847–2858.
(21) Jenkins, L. M. M., Ott, D. E., Hayashi, R., Coren, L. V., Wang, D., Xu, Q., Schito, M. L., Inman, J. K., Appella, D. H., and Appella, E. (2010) Small-molecule inactivation of HIV-1 NCp7 by repetitive intracellular acyl transfer. *Nature Chemical Biology* 1–3.
(22) Bain, D. L., Heneghan, A. F., Connaghan-Jones, K. D., and Miura, M. T. (2007) Nuclear Receptor Structure: Implications for Function. *Annu. Rev. Physiol. 69*, 201–220.
(23) Germain, P., Staels, B., Dacquet, C., Spedding, M., and Laudet, V. (2006) Overview of Nomenclature of Nuclear Receptors. *Pharmacological Reviews 58*, 685–704.
(24) Chawla, A., Repa, J. J., Evans, R. M., and Mangelsdorf, D. J. (2001) Nuclear receptors and lipid physiology: opening the X-files. *Science 294*, 1866–1870.
(25) Lee, Y.-K., Choi, Y.-H., Chua, S., Park, Y. J., and Moore, D. D. (2006) Phosphorylation of the hinge domain of the nuclear hormone receptor LRH-1 stimulates transactivation. *J. Biol. Chem. 281*, 7850–7855.
(26) Cutress, M. L., Whitaker, H. C., Mills, I. G., Stewart, M., and Neal, D. E. (2008) Structural basis for the nuclear import of the human androgen receptor. *Journal of Cell Science 121*, 957–968.

(27) Pratt, W. B., and Toft, D. O. (1997) Steroid receptor interactions with heat shock protein and immunophilin chaperones. *Endocrine Reviews 18*, 306–360.
(28) Bourguet, W., Germain, P., and Gronemeyer, H. (2000) Nuclear receptor ligand-binding domains: three-dimensional structures, molecular interactions and pharmacological implications. *Trends in Pharmacological Sciences 21*, 381–388.
(29) Moras, D., and Gronemeyer, H. (1998) The nuclear receptor ligand-binding domain: structure and function. *Curr. Opin. Cell Biol. 10*, 384–391.
(30) Dubbink, H. J. (2006) Androgen Receptor Ligand-Binding Domain Interaction and Nuclear Receptor Specificity of FXXLF and LXXLL Motifs as Determined by L/F Swapping. *Molecular Endocrinology 20*, 1742–1755.
(31) He, B., Gampe, R. T., Jr., Kole, A. J., Hnat, A. T., Stanley, T. B., An, G., Stewart, E. L., Kalman, R. I., Minges, J. T., and Wilson, E. M. (2004) Structural Basis for Androgen Receptor Interdomain and Coactivator Interactions Suggests a Transition in Nuclear Receptor Activation Function Dominance. *Molecular Cell 16*, 425–438.
(32) Foradori, C. D., Weiser, M. J., and Handa, R. J. (2008) Non-genomic actions of androgens. *Frontiers in Neuroendocrinology 29*, 169–181.
(33) Bishr, M., and Saad, F. (2013) Overview of the latest treatments for castration-resistant prostate cancer. *Nat Rev Urol* 1–8.
(34) Wirth, M. P., Hakenberg, O. W., and Froehner, M. (2007) Antiandrogens in the Treatment of Prostate Cancer. *European Urology 51*, 306–314.
(35) Ammannagari, N., and George, S. (2015) Anti-androgen therapies for prostate cancer: a focused review. *American Journal of Hematology/ …*.
(36) Chen, Y., Sawyers, C. L., and Scher, H. I. (2008) Targeting the androgen receptor pathway in prostate cancer. *Current Opinion in Pharmacology 8*, 440–448.
(37) Tran, C., Ouk, S., Clegg, N. J., Chen, Y., Watson, P. A., Arora, V., Wongvipat, J., Smith-Jones, P. M., Yoo, D., Kwon, A., Wasielewska, T., Welsbie, D., Chen, C. D., Higano, C. S., Beer, T. M., Hung, D. T., Scher, H. I., Jung, M. E., and Sawyers, C. L. (2009) Development of a second-generation antiandrogen for treatment of advanced prostate cancer. *Science 324*, 787–790.
(38) Chen, Y., Clegg, N. J., and Scher, H. I. (2009) Anti-androgens and androgen-depleting therapies in prostate cancer: new agents for an established target. *Lancet Oncology 10*, 981–991.
(39) Korpal, M., Korn, J. M., Gao, X., Rakiec, D. P., Ruddy, D. A., Doshi, S., Yuan, J., Kovats, S. G., Kim, S., Cooke, V. G., Monahan, J. E., Stegmeier, F., Roberts, T. M., Sellers, W. R., Zhou, W., and Zhu, P. (2013) An F876L Mutation in Androgen Receptor Confers Genetic and Phenotypic Resistance to MDV3100 (Enzalutamide). *Cancer Discovery 3*, 1030–1043.
(40) Bohl, C. E., Miller, D. D., Chen, J., Bell, C. E., and Dalton, J. T. (2005) Structural basis for accommodation of nonsteroidal ligands in the androgen receptor. *J. Biol. Chem. 280*, 37747–37754.
(41) McGinley, P. L., and Koh, J. T. (2007) Circumventing Anti-Androgen Resistance by Molecular Design. *J. Am. Chem. Soc. 129*, 3822–3823.
(42) Gunther, J. R., Parent, A. A., and Katzenellenbogen, J. A. (2009) Alternative

Inhibition of Androgen Receptor Signaling: Peptidomimetic Pyrimidines As Direct Androgen Receptor/Coactivator Disruptors. *ACS Chem. Biol. 4*, 435–440.
(43) Estébanez-Perpiñá, E. E., Arnold, L. A. L., Arnold, A. A. A., Nguyen, P. P., Rodrigues, E. D. E., Mar, E. E., Bateman, R. R., Pallai, P. P., Shokat, K. M. K., Baxter, J. D. J., Guy, R. K. R., Webb, P. P., and Fletterick, R. J. R. (2007) A surface on the androgen receptor that allosterically regulates coactivator binding. *Proc Natl Acad Sci U S A 104*, 16074–16079.
(44) Fu, M. (2000) p300 and p300/cAMP-response Element-binding Protein-associated Factor Acetylate the Androgen Receptor at Sites Governing Hormone-dependent Transactivation. *Journal of Biological Chemistry 275*, 20853–20860.
(45) Heinlein, C. A., and Chang, C. (2002) Androgen receptor (AR) coregulators: an overview. *Endocrine Reviews 23*, 175–200.
(46) Fu, M., Wang, C., Wang, J., Zhang, X., Sakamaki, T., Yeung, Y. G., Chang, C., Hopp, T., Fuqua, S. A. W., Jaffray, E., Hay, R. T., Palvimo, J. J., Jänne, O. A., and Pestell, R. G. (2002) Androgen receptor acetylation governs trans activation and MEKK1-induced apoptosis without affecting in vitro sumoylation and trans-repression function. *Mol. Cell. Biol. 22*, 3373–3388.
(47) Fu, M., Rao, M., Wang, C., Sakamaki, T., Wang, J., Di Vizio, D., Zhang, X., Albanese, C., Balk, S., Chang, C., Fan, S., Rosen, E., Palvimo, J. J., Jänne, O. A., Muratoglu, S., Avantaggiati, M. L., and Pestell, R. G. (2003) Acetylation of androgen receptor enhances coactivator binding and promotes prostate cancer cell growth. *Mol. Cell. Biol. 23*, 8563–8575.
(48) He, B., Minges, J. T., Lee, L. W., and Wilson, E. M. (2002) The FXXLF Motif Mediates Androgen Receptor-specific Interactions with Coregulators. *J. Biol. Chem. 277*, 10226–10235.

Chapter 2

ACETYLATION OF AR BY ARTIFICAL ACETYLTRANSFERASES MIMIC

2.1 Assessment of Modification Tolerance of MT-1 Domain

Previously, the Appella Lab reported that thiosalicylic acid amide (thiosalicylamide) derivatives such as MT-1 are able to catalyze the acetylation and the inactivation of the HIV Gag polyprotein. It is hypothesized that MT-1, upon entrance into the cell, is activated by cellular sources of acetate, presumably Ac-CoA to form the active form, SAMT-247. SAMT-247 is able to transfer acetate from its reactive thiophenol ester to proximal Cys39 on HIV gag by thioester exchange, and subsequently to the lysine residues within the zinc finger of the Gag polyprotein.

We envisioned that the MT-1 core could serve as an artificial acetyltransferases domain that catalyzes the acetylation of any protein of interest (POI) if conjugated to a proper targeting ligand. However, it was initially unclear if ligand conjugates of MT-1 would similarly acquire the acetate in cells, as MT-1 analogs with even modest sized N-alkyl modification had poor anti-HIV activity.[1] In order to assess the modification tolerance of MT-1 we synthesized a biotin conjugate YZ01 (Figure 2.1a). (Synthesis see P58) Structurally, YZ01 has the MT-1 domain conjugated by an amide bond a PEG alkyl chain with an azide terminus. The azide was "clicked" to the alkynated biotin which can be used to "fish" out the compound with streptavidin/avidin beads.

Because acetate thioester would be reactive and potentially lost to the nonspecific nucleophiles within the cellular milieu, we also synthesized the probe

analog YZ02 (Synthesis see P63) (Figure 2.1b), which is structurally similar to YZ01 having the MT-1 domain and the biotin groups, but contains a primary amine that could serve as an intramolecular acyl trap of the reactive thioester acetate.

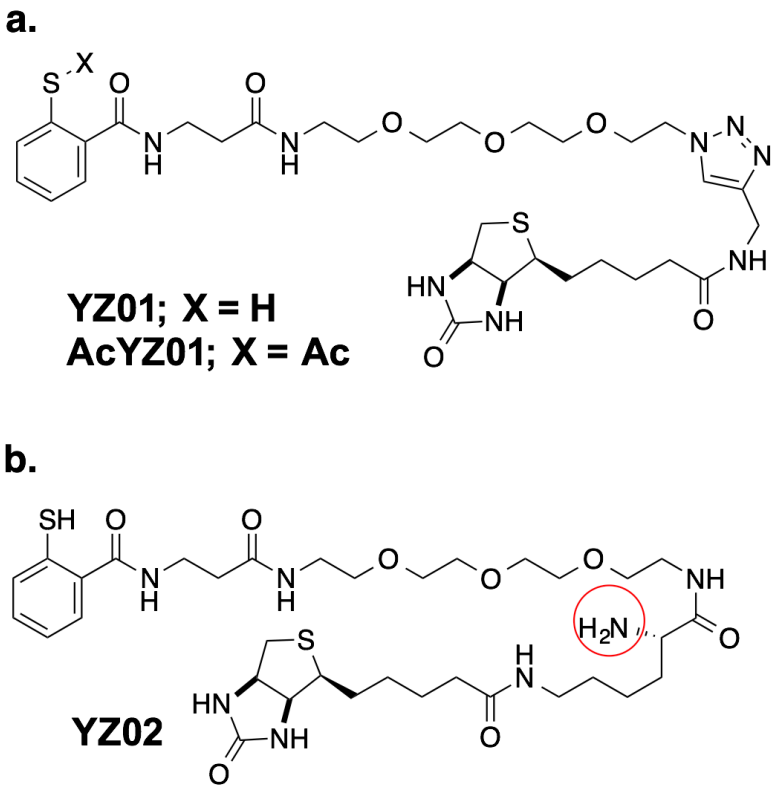

Figure 2.1. Biotin Conjugates Probe YZ01 and YZ02 Compounds.

HEK293t cells were cultured in media processed by dialysis to remove possible acetate sources before treatment with YZ01 or YZ02 in the presence of ^{14}C-labeled pyruvate or acetate. The cells were lysed and the biotin conjugates were isolated using streptavidin beads that were extensively washed and dried before the radio-labeling was measured by scintillation counting. As there is the potential for a lot of non-specific radioactive "labeling" of the streptavidin beads, we measure the

non-specific binding by treating identical aliquots of the cell lysate with a large excess of “unlabeled”, cold biotin prior to the isolation.

From scintillation counting, we found that both YZ01 and YZ02 were readily labeled in cells by ^{14}C-acetate despite the addition of the large tethered biotin ligand, indicating that the thiophenol core was acetylated in a similar manner to that of MT-1 (Figure 2.2a). Under the same experimental conditions, the amount of the ^{14}C-pyruvate derived radiolabel incorporation increased with increasing concentrations of the compounds and the YZ02 has roughly twice the amount of pyruvate label as YZ01 (Figure 2.2b) (See P49 for full experimental design).

Under similar experimental conditions, the cells treated with pre-acetylated AcYZ01 in the presence of ^{14}C-labeled acetate incorporated similar amounts of radiolabeled acetate. (Figure 2.2c) This demonstrates that the thiosalicylamide can be reacetylated in cells after acyl transfer occurs and is in principle capable of turnover.

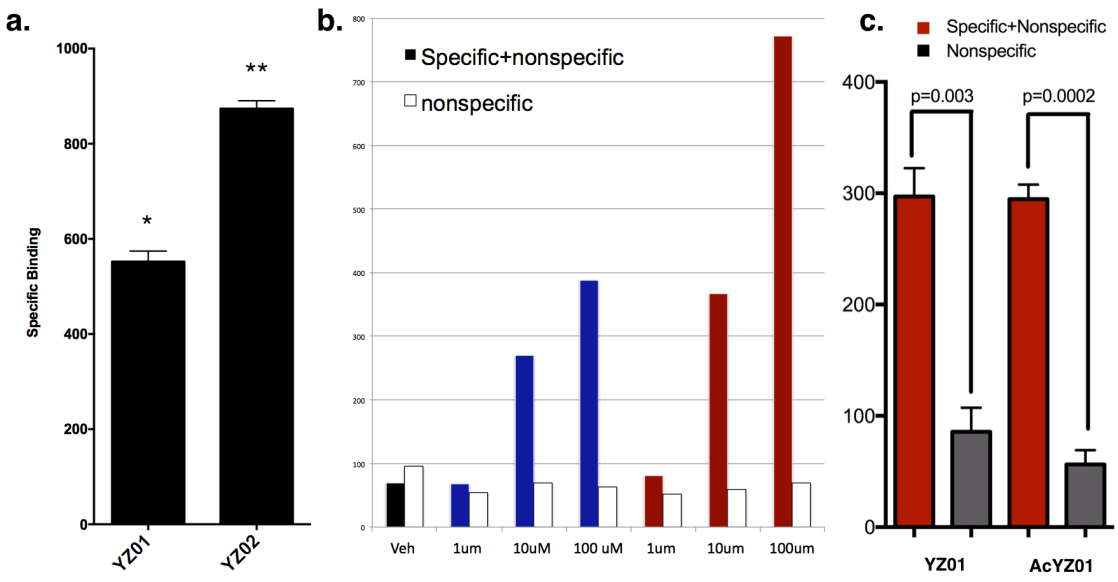

Figure 2.2. Cellular Labeling of Biotin Probes. a. Labeling of Biotin Probes (20 μM) by ^{14}C-acetate in HEK293t cells. b. Labeling of Biotin Probes (20 μM) by ^{14}C-pyruvate in HEK293t cells. c. Total and non-specific radiolabeling of YZ01 and AcYZ01 by ^{14}C-acetate in HEK293t cells.

2.2 Synthesis and Assessment of Artificial Acetyltransferase YZ03; Targeting Androgen Receptor

We then pursued the possibility of redirecting the acetate to a protein of interest. We synthesized the AR-targeting conjugate YZ03 (Figure 2.3a), which replaces the biotin handle of YZ01 with the AR-binding ligand tolfenamic acid, **3** (Figure 2.3a). Whereas many selective and high-affinity ligands are known to bind the ligand-binding pocket of the androgen receptor (AR), tolfenamic acid binds to an allosteric site on the surface of the AR ligand-binding domain (termed BF-3), that is flanked by several lysine residues on the receptor's surface.[2] Tolfenamic acid is a poor AR antagonist in cells (IC_{50} > 30 μM), however we have found that propargyl

amide 4 to be a submicromolar potent AR partial antagonist (IC50 ≈ 0.67 μM) in cellular reporter gene assays. (See P50 for full experimental design).

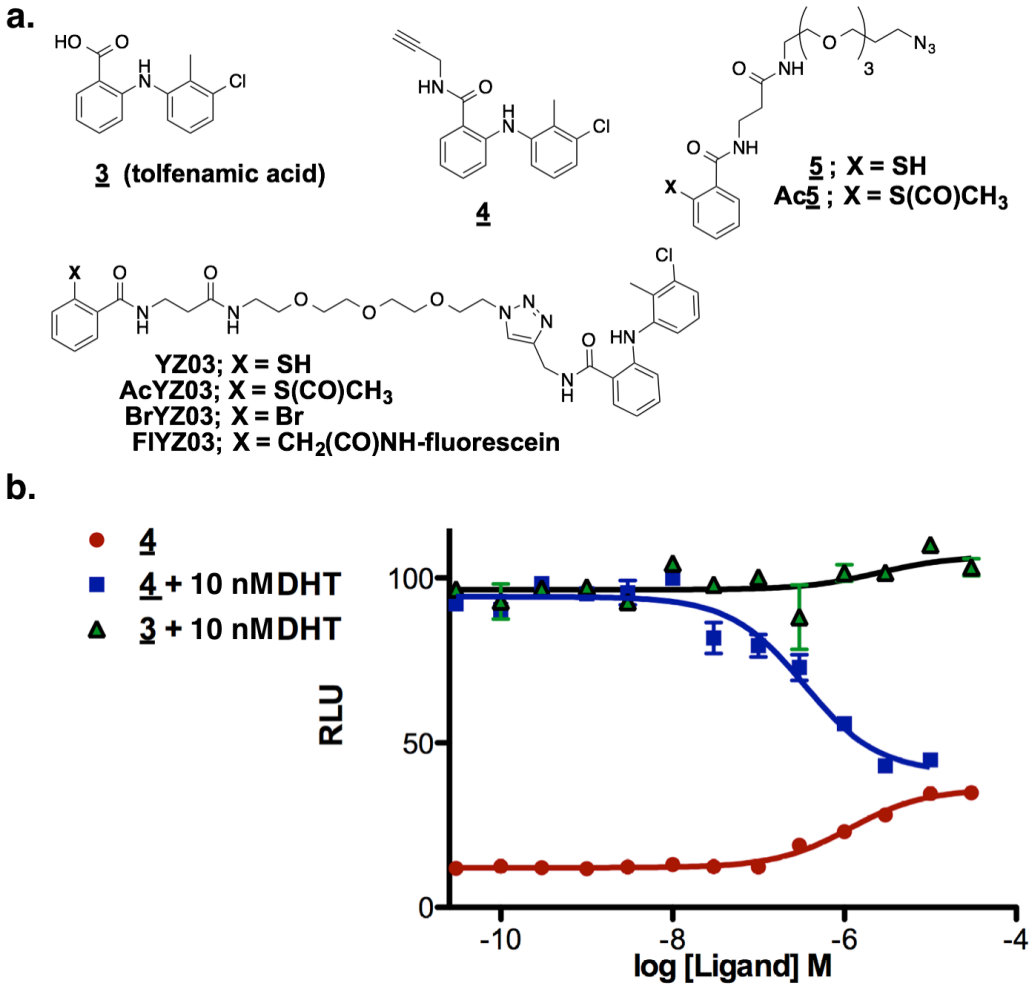

Figure 2.3. AR-directing ligands and reporter gene assay assessment for potency. a. Tolfenamic acid and tolfenamic acid derivatives and MT-1 derivatives. b. Ligand dependent AR transcription response determined by cellular reporter gene assays using AR-responsive luciferase reporter (ARE-Luc): (green) tolfenamic acid (3) + 10 nM DHT; (red) amide (4) ; (blue) amide (4) + 10 nM DHT. (RLU = relative light units)

In order to gain a better understanding about the binding of YZ03 to AR, we also synthesized the fluorescein labeled derivative, FlYZ03 (Figure 2.3a). We used a modified version of the standard *in vitro* TR-FRET coactivator association assay (Lanthascreen^{TM}, Invitrogen, Figure 2.4a), where GST tagged AR(LBD) was incubated with dihydrotestosterone (DHT), terbium labeled anti-GST antibody and increasing concentration of FlYZ03. (Figure 2.4b) The non-specific binding signal was obtained by incubation of just AR(LBD) the antibody and the FlYZ03, and specific binding was determined by subtracting the background signal. Limited solubility prevented us from obtaining a fully saturating binding curve, however we estimated the Kd of FlYZ03 to be 59 μM. To validate this Kd we performed a competitive binding assay where the concentration of FlYZ03 was kept constant and increasing concentration of AcYZ03 was added to compete off the signal. (Figure 2.4c) From the estimated Kd of FlYZ03 and the EC_{50} we obtained for AcYZ03, we calculated the Ki of AcYZ03 to be 60 μM, which is consistent with the Kd we estimated for FlYZ03 through direct binding. (See P57 for full experimental design).

From the binding study data, we believed that even by conjugating the tolfenamic amide **4**, to large substituents such as **5**, we are lowering the AR(LBD) binding affinity of the tolfenamic amide analog relative to **4**, but the tolfenamic acid conjugate YZ03 should still be able to get into the cell, become metabolically charged and subsequently transfer its S-acetyl group to proximal lysine residues on the ligand-binding domain of AR.

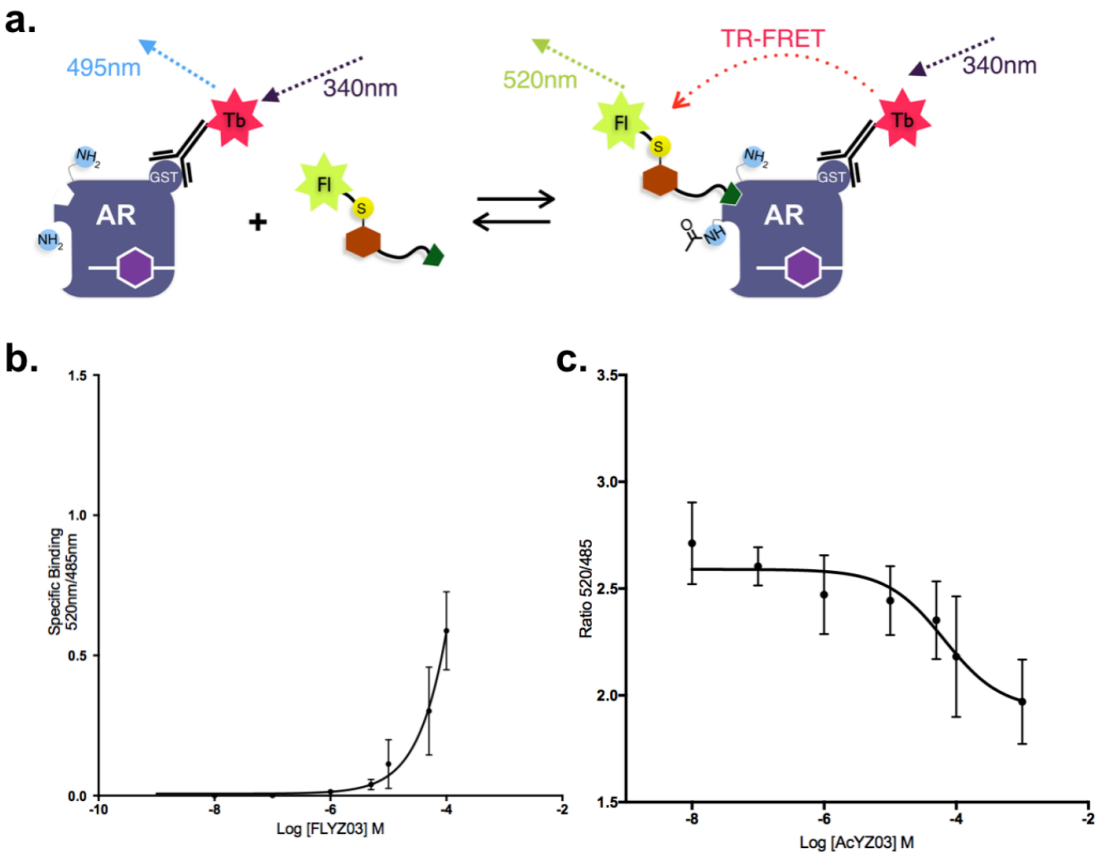

Figure 2.4. Direct and Competitive Binding of BF-3 Site Ligands by TR-FRET Assay. a. Scheme of modified TR-FRET assay using FLYZ03. b. Specific binding of FLYZ03 to AR(LBD) was evaluated by measuring difference between specific binding and nonspecific binding. c. Competitive assay of AcYZ03 versus 50 µM FLYZ03 for AR(LBD).

HEK293t cells transiently expressing full-length AR were treated with 20 µM (unacetylated) YZ03 or the combination of equal concentrations of unlinked fragments, tolfenamic amide **4** plus thiosalicylamide **5** for 16h. Acetylation of the low-abundance AR cannot be directly identified from the background of numerous endogenously acetylated proteins of the cell but can be readily detected by immunoprecipitation (IP) of AR. Imunoprecipitated AR was then analyzed by western blot using anti-

acetyllysine (anti-AcK) antibodies (Figure 2.5a). Treatment with YZ03 (lane 3), but not vehicle (lane 1) or the combination of **4** plus **5** (lane 2), resulted in a substantial increase in AR acetylation. Significantly, the intensity of YZ03 induced AR acetylation can be attenuated by the addition of the competing ligand tolfenamic amide **4** (Figure 2.5a, lanes 4 and 5) consistent with a ligand-directed process. We were unable to completely block all AR acetylation with **4** in cells as high concentrations (>50 μM) of **4** showed signs of cellular toxicity. Using purified AR ligand-binding domain, AR(LBD), we confirmed *in vitro* that AR(LBD) can be similarly acetylated using pre-acetylated YZ03, AcYZ03 (Figure 2.5b, lane 1). In vitro acetylation by AcYZ03 can be attenuated by 20 μM **4** and fully blocked by 50 μM **4** (Figure 2.5b, lanes 2 and 3). (See P52 for full experimental design)

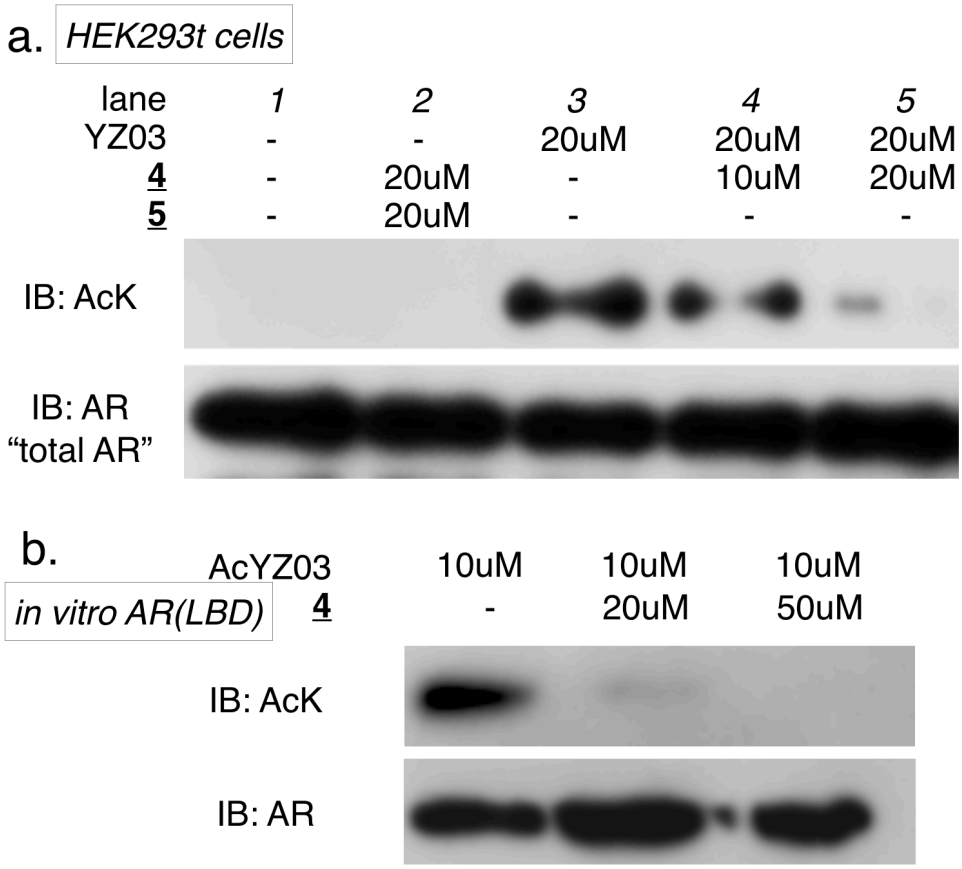

Figure 2.5. Cellular and *in vitro* acetylation of AR by AR-targeting thiosalicylamides. a. AR acetylation by YZ03 in AR-expressing HEK293t cells. Immunoprecipitated (IP) AR analyzed by western immunoblot (IB) using anti-acetyllysine (AcK) and anti-AR. b. *In vitro* acetylation of AR(LBD) by preacetylated AcYZ03.

We also confirmed that YZ03 is able to acetylate AR expressed at endogenous levels in the prostate cancer cell line CWR22Rv1. CWR22Rv1 cells were treated with 20μM YZ03 or equal concentrations of the two unlinked fragments, tolfenamic amide **4** plus probe **5** (Figure 2.6, lanes 1-3). Western analysis of the immunoprecipitated AR again shows that only the intact YZ03 promotes AR acetylation. A similar pattern is observed at 40 μM though the intensity is lower (Figure 2.6, lanes 4 and 5). AR

acetylation by YZ03 is substantially greater than endogenous acetylation levels which can be detected at longer exposures (Figure 2.6 middle). Based on comparison to acetylated protein standards, approximately 5% of AR is acetylated (See P51 for full experimental design).

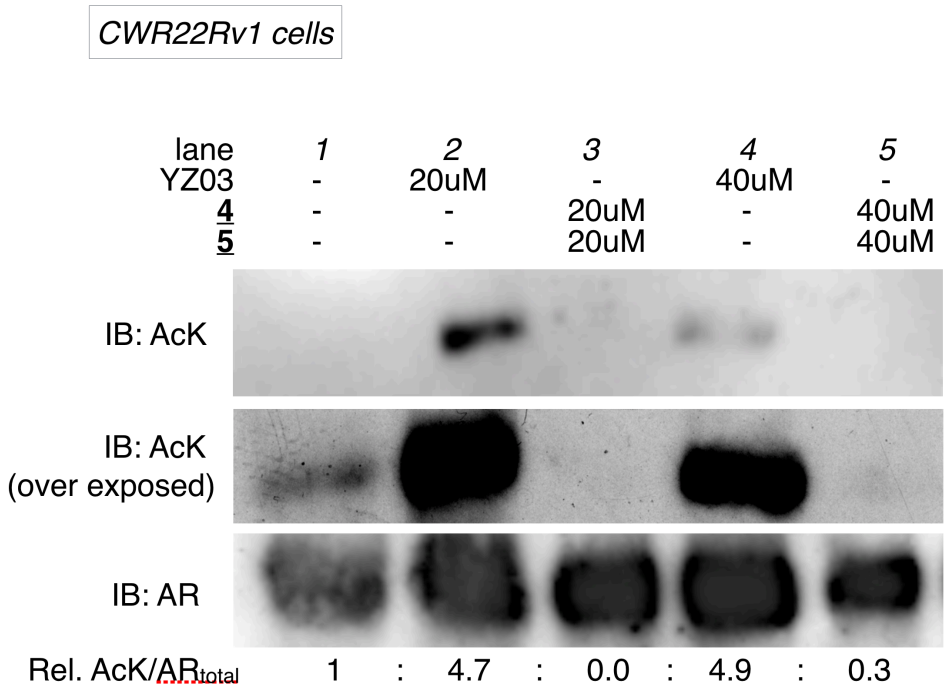

Figure 2.6. Endogenously expressed AR acetylation from CWR22Rv1 Cells.

2.3 Selectivity of YZ03 toward AR

As further evidence that acetylated YZ03 can serve as a proximity directed reagent, we used the S-acetylated analog of the control **5** (**Ac5**) and compared its ability to acetylate purified AR(LBD) in vitro to acetylation by AcYZ03 (Figure 2.7a). Again, only AcYZ03, and not the combination of **4** plus **Ac5,** caused detectable levels of AR(LBD) acetylation in vitro. As an additional control, we confirmed in HEK293t cells that the off-targeted biotin ligand conjugate (AcYZ01) did not significantly

acetylate AR under conditions where AcYZ03 caused substantial AR acetylation (Figure 2.7b). We also analyzed the AR content of the immunoprecipitated acetylome (i.e. IP with anti-AcK) of HEK293t cells treated with AcYZ03 (Figure 2.7c, lanes 1 and 2). Conversely, we selected HSP70 as prototypical off-target protein that contains a similar number of lysines (50 lysines) as AR (40 lysines). No HSP70 could be detected in the vehicle treated or AcYZ03 treated cells (Figure 2.7c).

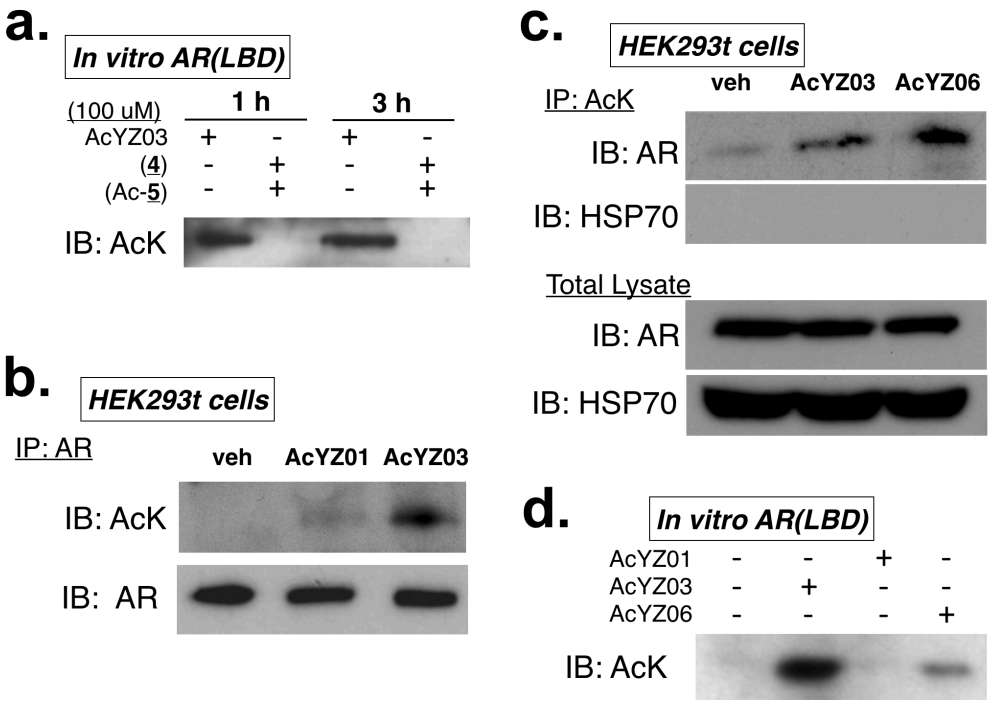

Figure 2.7. Selectivity and reactivity of AR-targeting thiosalicylamide conjugates. a. *In vitro* acetylation of purified AR(LBD); b. Acetylation of AR by AR-targeting (AcYZ03) and off-targeting (AcYZ01) in AR-expressing HEK293t cells; c. Analysis of AR and HSP70 content of cellular acetylome of AR-expressing HEK293t cells isolated by Anti-AcK IP; d. *In vitro* acetylation of purified AR(LBD).

Finally, we confirmed that neither YZ03 nor the biotin-conjugate YZ01 significantly affected the overall acetylation pattern of cellular proteins, suggesting

that YZ01 and YZ03 are not grossly modifying endogenous protein acetylation or deacetylation (Figure 2.8). Taken together, these studies provide additional support for YZ03 acting through a proximity directed acetyl transfer mechanism that uses an endogenous source of acetate to selectively target AR. (See P52 for full experimental design).

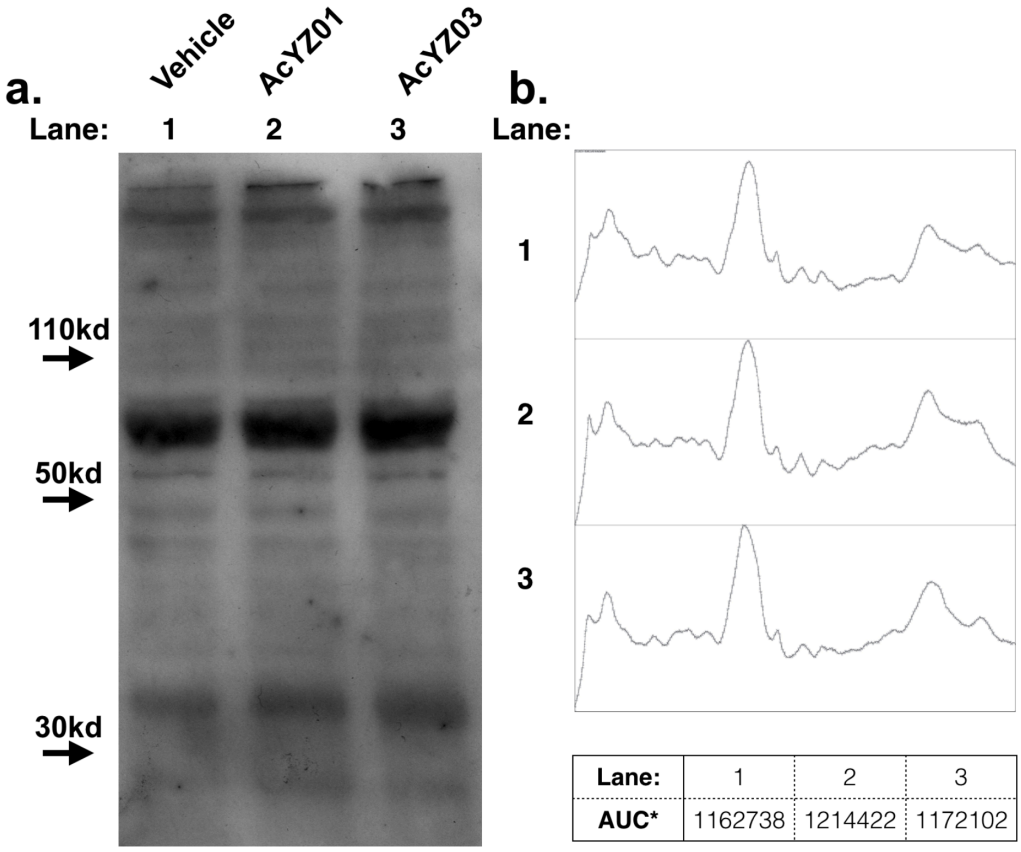

Lane:	1	2	3
AUC*	1162738	1214422	1172102

Figure 2.8. Western blot Analysis of Global Acetylation. a. Crude lysate from treated cells probed with anti-AcK antibody. b. Analysis of lysate acetylation by densitometry. *AUC=Area Under the Curve

2.4 Improvement of YZ compound

So far, we have successfully proven that the YZ03 compound is an acyltransfer catalyst that works through a proximity directed manner. In order to improve the efficiency of the proximity-directed acyltransfer catalyst, we chose to explore how thioester reactivity might change acyl-transfer efficiency.

We designed acyl transfer catalyst YZ06 (Figure 2.9a). Compared to YZ03, YZ06 has an intervening methylene group that breaks conjugation of the electron withdrawing amide with the thiophenol and is expected to form a less reactive thioester. *In vitro* acetyl transfer assays at 30°C, AcYZ06 is 4.6-times less effective than AcYZ03 as an acyltransfer reagent for AR(LBD) (Figure 2.6d). However, in acyl-transfer reactions performed in HEK293t cells, preacetylated YZ06 (AcYZ06) is 46% more effective at acetylating AR without detectable background acylation of control protein HSP70 (Figure 2.6c, lane 3). In CWR22Rv1 cells, (unacetylated) YZ06 is 2.2-times more efficient at catalyzing the overall acetyl group relay from cellular metabolites to AR (Figure 2.9b). This suggests that tuning the reactivity of the thiol can further improve acyl-relay efficiency, which does not simply parallel the reactivity of the intermediate thioester.

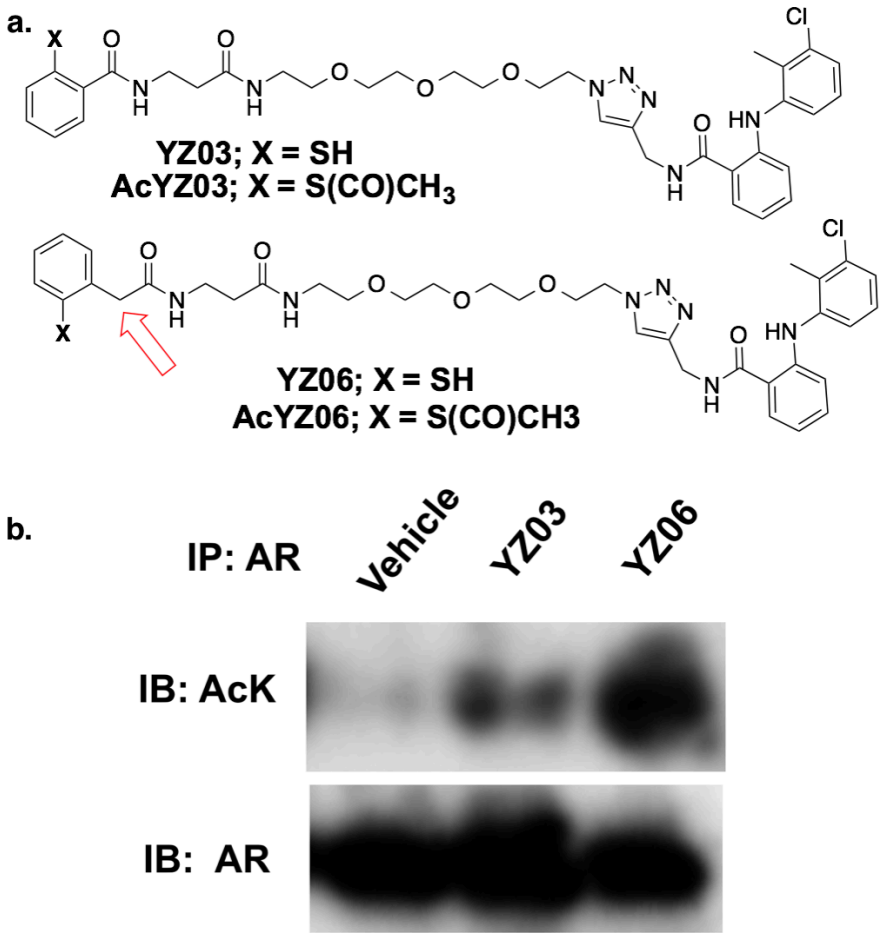

Figure 2.9. Acyltransfer catalyst YZ06 and cellular AR acetylation. a. Structure difference of YZ06 and YZ03. b. AR acetylation by YZ03 or YZ06 in CWR22Rv1 cells.

So far, we were able to modify the thiol reactivity independent of ligand binding function and confirm that although AcYZ06 is a less effective acylating agent than AcYZ03 in vitro, YZ06 is a more effective acyltransfer catalyst in cells. This suggests that catalyst efficiency is a balance between thiol nucleophilicity and acyl-

reactivity, which must function selectively in the presence of a large number of competing nucleophiles within the cell.[3]

REFERENCES

(1) He, B., Gampe, R. T., Jr., Kole, A. J., Hnat, A. T., Stanley, T. B., An, G., Stewart, E. L., Kalman, R. I., Minges, J. T., and Wilson, E. M. (2004) Structural Basis for Androgen Receptor Interdomain and Coactivator Interactions Suggests a Transition in Nuclear Receptor Activation Function Dominance. *Molecular Cell 16*, 425–438.
(2) He, B., Minges, J. T., Lee, L. W., and Wilson, E. M. (2002) The FXXLF Motif Mediates Androgen Receptor-specific Interactions with Coregulators. *J. Biol. Chem. 277*, 10226–10235.
(3) Zhang, Y., Mantravadi, P. K., Jobbagy, S., Bao, W., and Koh, J. T. (2016) Antagonizing the Androgen Receptor with a Biomimetic Acyltransferase. *ACS Chem. Biol.* acschembio.6b00659–6.

Chapter 3

ANTAGONIZING AR ACTIVITY WITH YZ03

3.1 Mapping Acetylation Sites of AR by Protein Mass Spectrometry

In order to elucidate the biological implications of AR acetylation by YZ03, we explored the sites of AR acetylation by YZ03. Recombinant AR(LBD) codon optimized with GST tag on the N-terminus was used to express the protein in E. coli. The purified AR(LBD) was incubated with pre-acetylated YZ03 (AcYZ03) at 30°C for 3h and tryptic digested fragments were analyzed by mass spectrometry (ESI-Orbitrap) and the data was processed by Proteome Discoverer™ Software. Two identical tryptic samples were cleaned by either C18 Ziptip Microcolumn or SCX (Strong Cation Exchange) Ziptip Microcolumn and provided two different mass spectra analyses (Figure 3.1a, b). Not all peptides identified by the software reach statistical confidence. The peptides are ranked by statistical confidence taking account of q-value, PEP value and XCorr value, indicated by color, green: strong confidence, yellow: moderate confidence and red: poor confidence. Based solely on the peptide ranked "strong confidence", we calculated the coverage to be around 30%. Of all the acetylated peptide observed, only one acetylated peptide arose to statistical confidendence; ^{718}WAK(Ac)LPGFR^{725} (Figure 3.1c), with acetylation at Lys720. (See P53 for full experimental design)

a.

	A2	Sequence	# PSMs	# Proteins	# Protein Groups	Protein Group Accessions	Modifications	ΔCn	q-Value	PEP	XCorr	Charge	MH+ [Da]	ΔM [ppm]	RT [min]
4		sp	AR(LBD)_Human	36.10	47.20 %	1	11	22	140	250	29.1	8.72			
1		WAkALPGFR	4	1	1	sp	K3(Acetyl)	0.0000	0	0.0054	2.18	2	1087.59526	-8.76	107.50
2		RFYQLTK	15	1	1	sp		0.0000	0	0.0134	2.03	2	955.52745	-8.95	56.00
3		QLVHVVK	9	1	1	sp		0.0000	0	0.00247	2.00	2	822.51183	-9.49	39.03
4		FYQLTK	5	1	1	sp		0.0000	0	0.00191	1.78	2	799.42742	-9.34	62.79
5		LLDSVQPIAR	21	1	1	sp		0.0000	0	0.00111	1.70	2	1111.63652	-9.46	81.41
6		LDSVQPIAR	1	1	1	sp		0.0000	0	0.00833	1.47	2	998.55419	-8.80	79.77
7		FFDELR	56	1	1	sp		0.0000	0	0.000345	1.42	2	826.40166	-9.39	84.75
8		VKPIYFH	1	1	1	sp		0.0000	0	0.00539	1.05	2	903.50060	-8.99	58.87
9		SFTNVNSR	6	1	1	sp		0.0000	0	0.0209	0.97	2	924.44426	-9.89	38.23
10		DSVQPIAR	1	1	1	sp		0.0000	0.023	0.262	1.24	1	885.47003	-10.02	79.86
11		SFTNVN	1	1	1	sp		0.0000	0.032	0.316	1.32	1	681.31390	-9.32	47.39
12		QKFFDELR	1	1	1	sp		0.0000	0.191	0.83	0.19	3	1082.56830	4.92	72.16
13		VLEAIEPGVVCAGH	4	1	1	sp		0.0000	0.731	1	0.06	3	1393.71769	2.29	64.65
14		MYSQcVR	1	1	1	sp	C5(Carbamyl)	0.0000	0.757	1	0.13	2	929.39513	-1.82	71.76
15		PTScSRR	3	1	1	sp	C4(Carbamyl)	0.0000	0.761	1	0.14	2	849.40282	3.79	48.61
16		DSVQPIAREL	1	1	1	sp		0.0000	0.806	1	0.03	2	1127.59636	-8.17	98.62
17		PGFRNL	1	1	1	sp		0.0000	0.826	1	0.03	2	703.39141	3.96	13.24
18		LSQEFGWL	1	1	1	sp		0.0000	0.835	1	0.05	2	979.49645	8.21	46.19
19		QFTFDLLIK	3	1	1	sp		0.0000	0.836	1	0.03	2	1124.62395	-9.89	129.45
20		WAKALPGFR	1	1	1	sp		0.0000	0.844	1	0.24	2	1045.59099	-3.09	135.25
21		ELDRIIAcK	1	1	1	sp	C8(Carbamyl)	0.1176			0.15	2	1103.58806	0.22	96.81
22		VkPIYFH	1	1	1	sp	K2(Acetyl)	0.7727			0.05	2	945.51842	-0.92	63.54
23		IIAckRk	1	1	1	sp	C4(Carbamyl); K5(Acetyl);...	0.2500			0.03	3	958.55692	6.91	34.18
24		YIkELDR	1	1	1	sp	K3(Acetyl)	0.9787			0.01	2	978.52678	1.30	57.09

b.

	A2	Sequence	# PSMs	# Proteins	# Protein Groups	Protein Group Accessions	Modifications	ΔCn	q-Value	PEP	XCorr	Charge	MH+ [Da]	ΔM [ppm]	RT [min]
2		sp	AR(LBD)_Human	65.83	74.40 %	1	10	30	119	250	29.1	8.72			
1		SHMVSVDFPEMMAEIISVQV...	4	1	1	sp		0.0000	0	0.000541	6.58	3	2474.21683	1.57	141.48
2		LLDSVQPIAR	10	1	1	sp		0.0000	0	0.0485	2.95	2	1111.64849	1.30	81.53
3		QLVHVVK	8	1	1	sp		0.0000	0	0.00781	2.23	2	822.52117	1.87	40.96
4		RFYQLTK	17	1	1	sp		0.0000	0	0.0158	2.23	2	955.53752	1.59	56.23
5		SFTNVNSR	3	1	1	sp		0.0000	0	0.0253	2.06	2	924.45586	2.66	40.45
6		FFDELR	30	1	1	sp		0.0000	0	0.0507	1.98	1	826.41034	1.11	86.60
7		FYQLTK	4	1	1	sp		0.0000	0	0.22	1.67	2	799.43608	1.50	64.51
8		ALPGFR	6	1	1	sp		0.0000	0	0.114	1.20	2	660.38310	0.44	65.99
9		VkPIYFH	2	1	1	sp	K2(Acetyl)	0.0000	0	0.324	1.02	2	945.51750	-1.89	85.98
10		VHVVkWAK	2	1	1	sp	K5(Acetyl)	0.0000	0.02	0.517	0.96	2	1008.59984	0.88	84.28
11		VKPIYFH	1	1	1	sp		0.0000	0.02	0.508	0.77	3	903.50910	0.42	60.54
12		ILSGkVK	2	1	1	sp	K5(Acetyl)	0.0000	0.106	0.645	1.12	2	786.50945	1.32	52.55
13		KNPTScSR	1	1	1	sp	C6(Carbamyl)	0.0200	0.334	0.773	0.49	1	935.43542	-1.02	135.51
14		WAkALPGFR	3	1	1	sp	K3(Acetyl)	0.0000	0.51	0.843	0.36	2	1087.60393	-0.79	94.40
15		FSIIPVDGLKN	1	1	1	sp		0.0000	0.51	0.841	0.07	2	1202.68682	7.32	90.41
16		NVLEAIEPGVVcAGH	1	1	1	sp	C12(Carbamyl)	0.0000	0.573	0.864	0.04	2	1550.77641	8.50	137.91
17		DSVQPIAR	1	1	1	sp		0.0000	0.67	0.91	0.29	1	885.48132	2.74	81.30
18		QITPQEFLcMkAL	1	1	1	sp	C9(Carbamyl); K11(Acetyl)	0.0000	0.867	1	0.24	2	1606.78679	-6.25	128.92
19		PTSCSRR	1	1	1	sp		0.0000	0.879	1	0.27	1	806.39301	-0.96	105.49
20		SGkVkPIYFH	1	1	1	sp	K3(Acetyl); K5(Acetyl)	0.0000	0.895	1	0.02	3	1259.67734	-0.78	50.35
21		IIACkRk	3	1	1	sp	K5(Acetyl); K7(Acetyl)	0.0000	0.919	1	0.04	2	915.54094	-3.87	85.41
22		PTScSRR	1	1	1	sp	C4(Carbamyl)	0.0000	0.922	1	0.03	2	849.39891	-0.80	59.24
23		KSRMYSQcVR	1	1	1	sp	C8(Carbamyl)	0.3095			0.29	2	1300.61290	-9.25	85.99
24		YFAPDLVFNEYR	1	1	1	sp		0.1071			0.25	3	1533.72260	-9.59	105.83
25		VVKWAK	1	1	1	sp		0.6515			0.23	2	730.45781	-4.45	11.56
26		SQEFGWLQITPQEFLcMk	1	1	1	sp	C16(Carbamyl); K18(Acetyl)	0.6182			0.21	3	2270.08060	8.13	120.33
27		ELDRIIAcK	2	1	1	sp	C8(Carbamyl)	0.6000			0.08	2	1103.58757	-0.22	107.37
28		ELDRIIAck	2	1	1	sp	C8(Carbamyl); K9(Acetyl)	0.1429			0.06	2	1145.60051	1.86	115.70
29		QITPQEFLcMK	1	1	1	sp	C9(Carbamyl)	0.2500			0.06	2	1380.66411	-0.71	119.84
30		NQPDSFAAL	1	1	1	sp		0.5714			0.06	3	962.45176	-6.31	38.58
31		PTScSRRFYQL	1	1	1	sp	C4(Carbamyl)	0.9000			0.04	2	1400.66875	-3.74	93.82
32		QFTFDLLIK	1	1	1	sp		0.3333			0.02	2	1124.63896	3.46	130.24
33		VVkWAk	1	1	1	sp	K3(Acetyl); K6(Acetyl)	0.8667			0.02	2	814.48033	-2.28	50.49
34		VkPIYFHT	1	1	1	sp	K2(Acetyl)	0.9130			0.02	2	1046.57085	3.71	84.31
35		ILSGkVk	1	1	1	sp	K5(Acetyl); K7(Acetyl)	0.8000			0.01	1	828.51715	-2.20	122.76
36		WAKALPGFR	1	1	1	sp		0.7500			0.01	2	1045.60161	7.07	135.55

c.

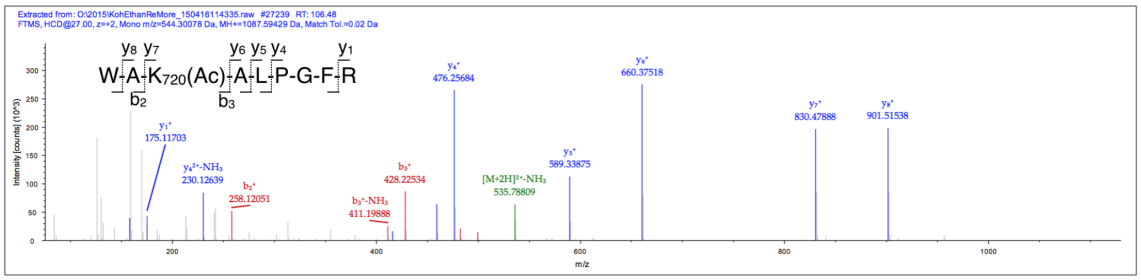

Figure 3.1. Analysis of acetylation site of AR by tandem mass spectrometry. a. Full peptide analysis of C-18 microcolumn treated AR(LBD) tryptic sample. b. Full peptide analysis of cation exchange microcolumn treated AR(LBD) tryptic sample.

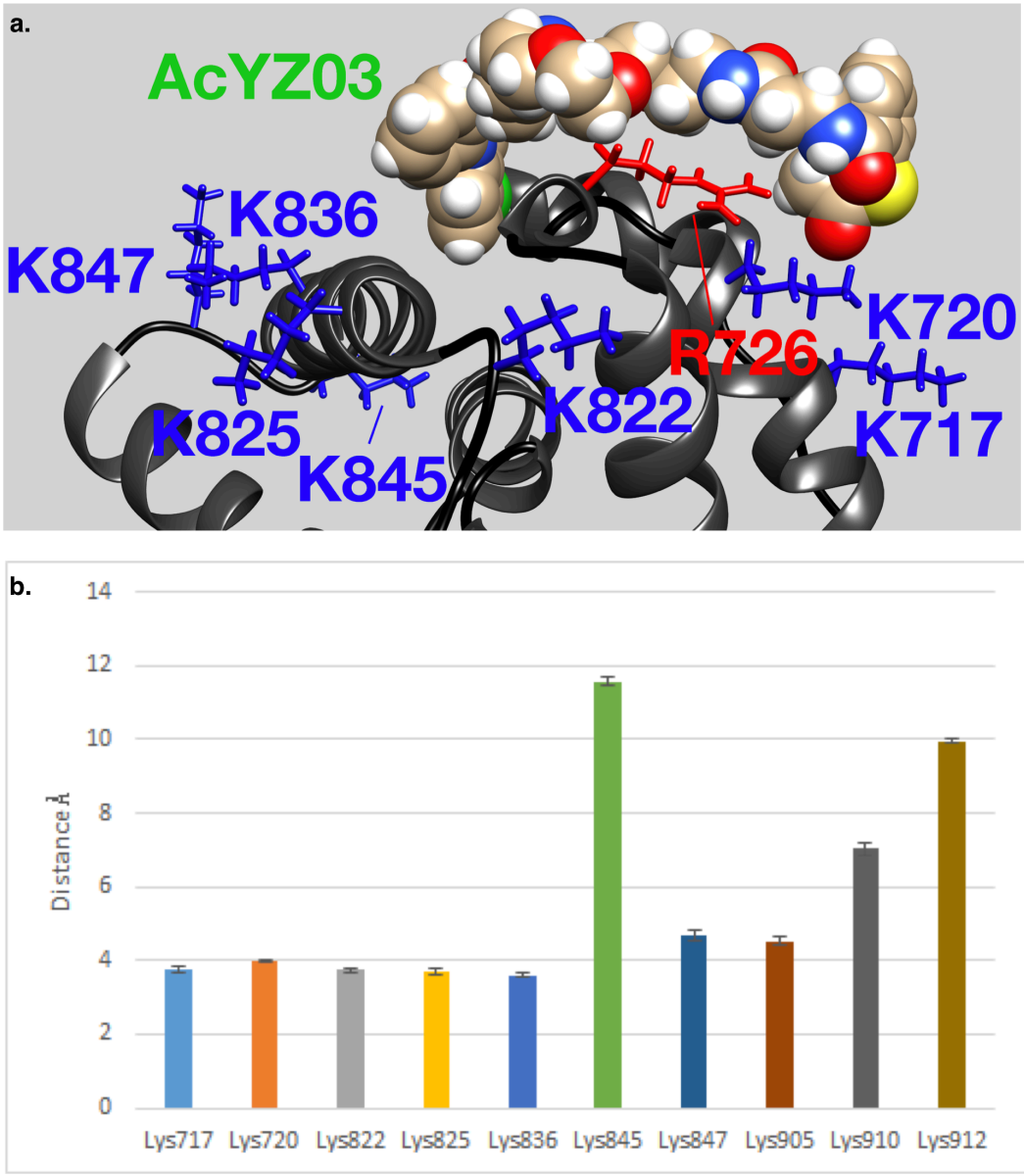

Figure 3.2. Lysine residues proximal to the AR BF-3 binding site. a. Structure of AcYZ03 directed towards Lys720 after steered molecular dynamics simulation (based on PDB:2PIX). b. Bar graph showing time-averaged distance, thioacetate carbonyl carbon to lysine-nitrogen, over the last 100 ps of simulation (± SD).

Steered molecular dynamics performed by graduate student Wei Bao suggests that in addition to Lys720, the thioacetate of AcYZ03 can readily access several other

lysine residues (Lys717, Lys822, Lys825 and Lys836) when bound to the BF-3 binding pocket (Figure 3.2a). The other accessible lysine residues might also be acetylated based on the length of AcYZ03, however they did not reach accepted standard of significance by our analysis. This may reflect artifacts intrinsic to our methods or perhaps Lys720 is more reactive, Lys720 is the second closest lysine after Lys836, to the BF-3 bound tolfenamic acid (Figure 3.2b) and is uniquely flanked by basic amino acid residues Lys717 and Arg726, which could account for an increased reactivity by effectively lowering Lys720's pKa (Figure 3.2a). (See P54 for full experimental design)

Lys720 is a critical residue for AR coactivator binding and is part of the "charge-clamp" motif used to bind the conserved amphipathic FXXLF helix of coactivors. Backbone carbonyl oxygens from F27 and V30 form hydrogen bonds with the side chain of K720. (Figure 3.3).[1] Mutations to Lys720 have been shown to reduce the association of coactivator peptides by almost 80%, however mutations to Lys717 do not show an appreciable affect on coactivator peptide association though Lys717 is in close proximity to the Lys720 and the binding pocket.[2] This suggests that the acetylation of Lys720 may similarly affect coactivator association by decreasing the number of hydrogen bond formed between Lys720 and the backbone of the peptide or interfering the helix dipole stabilization by the positive charged lysine residue.[2] This presents the intriguing possibility that YZ03 may be able to enhance the antagonist activity of BF-3 site ligands through proximity directed acyl transfers.

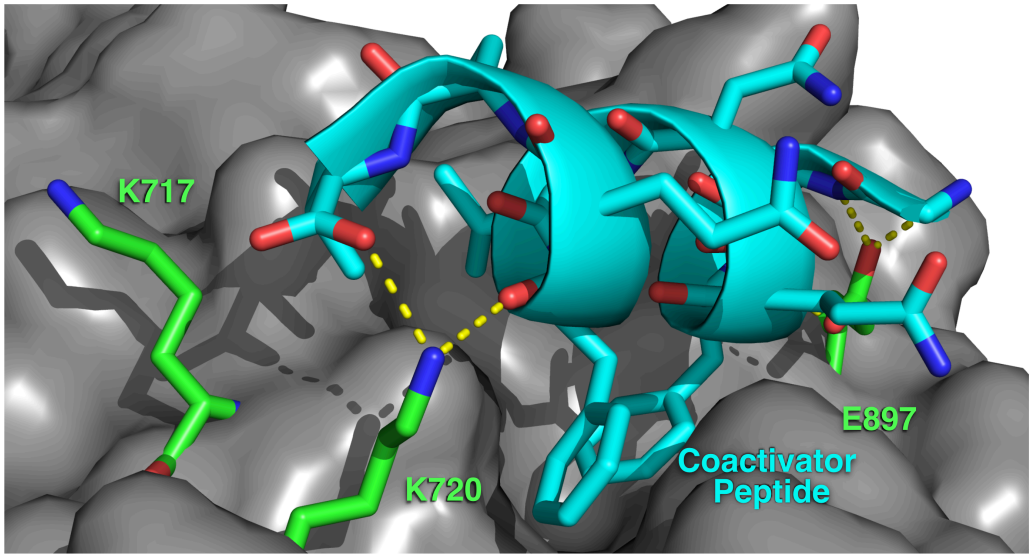

Figure 3.3. Lys720 forms H bond to the FXXLF coactivator peptide.

3.2 Evaluation of YZ03 as an Antagonist using Cellular Reporter Gene Assay

In order to evaluate the antagonist activity of YZ03, a cellular reporter gene assay was used to measure AR transcriptional activity at an AR response element to upregulate down stream luciferase expression.

We synthesized control compound, BrYZ03, a nonreactive isostere of YZ03 that has the thiol replaced by an isosteric bromine atom (Figure 2.3a). However, evaluation of YZ03's actual antagonist activity proved challenging as the parent ligand is already an effective AR antagonist, and at a 5% acetylation levels would be unlikely to cause a significant difference in transcriptional response compared to control. In reporter gene assays conducted in HEK293t cells, the isostere was a slightly more efficacious antagonist than AcYZ03 (Figure 3.4a). AcYZ06, shows even higher levels of acetylation in cells, but did not prove to be better than AcYZ03 at antagonizing AR activity (Figure 3.4b). As it is not likely that the distal bromine significantly alters ligand binding, we reasoned that the cellular bioavailability of YZ03 might be affected

by the propensity of the thiol to get oxidize over the course of the 18h cellular assay. The thiol is an intrinsic part of the YZ03's acyl transfer activity, therefore, we turned to *in vitro* studies to evaluate YZ03's antagonist activity.

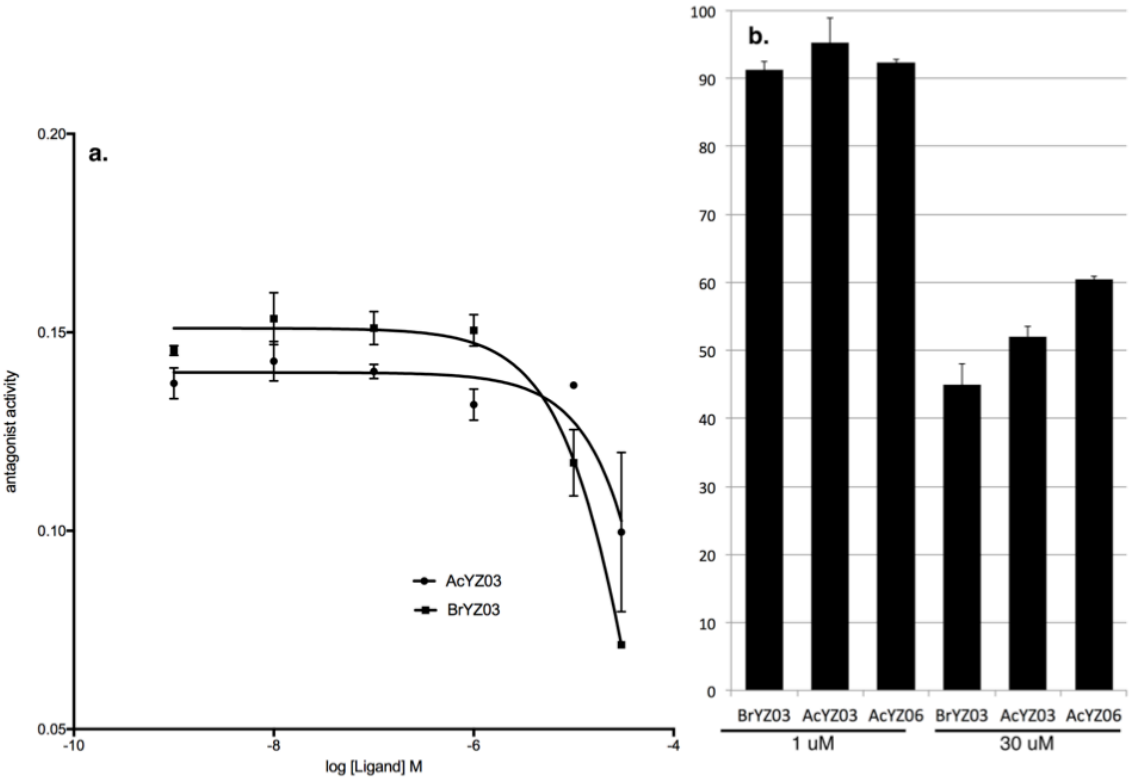

Figure 3.4. Reporter gene assay evaluation of antagonist activity of YZ03 and YZ06. **a**. Dose response curve of AcYZ03 and BrYZ03. b. Comparison of BrYZ03, AcYZ03 and AcYZ06 antagonist activity.

3.3 Assessment of Antagonist Activity of YZ03 with TR-FRET Assay

We used a standard in vitro TR-FRET coactivator association assay kit (Lanthascreen™, Invitrogen) to assess antagonist activity. The assay comes with expressed AR(LBD) with an N-terminal GST tag, Terbium conjugated anti-GST antibody and fluorescein labelled D11FXXLF peptide resembling GRIP1, SRC-1 and AIB-1 sequences. With the treatment of agonist (ex. DHT), the fluorescein labeled FXXLF peptide will bind preferably to the coactivator binding pocket induced by the DHT and give a TR-FRET signal (Figure 3.5a). If acetylation of Lysine720 affects the binding of the peptide, we should see a lower FRET signal when treated with AcYZ03 reagent (Figure 3.5b). (See P56 for full experimental design)

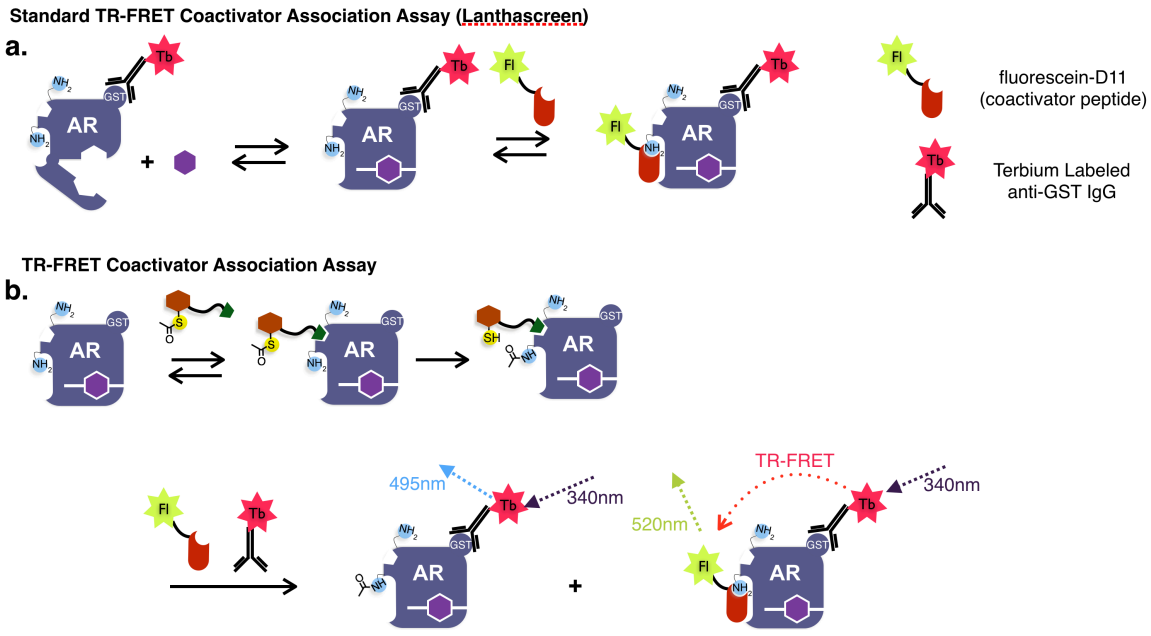

Figure 3.5. Scheme of TR-FRET used for antagonist assessment.

First we tried to incubate the AR(LBD), the antibody, the peptide, the DHT and YZ03 at the same time to allow for continuous monitoring of the reaction. Unfortunately, we saw no significant difference between the experiment and controls, even with longer incubation times (Figure 3.6).

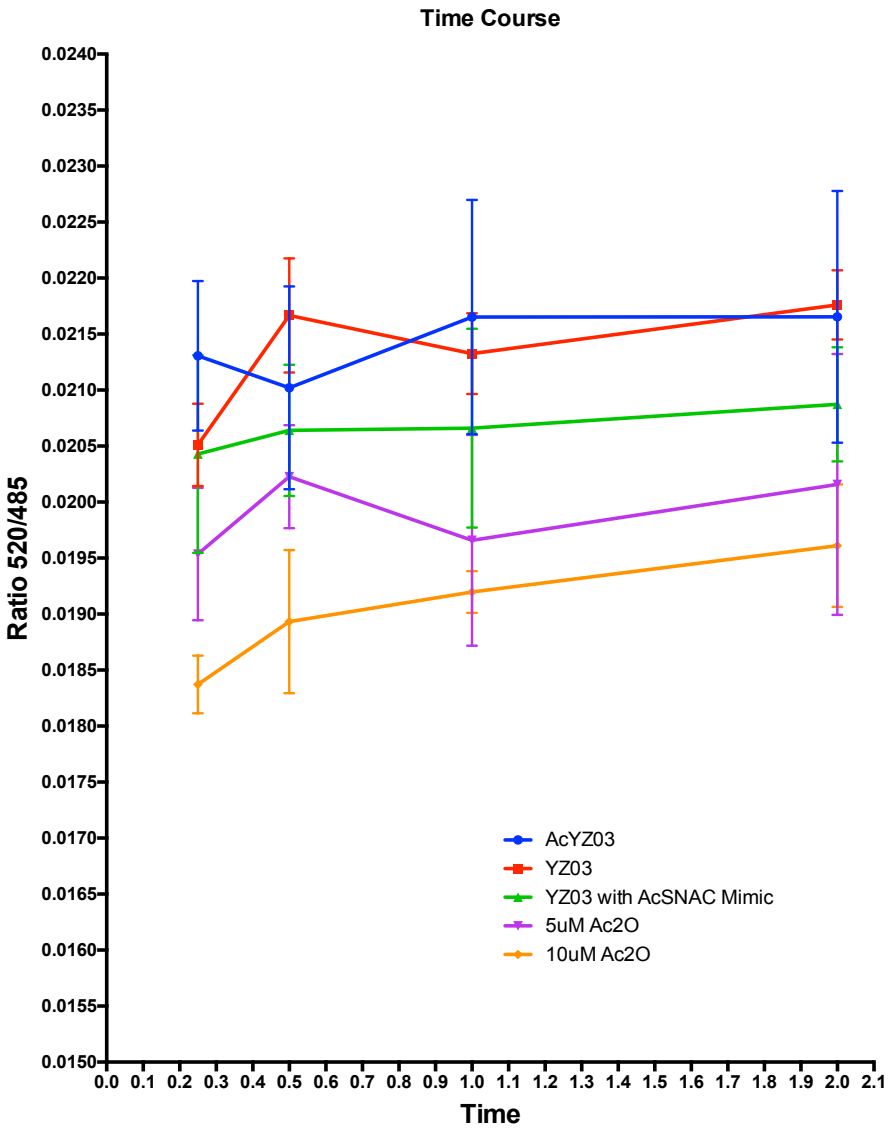

Figure 3.6. Continuous assay by TR-FRET by simultaneous incubation of YZ03 compounds.

We reasoned that with the FXXLF peptide bound, the lysine residue is hydrogen bonded and can no longer attack the carbonyl carbon of the thioester. Therefore, we first incubated the AR(LBD) with the YZ03 compounds such that the AR(LBD) is already acetylated before the fluorescein labeled peptide was added. Indeed, we saw a inhibitory effect from the addition of YZ03 and especially AcYZ03 (Figure 3.7a).

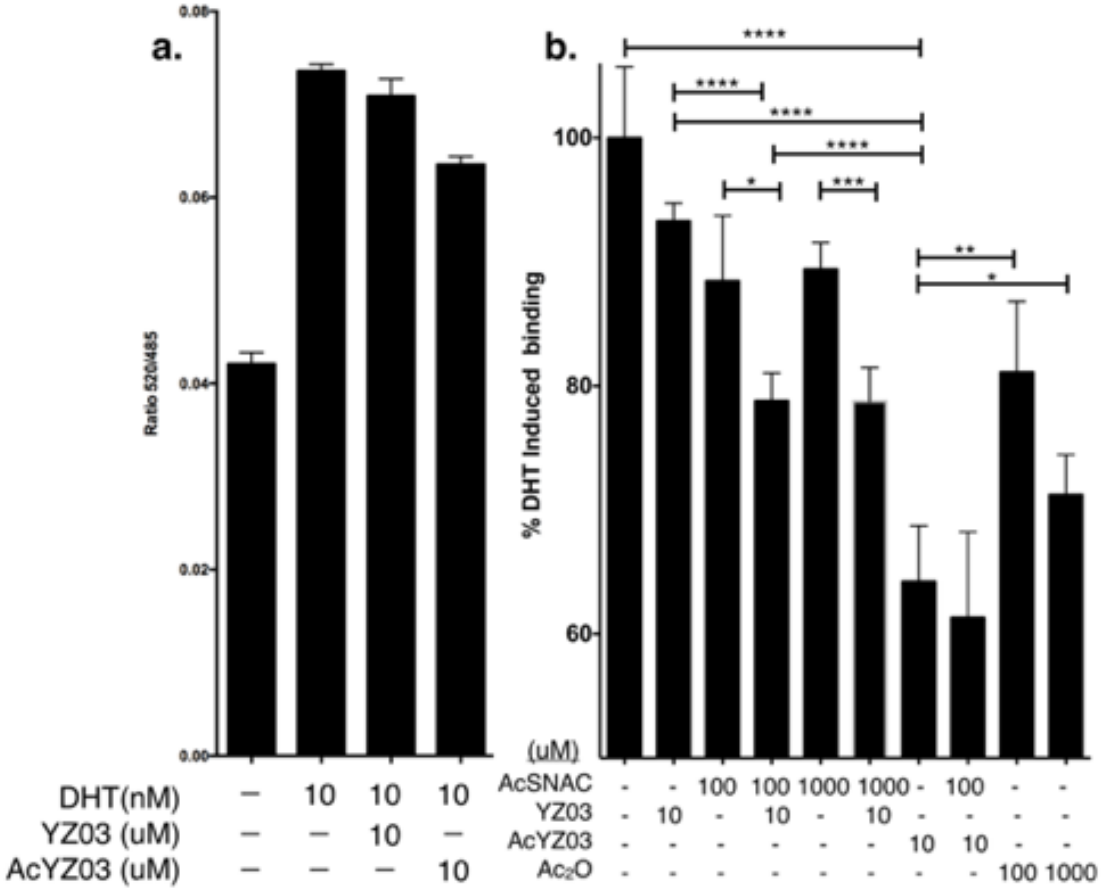

Figure 3.7. Coactivator peptide association assay. a. DHT was used to assess the background signal. b. Full set of experimental conditions normalized as percent DHT-Inductible.

By measuring the signal without adding DHT, we obtained the background signal level so that we could estimate the percent of inhibition based on induced signal

(Figure 3.7a). We then conducted a complete set of the experiments and controls and found that incubation of AR(LBD) with just 10 μM of AcYZ03 reduces dihydrotestosterone (DHT)-induced coactivator association by 36% ($p<0.0001$) or 5-times greater antagonism than the same concentration of unacetylated YZ03. Just 10 μM AcYZ03 is also significantly more effective than treatment with acetic anhydride at 100-times the concentration (1000 μM) (Figure 3.7b). Additionally, inhibition by unacetylated YZ03 can be enhanced 3-fold by the addition of 100 μM of the acetyl-CoA mimic, S-acetyl- N-acetyl cysteamine (AcSNAC) (Figure 3.7b). Together, these studies show that proximity directed acyl transfer reactions can be used as a novel approach to enhance the activity of weak antagonists that bind proximal to the coactivator binding interfaces.[3] (See P56 for full experimental design)

REFERENCES

(1) He, B., Gampe, R. T., Jr., Kole, A. J., Hnat, A. T., Stanley, T. B., An, G., Stewart, E. L., Kalman, R. I., Minges, J. T., and Wilson, E. M. (2004) Structural Basis for Androgen Receptor Interdomain and Coactivator Interactions Suggests a Transition in Nuclear Receptor Activation Function Dominance. *Molecular Cell 16*, 425–438.
(2) He, B., Minges, J. T., Lee, L. W., and Wilson, E. M. (2002) The FXXLF Motif Mediates Androgen Receptor-specific Interactions with Coregulators. *J. Biol. Chem. 277*, 10226–10235.
(3) Zhang, Y., Mantravadi, P. K., Jobbagy, S., Bao, W., and Koh, J. T. (2016) Antagonizing the Androgen Receptor with a Biomimetic Acyltransferase. *ACS Chem. Biol.* acschembio.6b00659–6.

Chapter 4

EXPERIMENTAL AND METHODS

General Methods and Materials:

All chemicals were brought from Sigma Aldrich and Acros Organics unless otherwise noted. Tolfenamic acid was purchased from Cayman chemicals and ASDI, Newark, DE.

1H and 13C spectra were recorded on Bruker AV 400, DRX-400 or AV-600 instruments. Chemical shifts are reported in δ and J values are reported in Hz.

RPMI 1640, Dulbecco's modified Eagle Media (DMEM), Sodium pyruvate solution, DPBS were purchased from MediaTech. Phenol red free RPMI 1640 was purchased from Gibco. EDTA free protease cocktail minitab was purchased from Roche Applied science. Anti-acetyllysine, Streptavidin-HRP, Agarose-A beads were purchased from cell signaling. Anti-AR (N-20) antibody and secondary antibodies were purchased from Santa Cruz biotechnologies, CA. High capacity streptavidin beads were purchased from Thermo Scientific.

Methods for Cellular radio-labeling studies of Biotin Probes YZ01 and YZ02 with ^{14}C-acetate or Pyruvate :

HEK293t Cells (300,000 cells/well) were seeded individually into 32 mm wells (6-well plate) in DMEM supplemented with 10% CCS, 4 mM L-Glutamine. After 12-16 hours the media was changed to pyruvate-free DMEM supplemented with 10% dialyzed CCS (1 ml). After 5 h acetylation probe YZ01 or YZ02 was added along with

2 μCi 14C-pyruvate (or 5 μCi 14C-acetate) at indicated concentrations. The cells were incubated at 37°C for 16 h before the media was remove and retained. The cells were lysed with 200 μL lysis buffer (5% glycerol, 0.05% tritonx-100 in PBS) followed by washing with 200 μL DPBS. Lysates were then combined with the cell media and centrifuged (12,000 rpm, 20 min). The supernatant was then divided into two 450 μL aliquots. Control aliquots were treated with 50 μL of 200 mM "cold" (unlabeled) biotin (buffered with an equivalent of triethylamine) in DMSO to block specific binding of YZ01 or YZ02. To the remaining aliquot was added 50 μL DMSO. Streptavidin-argrose Beads (50 μL, Thermo Scientific, #20357) were added to both aliquots and rocked on a rocker platform for 3.5 hrs at 4°C. The slurry was added to a spin column and washed with lysis buffer (7 x 500μL). The beads were wetted with 100μL of methanol dried for 12 hrs prior to addition of scintillation cocktail. After mixing with scintillation cocktail the specific activity was measured in a microbeta scintillation counter.

Transcription/antagonist response by cellular (luciferase) reporter gene assay: Twenty-four hours prior to transfection, HEK293T cells were seeded at a density of 75,000 cells per well in 24-well cell culture plates and grown in phenol red free Dulbecco's Modified Eagle Medium (DMEM) supplemented with 10% cosmic calf serum (CCS) (HyClone, Logan, UT). Transfections were performed using $Ca_3(PO_4)_2$ following general protocol (Short Protocol in Molecular Biology) and using 0.08 ug hAR(wt), 0.16 ug of ARE-Luciferase reporter, 0.08ug of Renilla-luc as internal standard. Five hours after transfection the wells were washed with DPBS and media was added containing appropriate ligands. The cells were allowed to incubate for 36 h

before harvesting by passive lysis buffer. Cell extracts were immediately assayed using the Dual Luciferase Assay (Promega #E1960, Madison, WI) with a Perkin-Elmer Microbeta Luminometer. All experiments were run in triplicates. Activity is reported in relative light unit (RLU), determined as the ratio of inducible firefly luciferase luminescence divided by the luminescence of the renilla luciferase control.

Androgen Receptor Acetylation in CWR22Rv1 cells by Synthetic Acyltransferase YZ03 (IP:AR followed by IB: Anti-AcK):

CWR22Rv1 cells were seeded in 100 mm dish with RPMI 1640 media supplemented with 10% FBS. After the cell reached 60% confluence, the media was changed to phenol red-free RPMI 1640 supplemented with 1mM pyruvate and incubated for an additional 12 h. The media was then changed to phenol red-free RPMI containing YZ03, HDAC inhibitor SAHA (50μM) and incubated for 16 hrs. The cells were then washed with ice cold DPBS and lysed with RIPA buffer (pH 7.4 PBS with 0.1% SDS, 1% Sodium Deoxycholate and 1.5M NaCl, 1 ml) followed by sonication (Branson Sonifier 200 watt 2 x 2s pulses @40%) and centrifugation (12,000 rpm, 20 mins). The supernatants were saved and the total protein levels were determined by Bradford assay. To 500 μL of lysate was added 5μL anti-AR (N20, Santa Cruz) and the solution rock at 4°C for 12 hours. Protein A beads (20 μL, Cell Signaling) was added and the solution was rocked for an additional 3.5 h. The beads were washed with PBS buffer (3 x 500 μL), denatured and the protein analyzed by 12% SDS-PAGE followed by western blot onto PVDF membrane which was probed with anti-AcK (1:1000, Cell Signaling, #9441S) and visualized by chemiluminescence using HRP conjugated secondary antibodies and film.

Androgen Receptor Acetylation by AcYZ01 (control) vs AcYZ03 in HEK293T cells (IP:AR followed by IB: Anti-AcK):

HEK293T (1,000,000 cells/well) cells were seeded individually into 100 mm dish. Standard calcium phosphate transfection of 20 ug pSG5-hAR DNA were performed when the cells reached 20% confluent. The cells were grown over night before the media was changed to phenol red-free DMEM containing 5μM SAHA and either 20μM AcYZ01 or AcYZ03 (or vehicle DMSO) for three hours. The cells were then washed with ice cold DPBS and lysed with RIPA buffer (pH 7.4 PBS with 0.1% SDS, 1% sodium deoxycholate and 1.5M NaCl, 1 ml). To 500 μL of lysate was added 5μL anti-AR (N20, Santa Cruz) and the solution rocked at 4oC for 12 hours. Protein A beads (20 μL, GenScript, L00273) was added and the solution was rocked for an additional 3.5 hrs. The beads were washed with PBS buffer (3 x 500 ul), denatured and the protein analyzed by 12% SDS-PAGE followed by western blotting onto PVDF membrane which was probed with anti-AcK (1:1000, Cell Signaling) and visualized by chemiluminescence using HRP conjugated secondary antibodies and film.

Androgen Receptor Acetylation Selectivity Assay; AR vs HSP70 by AcYZ03 and AcYZ06 (IP:anti-AcK followed by IB: AR or HSP70):

HEK293T (1,000,000 cells/well) cells were seeded individually into 100 mm dish. Standard calcium phosphate transfection of 20 ug hAR DNA were performed HEK293T cells when the cells were 20% confluent. The HEK293T cells were grown over night before the media was changed to phenol red-free DMEM containing 5μM SAHA, and either 20μM AcYZ03 or AcYZ06 (or DMSO as vehicle control) for three

hours. The cells were then washed with ice cold DPBS and lysed with RIPA buffer (pH 7.4 PBS with 0.1% SDS, 1% Sodium Deoxycholate and 1.5M NaCl, 1 ml). To 500 µL of lysate was added 5µL anti-AcK and the solution rocked at 4oC for 12 hours. Protein A beads (20 µL, GenScript, L00273) was added and the mixture was rocked for an additional 3.5 hrs. The beads were washed with PBS buffer (3 x 500 ul), denatured and the protein analyzed by 12% SDS-PAGE followed by western blotting onto PVDF membrane. The blot was cut along the 90kD mark of the protein ladder and the top portion (>90kD) probed with anti-AR and the bottom portion (<90 kD) probed with anti-HSP70. Both were visualized together by chemiluminescence using HRP conjugated secondary antibodies and film.

MS/MS analysis of acetylation site of AR(LBD):

The protocol was adapted from the published article (*Journal of Biological Chemistry 275, 26164–26171)*, and summarized as following: The codon-optimized sequence for the Androgen receptor Ligand-binding Domain (AR-LBD; residues 670-919) was subcloned into pET-41a vector with N-terminal GST fusion tag. AR(LBD) was expressed in BL21DE3 cells, supplemented with 10 µM DHT and purified by GST column. Protein quantification was performed by Bradford assay. Approximately 10 µM AR(LBD) was incubated with 50 µM AcYZ03 in PBS buffer (pH 7.4) for one hour at 30°C. Acetylated AR(LBD) was resolved by SDS-PAGE gel, which was stained by coommasie blue. The band corresponding to GST-AR(LBD) (~57 kDa) was excised, dehydrated and digested with trypsin. The digest product was acidified by formic acid and prepped by C18 ZipTip microcolumn with elution by 60% acetonitrile. Alternatively acidified digest was prepped by SCX (strong cation

exchange) microcolumn using NH4OH elution. Time program on the Orbitrap was from 5% to 95% ACN in 1 h, with C-18 Acclaim PepMap Column and flow rate set to be 300 nL/min. Raw data was obtained, and analyzed by Proteome Discoverer™ Software (Thermo Scientific, V1.4). AR(LBD) sequence along with the cRAP protein (The Common Repository of Adventitious Proteins) sequence data as a source of possible sources of contamination was indexed into the Proteome Discover™ and was used to identify the possible peptide hits from the MS/MS data. The tolerance was set to be 10 ppm for the precursor mass and for the fragment mass tolerance was set to be 0.02 Da.

Molecular Dynamics Simulations:

Simulation System Setup: The protein structure was obtained from the crystal structure of flufenamic acid bound AR(LBD) (PDBID: 2PIX). Tolfenamic acid was removed for docking of AcYZ03 by Autodock vina[1] with protonation states assigned using the H++ server[2].

Force field parameters for YZ03 were calculated as follows; RESP charges were calculated with Gaussian09 using DFT/6-31G(d) as the basis set. Then, topology parameters were generated with the general Amber force filed (GAFF) by ANTECHAMBER[3]. Protein topology parameters were generated using Amber 14SB force field[3]. The protein-ligand system was then solvated with the TIP3PBOX water model in a cubic periodic unit cell. Each side of the unit cell is at least 10 Å from the nearest solute atom. The system the was neutralized by adding sodium cations. The Amber14 package was used to perform all MD simulations. The system was first minimized by 50000 steps of steepest descent minimization followed by another

50000 steps conjugated gradient minimization. The system was then heated from 0K to 300K over 500 ps with NVT ensemble, with a 10 Kcal•mol-1•Å-2 restraint on the protein-ligand complex. Then 5ns equilibrium MD was performed with the unconstrained NPT ensemble. SHAKE algorithm was employed to constrain bonds containing hydrogen atoms, 2fs step was used for all MD simulations. The Particle Mesh Ewald method was used to calculate electrostatic interactions with a nonbonded cutoff distance of 10 Å.

Steered Molecular Dynamics (SMD): To determine which lysines might be acetylated by YZ03 from its bound state, the closet possible distances between the side-chain nitrogen of each lysine and the carbonyl carbon of the thioester of AcYZ03 were calculated by SMD using a small pulling constant. The equilibrated complex was used as a starting point for each SMD. For each simulation, a 0.5 Kcal•mol-1•Å-2 constant pulling force between the carbonyl carbon of the YZ03 thioester and the epsilon nitrogen of lysine was used to pull the YZ03 side chain thioester to each surface lysine within 36Å (linear distance) from the tolfenamic acid carbonyl. To avoid drifting of the protein or pulling YZ03 from the binding site, a 5 Kcal•mol-1•Å-2 force was used to constraint the lysine backbone and YZ03's tolfenamic acid core.

For each lysine, 500ps SMD was performed at 300K. All trajectories were visually inspected to confirm their unimpeded access to the target lysine, or to the closest distance thereof. Trajectories of the last 100 ps were used to calculate average distances.

Inhibition of Coactivator Association by YZ03 by TR-FRET:

TR-FRET Androgen Receptor Coactivator Assay, Lanthascreen (FisherScientific, A15878) was performed following manufacturer's protocol. The AR(LBD) was incubated with 5nM DHT plus indicated amounts of test compounds or controls for 3 h at 30°C. After incubation, fluorescein labeled coactivator peptide was added and the fluorescence signal was measure using 520 nm and 485 nm filters using 100 microsecond delay, and the signal determined ratiometrically. Evaluation of coactivator association in the absence and presence of 5 nM DHT was used to determine the DHT-inducible response.

Assessment of Binding Constant of FLYZ03:

A TR-FRET Androgen Receptor Coactivator Assay based on the commercial Lanthascreen (FisherScientific, A15878) coactivator binding assay was developed to assess the direct binding of the YZ03 derivative FLYZ03. AR(LBD) was incubated with 10nM DHT, anti-GST-terbium antibody and increasing concentrations of FLYZ03. Fluorescence signal was measured using 520 nm and 485 nm emission filters using a 100 microsecond delay, and the signal determined ratiometrically. The signal from nonspecific controls was determined from incubation of DHT and anti-GST-terbium antibody (i.e. no GST-AR) at the same concentration of FLYZ03. The specific binding signal was obtained by subtracting the signal obtained from nonspecific controls. The signal was plot against FLYZ03 concentration using Prism software, with nonlinear regression fit to a sigmoidal dose-response equation. From

the plot which did not fully saturate due to solubility limitations, the Kd of FLYZ03 was estimated to be to be 59 μM.

To confirm the validity of this approximate Kd, a competitive binding assay was performed with AcYZ03. For the competition assay, FLYZ03 was kept at a constant 50μM concentration and titrated against increasing concentrations of AcYZ03. The signal was measured using the same method described above. Based on the estimated Kd of FLYZ03 calculated above (59 μM), and the observed EC50 of AcYZ03, the calculated Ki of AcYZ03 was 60 μM which is consistent with the Kd of FLYZ03 as the probe and competitor share the same binding core.

Synthesis of YZ01

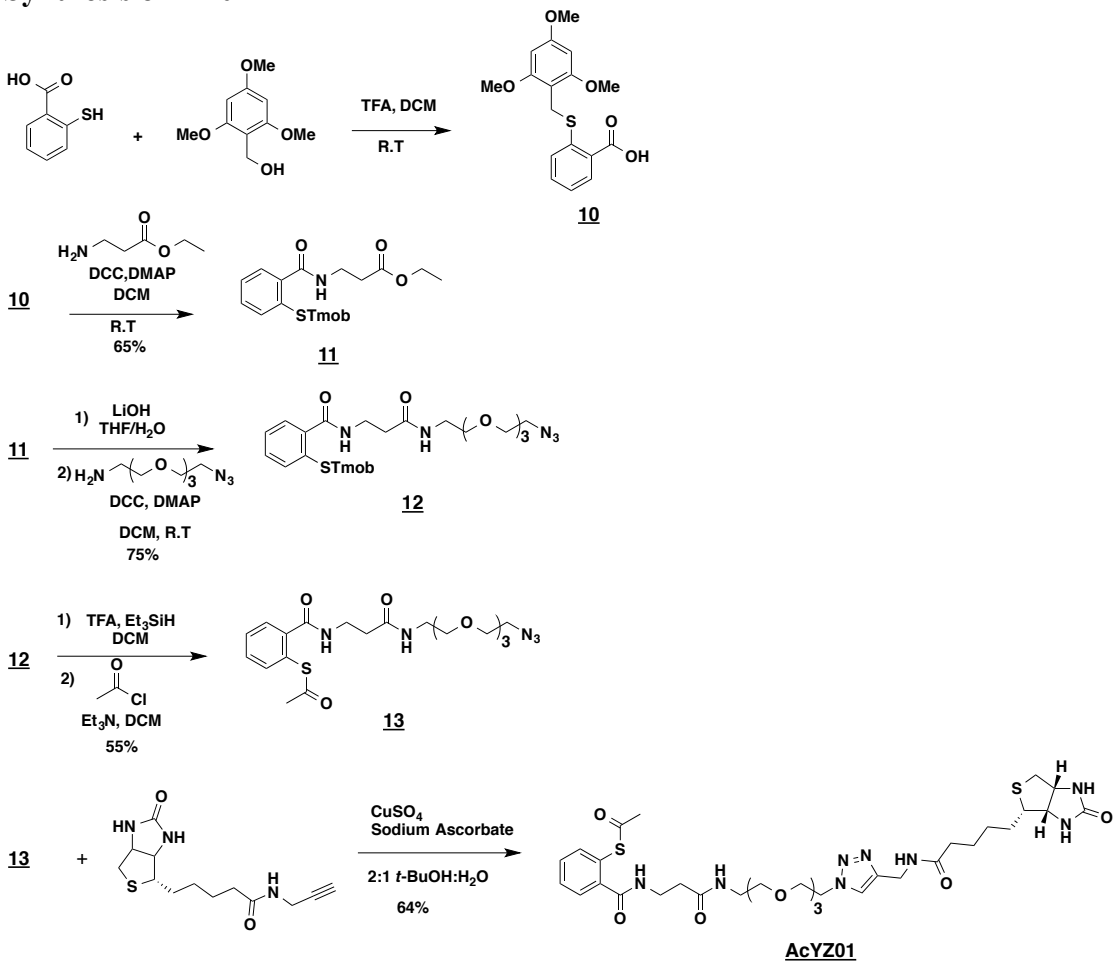

Ethyl 3-(2-((2,4,6-trimethoxylbenzyl)thiol)benzamido)propanoate, 11: To a solution of 2-mercaptobenzoic acid (1 g 6.49 mmol) and (2,4,6-trimethoxyphenyl)methanol (1.29 g, 6.49 mmol) in distilled DCM (65 ml) was added trifluoroacetic acid (0.626 ml, 8.43 mmol). After 30 min at RT the solution was washed with sat. $NaHCO_3$ (3 x 20 ml). The combined aqueous washings were back extracted with DCM (3 x 10 ml). The combined organic extracts were dried over Na_2SO_4 followed by concentration in vacuo to afford a light yellow solid. The metastable product 10 was applied to next step without further purification. ^{1}H NMR

(400 MHz, $CDCl_3$) δ 8.27 (dd, J = 7.9, 1.6 Hz, 1H), 7.59 (dd, J = 7.8, 1.3 Hz, 1H), 7.48 (td, J = 7.6, 1.6 Hz, 1H), 7.37 (td, J = 7.6, 1.3 Hz, 1H), 6.06 (s, 2H), 4.20 (s, 2H), 3.82 (s, 3H), 3.71 (s, 6H). To a solution of 10 (800 mg, 2.39mmol) in 24 ml distilled DCM was added DCC (822.64 mg, 3.99 mmol). The solution was stirred for 15 min before ethyl-3-aminopropanoate (311.2 mg, 2.66 mmol) and DMAP was added. The reaction was stirred under N_2 for 16 h. The solution was washed with H_2O (3 x 10 ml), dried over Na_2SO_4 then concentration in vacuo. The residue was purified by flash column chromatography (EtOAc: Hexane = 3:7, Rf = 0.45) to give 11 as white solid. ^1H NMR (400 MHz, $CDCl_3$) δ 7.75 (dd, J = 7.4, 1.7 Hz, 1H), 7.62 (bs. 1H), 7.42 (dd, J = 7.3, 1.7 Hz, 1H), 7.30 -7.23 (m, 2H), 6.06 (s, 2H), 4.18- 4.11 (m, 4H), 3.81 (s, 3H), 3.73- 3.65 (m, 8H), 2.66 (t, J = 6.4 Hz, 2H), 1.25 (t, J = 7.1 Hz, 3H). ^{13}C NMR (101 MHz, CDCl3) δ 172.36 , 167.92 , 160.73 , 158.84 , 137.09 , 134.35 , 133.60, 130.19, 129.44, 126.69 , 105.80 , 90.28 , 60.74 , 55.64 , 55.07 , 35.51 , 34.19, 28.77 , 14.22 . HR-ESI MS m/e calcd for [$C_{22}H_{27}NO_6S$] 434.1637, found 434.1648.

N-(1-azido-13-oxo-3,6,9,trioxa-12-azapentadecan-15-yl)-2-(2,4,6-trimethoxylbenzyl)thio)benzamide, 12 : To a solution of 11 (267.3 mg 0.62 mmol) in 3 ml distilled THF was added 1.23 ml 1M LiOH solution. The reaction was stirred at RT for 90 min before 2 ml of 1M HCl was added followed by 5 ml Sat. NaCl. The mixture was extracted with DCM (5 x 15 ml). The combined organic extracts were dried over Na_2SO_4 then concentration in vacuo to afford crude acid intermediate, which was applied to next step without further purification.

To a solution of acid intermediate (250 mg, 0.62mmol) in 6 ml distilled DCM was added DCC (190.8 mg 0.92 mmol). After 15 mins, 11-azido-3,6,9-trioxaundecan-1-

amine (116.2 ul, 0.95 mmol) and DMAP were added sequentially. The solution was stirred under N_2 for 16 hrs and then was washed with H_2O (3 x 5 ml). The aqueous washings were back extracted with DCM (3 x 15 ml). The combined organic extracts were combined and dried over Na_2SO_4 and concentration in vacuo. The residue was purified by flash column chromatography (MeOH: DCM = 3 : 97 Rf = 0.3) to give 12 as oil. ^{1}H NMR (400 MHz, $CDCl_3$) δ 7.68 (dd, J = 7.6, 1.6 Hz, 1H), 7.54 (bt, J = 5.9 Hz, 1H), 7.47-7.31 (dd, J = 7.6, 1.6 Hz, 1H), 7.31-7.21 (m, 2H), 6.39 (bs, 1H), 6.07 (s, 2H), 4.13 (s, 2H), 3.81 (s, 3H), 3.74-3.62 (m, 12H), 3.64-3.58 (m, 2H), 3.61-3.54 (m, 2H), 3.51 (m, 2H), 3.41 (m, 4H), 2.53 (t, J = 6.3 Hz, 2H), 1.82 (bs, 2H). ^{13}C NMR (101 MHz, $CDCl_3$) δ 171.38, 168.25 , 160.72 , 158.98 , 137.14 , 134.85 , 133.16 , 130.11 , 128.95 , 126.61 , 105.71 , 90.34 , 70.68 , 70.59 , 70.56 , 70.22 , 70.05 , 69.69 , 55.66 , 55.38 , 50.67 , 39.19 , 36.33 , 36.00 , 28.53. HR-ESI MS m/e calcd for [C28H39N5O8S] 606.2598, found 606.2607

S-(2-((1-azido-13-oxo-3,6,9-trioxa-12-azapentadecan-15-yl)carbamoyl)phenyl) ethanethioate, 13: To a solution of 12 (117.4 mg 0.194 mmol) in 2 ml distilled DCM was added 245 µl TFA and 144ul triethylsilane. After 1 h at RT, 5 ml H_2O was added to the solution. The mixture partitioned and the aqueous layer extracted with DCM (5 x 20 ml). The combined organic extracts were dried over Na_2SO_4 and concentration in vacuo to afford crude intermediates. The residue was applied to next step without further purification.

To the residue in 2 ml distilled DCM was added sequentially acetyl chloride (16 ul, 0.233 mmol) and triethylamine (54.5 ul 0.388 mmol). The reaction was stirred at RT under N2 for 16 h and then was washed with 5 ml H_2O and dried over Na_2SO_4 and

concentration in vacuo. The residue was purified by flash column chromatography (MeOH: DCM = 1: 33, Rf = 0.25) to give 13 as light yellowish oil. ^{1}H NMR (400 MHz, $CDCl_3$) δ 7.60 (dd, J = 5.8, 3.0 Hz, 1H), 7.55-7.41 (m, 3H), 6.88 (bs, 1H), 6.34 (bs, 1H) 3.75-3.60 (m, 12H), 3.60-3.53 (m, 2H), 3.48 (q, J = 5.1 Hz, 2H), 3.43-3.35 (m, 2H), 2.52 (t, J = 7.1 HZ, 2H), 2.46 (s, 3H). ^{13}C NMR (101 MHz, $CDCl_3$) δ 194.65, 171.40, 168.21, 140.84, 136.52, 130.43, 129.96, 128.44, 125.39, 70.69, 70.64, 70.54, 70.21, 70.06, 69.64, 50.67, 39.28, 35.83, 35.39 , 30.36 . HR-ESI MS m/e calcd for [$C_{20}H_{29}N_5O_6S$] 468.1917, found 468.1927.

S-(2-((13-oxo-1-(4-((5-(2-oxohexahydro-1H-thieno[3,4-d]imidazol-4-yl)pentanamido)methyl)-1H-1,2,3-triazol-1-yl)-3,6,9-trioxa-12-azapentadecan-15-yl)carbamoyl)phenyl) ethanethioate, AcYZ01: To a solution of 13 (63 mg 0.135 mmol) and biotin propargylamide (39.93 mg 0.142mmol) in dry DMF was added 14.2 µL 1M $CuSO_4$, 14.2 µL 1M ascorbic acid and TBTA (7.53 mg 0.0142mmol). The solution was stirred at RT under N_2 for 16 h, followed by removal of DMF by rotary evaporation. The residue was purified by flash column chromatography on SiO_2 (MeOH: DCM = 1: 6 Rf = 0.3) to give AcYZ01 as a yellowish oil. A solution of AcYZ01 in degassed MeOH was purged in NH_3 for 20 min to give the free thiol YZ01 quantitatively. The solution was concentrated in vacuo, and used as a stock solution in DMSO. ^{1}H NMR (400 MHz, $CDCl_3$) δ 7.86 (bs, 2H), 7.62-7.48 (m, 4H), 7.07 (bs, 1H), 7.01 (s, 1H), 6.36 (s, 1H), 4.55 (m, 4H), 4.38 (m, 2H), 3.92 (t, J = 7.0 Hz, 2H), 3.87 (t, J = 4.9 Hz, 2H), 3.64-3.56 (m, 4H), 3.53 (t, J = 5.1 Hz, 2H), 3.47-3.34 (m, 2H), 3.20-3.09 (m, 1H), 2.94 (dd, J = 12.8, 4.9 Hz, 1H), 2.79 (d, J = 12.8 Hz, 1H), 2.54 (t, J = 7.0 Hz, 2H), 2.42 (s, 3H), 2.29 (s, 2H), 2.22 (m, 3H), 1.79-1.61 (m, 8H). ^{13}C NMR (101

MHz, $CDCl_3$) δ 192.87, 173.34 , 171.86 , 170.61 , 164.44 , 145.15 , 140.69 , 136.83 , 131.20 , 130.02 , 128.23 , 125.26 , 123.77 , 70.37 , 70.06 , 69.92 , 69.19 , 61.55 , 60.27 , 55.56 , 50.12 , 42.53 , 40.75 , 39.48 , 35.65 , 34.82 , 34.38 , 30.38 , 29.66 , 27.83 , 26.39 , 25.28. HR-ESI MS m/e calcd for [$C_{33}H_{48}N_8O_8S_2$] 747.2958, found 747.2964

Synthesis of YZ02

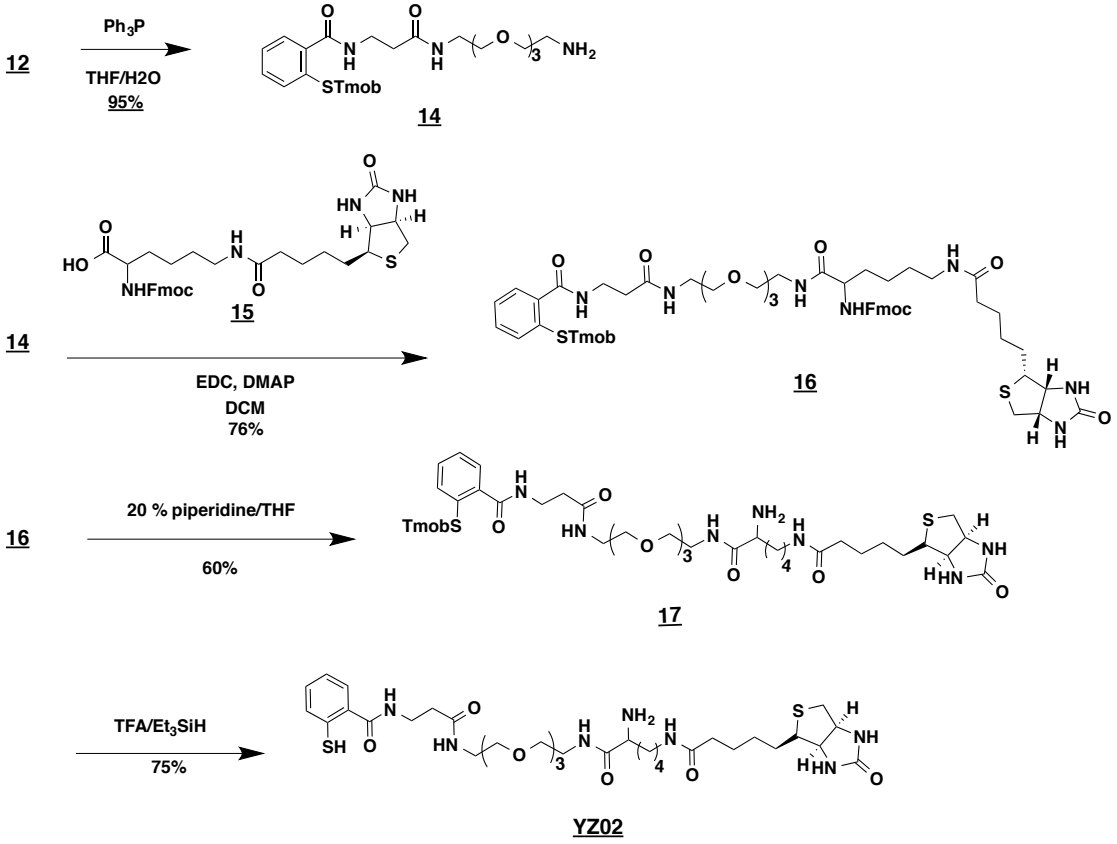

N-(1-amino-13-oxo-3,6,9-trioxa-12-azapentadecan-15-yl)-2-((2,4,6-trimethoxybenzyl)thio)benzamide, 14: To a solution of 12 (203 mg 0.335 mmol) in 3.4 ml distilled THF is added Ph_3P (169.2 mg 0.67 mmol) and 0.13 ml H_2O. The solution was reflux for 2 h then was partitioned between 1M HCl and ethyl ether. The organic layer was extracted with 1M HCl (2 x 10 ml). The combined aqueous extracts were made basic with NaOH to pH > 10, and back extracted with DCM (5 x 15 ml). The organic extracts were combined, dried over Na_2SO_4, and concentration in vacuo. The residue was purified by flash column chromatography (NH_3 Sat. MeOH: DCM = 1:12 Rf = 0.3) to give pure 14 as light yellow oil. ^1H NMR (400 MHz, $CDCl_3$) δ 7.67 (dd, J = 7.6, 1.6 Hz, 1H), 7.56 (bs, 1H), 7.43 (dd, J = 7.7, 1.1 Hz, 1H), 7.35 (bs, 1H),

7.31-7.21 (m, 2H), 6.07 (s, 2H), 4.13 (s, 2H), 3.81 (s, 3H), 3.75-3.65 (m, 8H), 3.62-3.53 (m, 8H), 3.52-3.48 (m, 4H), 3.45-3.39 (m, 2H), 2.85 (t, J = 5.0 Hz, 2H), 2.54 (t, J = 6.4 Hz, 2H), 2.1-1.7 (bs, 2H). ^{13}C NMR (101 MHz, $CDCl_3$) δ 171.56, 168.28, 160.73 , 158.98 , 137.26 , 134.97 , 133.07 , 130.08 , 128.89 , 126.55 , 105.74 , 90.34 , 73.19 , 70.51 , 70.50 , 70.18 , 70.06 , 69.94 , 55.66 , 55.37 , 41.56 , 39.17 , 36.39 , 35.79 , 28.40. HR-ESI MS m/e calcd for [$C_{28}H_{41}N_3O_8S$] 580.2693, found 580.2690.

(9H-fluoren-9-yl)methyl (1,5,19,26-tetraoxo-30-(2-oxohexahydro-1H-thieno[3,4-d]imidazol-4-yl)-1-(2-((2,4,6-trimethoxybenzyl)thio)phenyl)-9,12,15-trioxa-2,6,18,25-tetraazatriacontan-20-yl)carbamate, 16: To a solution of 14 (80.7 mg 0.1357 mmol) in 1.5 ml distilled DCM was added 1-[3-(Dimethylamino)propyl]-3-ethylcarbodiimide hydrochloride (EDC) (39 mg 0.204 mmol). The solution was stirred for 15 min before 15 (70.78 mg 0.1221 mmol) (JACS, 2004, 126 (44), pp 14435–14446) and DMAP (4.98 mg 0.041 mmol) were added sequentially. The reaction was stirred under N_2 for 16 h and then was washed with H_2O (3 x 5ml). The combined aqueous washings were back extracted with DCM (3 x 15 ml). The combined organic extracts were combined and dried over Na_2SO_4 and concentration in vacuo. The residue was purified by flash column chromatography (NH_3 Sat. MeOH: DCM = 1:9 Rf = 0.3) to give pure 16 as yellowish oil. ^{1}H NMR (400 MHz, $CDCl_3$) δ 7.87 (s, 1H), 7.77 (d, J = 7.5 Hz, 2H), 7.65-7.53 (m, 4H), 7.45-7.25 (m, 5H), 7.19 (t, J = 7.5 Hz, 1H), 6.85 (bs, 1H), 6.16 (bs, 1H), 6.05 (s, 2H), 6.04 (d, J = 8.6 HZ, 1H) 5.76 (s, 1H), 4.49-4.41 (bs, 1H), 4.32 (d, J = 7.2 Hz, 2H), 4.13 (s, 2H), 3.80 (s, 3H), 3.75-3.39 (m, 24H), 3.16-2.98 (m, 2H), 2.71 (d, J = 12.8 Hz, 1H), 2.56 (t, J = 6.1 Hz, 2H), 2.09-2.02 (m, 3H), 1.82-1.57 (m, 8H), 1.55-1.35 (m, 4H), 0.98-0.73 (m, 6H). ^{13}C NMR (101 MHz,

$CDCl_3$) δ 173.30, 172.46 , 171.88 , 168.83 , 163.91 , 160.79 , 158.99 , 156.34 , 143.92 , 143.73 , 141.25 , 141.22 , 136.58 , 135.69 , 131.84 , 130.24 , 128.48 , 127.75 , 127.14 , 126.12 , 125.22 , 120.00 , 105.39 , 90.37 , 70.30 , 70.27 , 69.89 , 69.76 , 69.69 , 67.04 , 61.88 , 60.21 , 55.95 , 55.70 , 55.39 , 54.65 , 47.07 , 39.23 , 39.15 , 39.03 , 36.67 , 35.69 , 35.04 , 32.88 , 31.94 , 29.75 , 27.94 , 27.53 , 25.14 , 23.07 , 22.71 . HR-ESI MS m/e calcd for [$C_{59}H_{77}N_7O_{13}S_2$] 1156.4735, found 1156.4723.

N-(18-amino-3,17,24-trioxo-28-(2-oxohexahydro-1H-thieno[3,4-d]imidazol-4-yl)-7,10,13-trioxa-4,16,23-triazaoctacosyl)-2-mercaptobenzamide, YZ02: A solution of 16 (30.9 mg 0.027mmol) in 20% piperidine/ THF was stirred for 60 min at RT followed by removal of solvent by rotary evaporation to afford crude 17; HR-ESI MS m/z calcd for [$C_{44}H_{67}N_7O_{11}S_2$] 934.4418, found 934.4414,The residue was applied to next step without further purification.

To a solution of 17 (15.1 mg 0.0162 mmol) in distilled 0.2 ml DCM was added TFA (20.42 μL 0.275 mmol) and Triethylsilane (12 μL 0.05 mmol). The solution was stirred under N2 for 60 mins, followed by removal of solvent by rotary evaporation. The residue was purified by flash column chromatography on C-18 reverse phase column (MeOH: H_2O (w/ 3% TFA) = 3: 2) to give pure YZ02 as the free thiol. ^1H NMR (400 MHz, MeOD) δ 7.64 (d, J = 7.8 Hz, 1H), 7.48 (d, J = 7.6 Hz, 1H), 7.41-7.25 (t, J = 13.6 HZ, 1H), 7.25-7.11 (t, J = 13.6 HZ, 1H), 4.49-4.36 (m, 1H), 4.25-4.13 (m, 1H), 3.75 (t, J = 6.5 Hz, 2H), 3.65-3.51 (m, 14H), 3.47-3.18 (m, 5H), 3.16-3.00 (m, 3H), 2.82 (dd, J = 12.6, 5.0 Hz, 1H), 2.60 (d, J = 12.8 Hz, 1H), 2.48 (t, J = 6.3 Hz, 2H), 2.09 (t, J = 6.8 Hz, 2H), 1.85-1.10 (m, 13H). ^{13}C NMR (101 MHz, MeOD) δ 174.81, 172.47 , 169.12 , 168.85 , 164.80 , 136.55 , 134.16 , 130.99 , 127.69 , 126.53 , 126.17 ,

70.19 , 70.12 , 69.80 , 69.77 , 69.11 , 68.88 , 62.07 , 60.26 , 55.65 , 53.00 , 39.69 , 39.14 , 39.00 , 38.46 , 36.30 , 35.39 , 35.25 , 30.87 , 28.70 , 28.39 , 28.11 , 25.48 , 21.80. HR-ESI MS m/e calcd for 1156.4735, found 1156.4723. HR-ESI MS m/e calcd for [$C_{34}H_{55}N_7O_8S_2$] 753.3520, found 753.3535.

Synthesis of YZ03

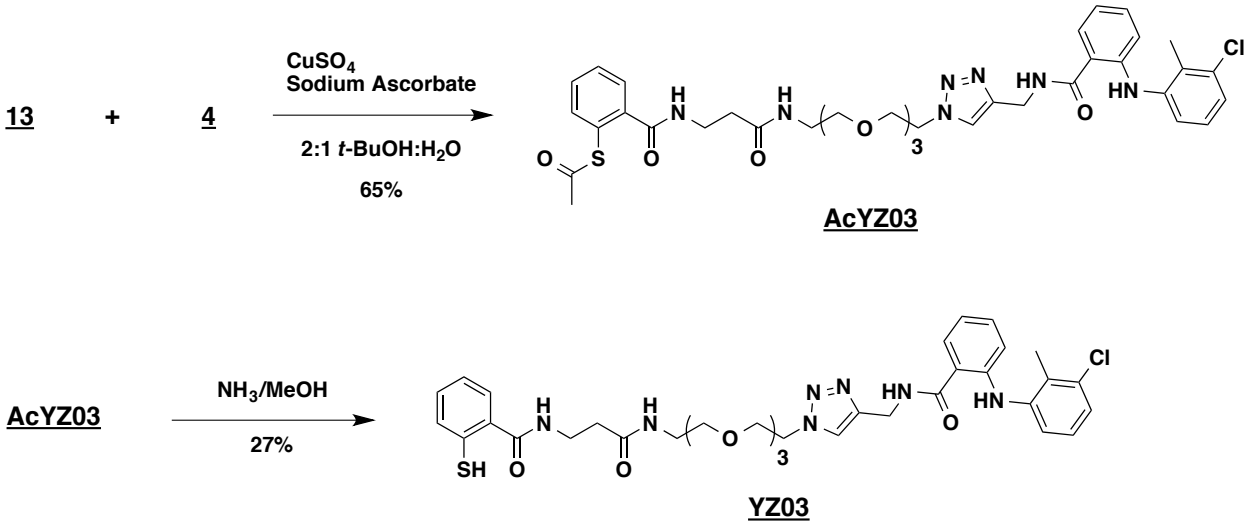

S-(2-((1-(4-((3-((3-chloro-2-methylphenyl)amino)benzamido)methyl)-1H-1,2,3-triazol-1-yl)-13-oxo-3,6,9-trioxa-12-azapentadecan-15-yl)carbamoyl)phenyl) ethanethioate AcZ03: To a solution of 13 (40 mg 0.085 mmol) and 4 (25.53 mg 90μmol) in dry DMF was added 9 ul 1M CuSO4, 9 ul 1M ascorbic acid and TBTA (4.78 mg 9μmol). The solution was stirred at room temperature under N_2 for 16 hr, followed by removal of DMF by rotary evaporation. The residue was purified by flash column chromatography (MeOH: DCM = 1 : 19) to give AcYZ03 as a yellowish oil. A solution of AcYZ03 in degassed MeOH was purged in NH3 for 20 min to give

YZ03 as the free thiol. The solution was concentrated in vacuo, redissolved in DMSO to use without further purification. ^{1}H NMR (400 MHz, $CDCl_3$) δ 9.40 (s, 1H), 7.79-7.75 (m, 1H), 7.62-7.54 (m, 1H), 7.51 (d, J = 7.9 Hz, 1H), 7.48-7.41 (m, 2H), 7.37 (bs, 1H), 7.24 (d, J = 7.7 Hz, 2H), 7.17-7.06 (m, 2H), 7.02-6.95 (m, 2H), 6.89 (bs, 1H), 6.77- 6.69 (m, 1H), 4.75-4.69 (m, 1H), 4.66 (d, J = 5.6 Hz, 2H), 4.59-4.51 (m, 2H), 3.95-3.85 (m, 2H), 3.71 -3.39 (m, 15H), 2.53 (t, J = 12 HZ, 1H), 2.44 (s, 2H), 2.37 (s, 3H), 1.98 (s, 1H). ^{13}C NMR (101 MHz, $CDCl_3$) δ 194.81, 171.59, 169.55, 168.35 , 146.20 , 144.48 , 141.29 , 140.90 , 136.54 , 135.47 , 132.47 , 130.43 , 129.96 , 129.73, 128.44 , 127.97 , 126.77 , 125.32 , 124.28 , 123.51 , 120.37 , 117.79 , 117.02 , 115.17 , 70.56 , 70.48 , 70.44 ,70.05, 69.76 , 69.40 , 50.36 , 39.18 , 36.31 , 35.47 , 35.17 , 30.37 , 14.94 . HR-ESI MS m/e calcd for [$C_{37}H_{44}ClN_7O_7S$] 766.2790, found 766. 2800.HPLC trace of AcYZ03 was reported with >95% purity.

Synthesis of YZ06

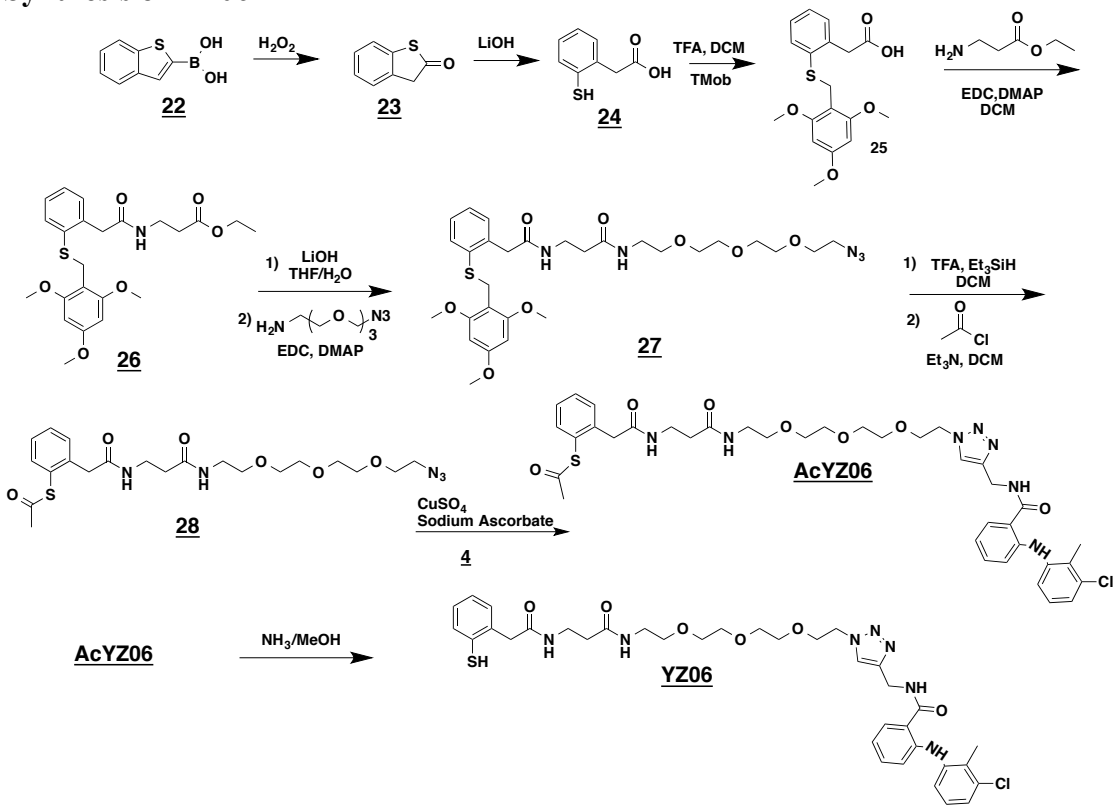

ethyl 3-(2-(2-((2,4,6-trimethoxybenzyl)thio)phenyl)acetamido)propanoate, 26:

Compound 26 was made from 2-(2-mercaptophenyl)acetic acid, 24 following the reported method of Chen et al. and the crude reaction product was used directly in the next reaction to avoid oxidation (Bioconjugate Chemistry, 2010 , vol. 21, # 5 p. 979 - 987): To a solution of 24 (157 mg, 0.935 mmol) and (2,4,6-trimethoxyphenyl)methanol (185.2 mg, 0.935 mmol) in 10 mL dried DCM was added drop wise TFA (90 μL, 1.22 mmol). The reaction was stirred under N_2 at room temperature for 30 mins, solvent and TFA was reduced in vacuo. The crude product, 25 was applied to the next reaction without further purification.

To a solution of 25 (180 mg, 1.07 mmol) in 10 mL dry DCM was added 1-[3-(Dimethylamino)propyl]-3-ethylcarbodiimide hydrochloride (EDC) (307.7 mg, 1.605

mmol). The reaction was stirred for 15 mins under N_2 before ethyl 3-aminopropanoate (164.2mg, 1.07mmol) was added followed by the addition of DMAP (261.3mg, 2.14 mmol). The reaction was stirred under N_2 for 16 h before 1 ml 1N HCl was added and aqueous layer was extracted with DCM (2 X 10 mL). The combined organic extracts were combined, dried over Na_2SO_4 and reduced in vacuo. The product was purified by flash chromatography (20% EtOAc/DCM) to give 26 as an oil. ^{1}H NMR (400 MHz, $CDCl_3$) δ 7.50 – 7.48 (m, 1H), 7.30 – 7.27 (m, 1H), 7.23 – 7.20 (m, 2H), 6.09 (s, 2H), 4.10 (s, 2H), 4.06 (q, J = 7.1 Hz, 2H), 3.82 (s, 3H), 3.72 (s, 6H), 3.44 (q, J = 6.2 Hz, 2H), 2.48 (t, J = 6.3 Hz, 2H), 1.698 (s, 2H), 1.20 (t, J = 7.1 Hz, 3H). ^{13}C NMR (101 MHz, $CDCl_3$) δ 172.13, 171.03, 160.67, 159.02, 136.81, 136.62, 133.17, 130.32, 127.68, 127.26, 105.96, 90.39, 60.59, 55.67, 55.36, 42.04, 35.07, 34.08, 28.22, 14.14. HR-ESI MS m/e calcd for [$C_{23}H_{29}NO_6S$] 447.1716, found 447.1718.

N-(2-(2-(2-(2-azidoethoxy)ethoxy)ethoxy)ethyl)-3-(2-(2-((2,4,6-trimethoxybenzyl)thio)phenyl)acetamido)propanamide, 27: To a solution of 26 (54.35 mg, 0.1216 mmol) in 1 mL THF was added 1N LiOH (0.2432 mL). The reaction was stirred for 4 hours before 1 mL 1M HCl was added. The THF was removed in vacuo, and the aqueous layer was extracted exhaustively with DCM. The organic layers were combined, dried over Na_2SO_4 and reduced in vacuo. To a solution of the crude acid product (51 mg, 0.1216 mmol) in 3 mL dried DCM was added 1-[3-(Dimethylamino)propyl]-3-ethylcarbodiimide hydrochloride (EDC) (47 mg, 0.2432 mmol). The reaction was stirred for 15 mins under N_2 before ethyl 11-azido-3,6,9-trioxaundecan-1-amine (48μL, 0.2432mmol) was added followed by the addition of DMAP (261.3mg, 2.14 mmol). The reaction was stirred under N_2 for 16 hours before

1ml 1N HCl was added and aqueous layer was extracted with DCM (2 X 10mL). The organic layers were combined, dried over Na2SO4 and reduced in vacuo. The product was purified by flash chromatography (5% MeOH/DCM) to give 27 as an oil. ^{1}H NMR (400 MHz, $CDCl_3$) δ 7.50 – 7.43 (m, 1H), 7.28 – 7.26 (m, 1H), 7.25 —7.17 (m, 2H), 6.24 — 6.17 (m, 2H), 6.10 (s, 2H), 4.10 (s, 2H), 3.83 (s, 3H), 3.73 (s, 6H), 3.71 (s, 2H), 3.70 — 3.64 (m, 8H), 3.63 — 3.59 (m, 2H), 3.51 (t, J = 5.2Hz, 2H), 3.47 (q, J = 6.2Hz, 2H), 3.4 (t, J = 5.0 Hz, 2H), 3.37 (q, J = 5.3 Hz, 2H), 2.36 (t, J = 6.3 Hz, 2H). ^{13}C NMR (101 MHz, $CDCl_3$) δ 171.47, 171.38 , 160.73 , 159.05 , 136.93 , 136.35 , 132.89 , 130.34 , 127.70 , 127.71 , 105.98 , 90.50 , 70.70 , 70.64 , 70.59 , 70.05 , 69.54 , 55.71 , 55.37 , 50.69 , 41.91 , 39.29 , 35.97 , 35.90 , 28.14. HR-ESI MS m/e calcd for [$C_{29}H_{41}N_5O_8S$] 619.2676, found 619.2655.

S-(2-(1-(4-((2-((3-chloro-2-methylphenyl)amino)benzamido)methyl)-1H-1,2,3-triazol-1-yl)-13,17-dioxo-3,6,9-trioxa-12,16-diazaoctadecan-18-yl)phenyl) ethanethioate, AcZ06 was made from S-(2-(1-azido-13,17-dioxo-3,6,9-trioxa-12,16-diazaoctadecan-18-yl)phenyl) ethanethioate, 28: To a solution of 27 (85.3mg, 0.138 mmol) in 2 mL DCM was added TFA (174 µL, 2.34 mmol) and Et_3SiH (70 µL, 0.434 mmol) at 0oC. The reaction was stirred for 30 mins than the solvent was removed in vacuo, and applied to high vacuum for 3 hours to remove the trace amount of the TFA. To the residue in 2 mL dried DCM was added Acetyl chloride (25.6 µL, 29 mmol) and Et_3N(78 µL, 55 mmol) at -78°C. The reaction was slowly warmed up to RT and stirred for 16 hours. The solvent was removed in vacuo and the crude product 28 was applied to next step without purification. HR-ESI MS m/e calcd for [$C_{21}H_{31}N_5O_6S$+Na] 504.1887, found 504.1879.

To a solution of 28 (17 mg, 0.035 mmol) in 1 mL DMF was added 2-((3-chloro-2-methylphenyl)amino)-N-(prop-2-yn-1-yl)benzamide (12.6 mg, 0.042 mmol), 1N $CuSO_4$ (4 μL), 1N ascorbic acid (4μL) and TBTA (2 mg, 0.0035 mmol). The reaction was stirred for 16 hours before the solvent was removed under vacuum. The product was purified by flash column chromatography (5 % MeOH/DCM) to give AcYZ06 as an oil. HR-ESI MS m/e calcd for $C_{38}H_{46}ClN_7O_7S$ 802.2700, found 802.2693. A solution of AcYZ06 in degassed MeOH was purged in NH_3 for 20 min to give YZ06 with free thiol. The solution was concentrated in vacuo, redissolved in DMSO to use without further purification. ^{1}H NMR (400 MHz, $CDCl_3$) δ 9.35 (s, 1H), 7.72 (s, 2H), 7.51 – 7.43 (m, 1H), 7.39 – 7.35 (m, 2H), 7.35 – 7.29 (m, 2H), 7.24 (td, J = 7.3, 2.2 Hz, 1H), 7.19 – 7.12 (m, 2H), 7.04 (dd, J = 8.0, 1.4 Hz, 1H), 7.00 (t, J = 7.8 Hz, 1H), 6.93 – 6.85 (m, 1H), 6.70 – 6.60 (m, 2H), 6.21 (d, J = 6.7 Hz, 1H), 4.61 (d, J = 5.3 Hz, 2H), 4.45 (t, J = 5.0 Hz, 2H), 3.81 (t, J = 5.0 Hz, 2H), 3.56 (s, 2H), 3.54 – 3.33 (m, 13H), 3.29 (q, J = 5.3 Hz, 2H), 2.34 (s, 3H), 2.27 (s, 3H). ^{13}C NMR (101 MHz, $CDCl_3$) δ 194.39, 171.38, 170.42, 169.54, 146.30, 141.35, 138.94, 136.94, 135.49, 133.09, 132.43, 131.31, 131.18, 130.75, 129.85, 128.30, 128.04, 127.94, 126.73, 124.34, 120.55, 117.77, 117.09, 115.17, 70.58, 70.48, 70.47, 70.13, 69.70, 69.37, 50.38, 42.18, 39.15, 36.03, 35.56, 35.19, 30.28, 14.89. HR-ESI MS m/e calcd for [$C_{38}H_{46}ClN_7O_7S$+Na] 802.2700, found 802.2693. HPLC trace of AcYZ06 was reported with >95% purity.

Synthesis of BrYZ03

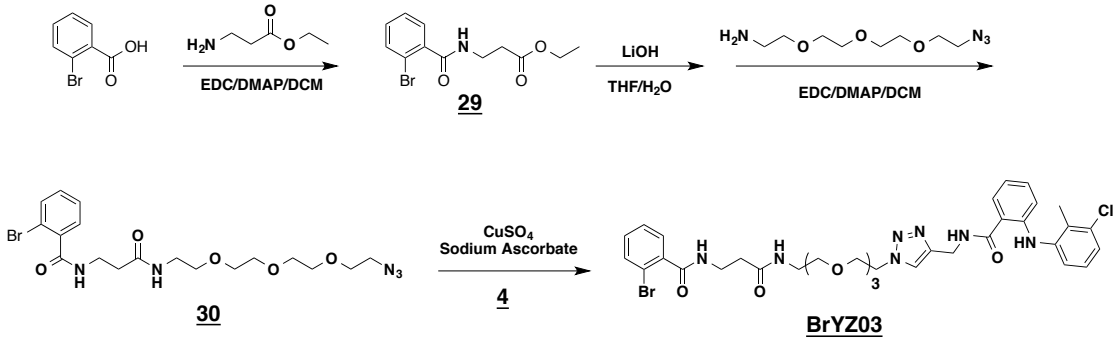

Ethyl 3-(2-bromobenzamido)propanoate, 29: To a solution of 2-Bromobenzioc acid (100mg, 0.497mmol) in 5 mL dried DCM was added 1-[3-(Dimethylamino)propyl]-3-ethylcarbodiimide hydrochloride (EDC) (143mg, 0.746mmol). The reaction was stirred for 15 mins under N_2 before ethyl 3-aminopropanoate (76.3mg, 0.497mmol) was added followed by the addition of DMAP (91mg, 0.7455 mmol). The reaction was stirred under N2 for 16 hours before 1ml 1N HCl was added and aqueous layer was extracted with DCM (2 X 10mL). The organic layers were combined, dried over Na_2SO_4 and reduced in vacuo. The product was purified by flash chromatography (20% EtOAc/DCM) to give 29 as an oil.

^{1}H NMR (400 MHz, $CDCl_3$) δ 7.56 (d, J = 8.0, 1H), 7.48 (d, J = 7.6, 1H), 7.34 (t, J = 7.5, 1H), 7.30 – 7.22 (m, 1H), 6.66 (bs, 1H), 4.15 (q, J = 7.1 Hz, 2H), 3.72 (q, J = 6.0 Hz, 2H), 2.67 (t, J = 5.9 Hz, 2H), 1.27 (t, J = 7.1 Hz, 3H). ^{13}C NMR (101 MHz, $CDCl_3$) δ 172.60, 167.68, 137.76, 133.29, 131.23, 129.34, 127.53, 119.24, 60.87, 35.34, 33.84, 14.23. HR-ESI MS m/e calcd for [$C_{12}H_{14}BrNO_3$] 299.0153, found 299.0157.

N-(1-azido-13-oxo-3,6,9-trioxa-12-azapentadecan-15-yl)-2-bromobenzamide, 30: To a solution of 18 (100mg, 0.334mmol) in 1 mL THF was added 1N LiOH (0.668 mL). The reaction was stirred for 2 hours before 1 mL HCl was added to quench the

reaction. The THF was removed in vacuo, and the aqueous layer was extracted copiously with DCM. The organic layers were combined, dried over Na_2SO_4 and reduced in vacuo. To a solution of the acid product in 3 mL dried DCM was added 1-[3-(Dimethylamino)propyl]-3-ethylcarbodiimide hydrochloride (EDC) (96.8mg, 0.501 mmol). The reaction was stirred for 15 mins under N_2 before ethyl 11-azido-3,6,9-trioxaundecan-1-amine (66μL, 0.334mmol) was added followed by the addition of DMAP (12.2mg, 0.1 mmol). The reaction was stirred under N_2 for 16 hours before 1ml 1N HCl was added and aqueous layer was extracted with DCM (2 x 10mL). The organic layers were combined, dried over Na_2SO_4 and reduced in vacuo. The product was purified by flash chromatography (5% MeOH/DCM) to give 30 as an oil. ^{1}H NMR (400 MHz, $CDCl_3$) δ 7.54 (dd, J = 8.0, 1.3 Hz, 1H), 7.44 (dd, J = 7.6, 1.8 Hz, 1H), 7.35 – 7.26 (m, 1H), 7.23 (td, J = 7.7, 1.8 Hz, 1H), 7.00 (t, J = 5.6 Hz, 1H), 6.59 (t, J = 5.5 Hz, 1H), 3.74 – 3.66 (m, 4H), 3.64 – 3.55 (m, 6H), 3.52 (dd, J = 5.6, 4.5 Hz, 2H), 3.45 – 3.33 (m, 6H), 2.57 – 2.49 (m, 2H). ^{13}C NMR (101 MHz, $CDCl_3$) δ 171.62, 167.90, 138.02, 133.21, 131.07, 129.12, 127.46, 119.33, 72.48, 70.62, 70.49, 70.18, 69.99, 69.60, 61.65, 39.22, 36.03, 35.07. HR-ESI MS m/e calcd for [$C_{18}H_{26}BrN_5O_5$] 471.1182, found 471.1196.

2-bromo-N-(1-(4-((2-((3-chloro-2-methylphenyl)amino)benzamido)methyl)-1H-1,2,3-triazol-1-yl)-13-oxo-3,6,9-trioxa-12-azapentadecan-15-yl)benzamide, BrYZ03 : To a solution of 19 (50mg, 0.106 mmol) in 5 mL DMF was added 2-((3-chloro-2-methylphenyl)amino)-N-(prop-2-yn-1-yl)benzamide (31.8 mg, 0.106 mmol), 1N CuSO4 (10 μL), 1N ascorbic acid (10μL) and TBTA (5.8mg, 0.011mmol). The reaction was stirred for 16 hours before the solvent was removed by high vacuum. The

product was purified by flash column chromatography (5 % MeOH/DCM) to give BrYZ03 as oil. ^{1}H NMR (400 MHz, $CDCl_3$) δ 9.42 (s, 1H), 7.79 (s, 1H), 7.54 (m, 2H), 7.46 (dd, J = 7.6, 1.8 Hz, 1H), 7.33 (d, J = 1.3 Hz, 2H), 7.30 – 7.19 (m, 3H), 7.19 – 7.04 (m, 2H), 6.99 (dd, J = 8.5, 1.1 Hz, 1H), 6.92 (t, J = 6.1 Hz, 1H), 6.82 (t, J = 5.5 Hz, 1H), 6.72 (t, J = 0.9 Hz, 1H), 4.70 (d, J = 5.6 Hz, 2H), 4.54 (t, J = 5.0 Hz, 2H), 3.90 (t, J = 5.5, 2H), 3.72 (q, J = 5.9 Hz, 2H), 3.64 – 3.58 (m, 2H), 3.58 – 3.47 (m, 8H), 3.44 (t, J = 5.1 Hz, 2H), 2.58 (t, J = 6.0 Hz, 2H), 2.36 (s, 3H). ^{13}C NMR (101 MHz, $CDCl_3$) δ 171.66, 169.56, 167.99, 146.16, 144.43, 141.28, 137.96, 135.46, 133.25, 132.46, 131.13, 129.69, 129.17, 127.93, 127.49, 126.76, 124.27, 123.47, 120.36, 119.33, 117.79, 117.03, 115.17, 70.55, 70.46, 70.42, 70.11, 69.71, 69.40, 50.31, 39.20, 36.16, 35.24, 35.13, 14.94. HR-ESI MS m/e calcd for [$C_{35}H_{41}BrClN_7O_6$] 769.1965, found 769.1990.

REFERENCES

(1) Pratt, W. B., and Toft, D. O. (1997) Steroid receptor interactions with heat shock protein and immunophilin chaperones. *Endocrine Reviews 18*, 306–360.
(2) Gordon, J. C., Myers, J. B., Folta, T., Shoja, V., Heath, L. S., and Onufriev, A. (2005) H++: a server for estimating pKas and adding missing hydrogens to macromolecules. *Nucleic Acids Research 33*, W368–W371.
(3) Trott, O., and Olson, A. J. (2009) AutoDock Vina: Improving the speed and accuracy of docking with a new scoring function, efficient optimization, and multithreading. *J. Comput. Chem.* NA–NA.

Appendix A

PERMISSION LETTER

Appendix B

^{1}H and ^{13}C NMR SPECTRA

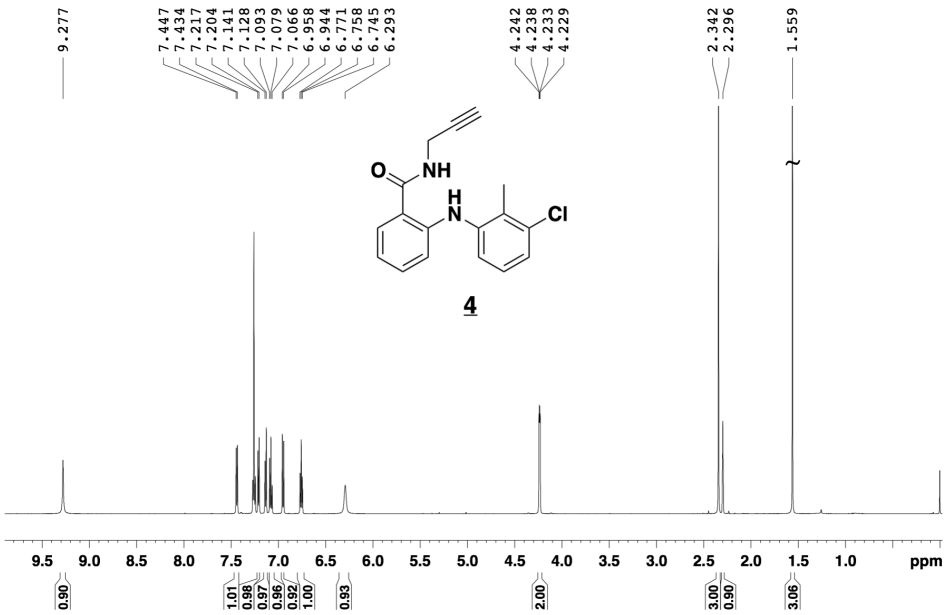
9.277
7.447
7.434
7.217
7.204
7.141
7.128
7.093
7.079
7.066
6.958
6.944
6.771
6.758
6.745
6.293
4.242
4.238
4.233
4.229
2.342
2.296
1.559
O
NH
H
N
Cl
4
9.5 9.0 8.5 8.0 7.5 7.0 6.5 6.0 5.5 5.0 4.5 4.0 3.5 3.0 2.5 2.0 1.5 1.0 ppm
0.90
1.01
0.98
0.97
0.96
0.92
1.00
0.93
2.00
3.00
0.90
3.06

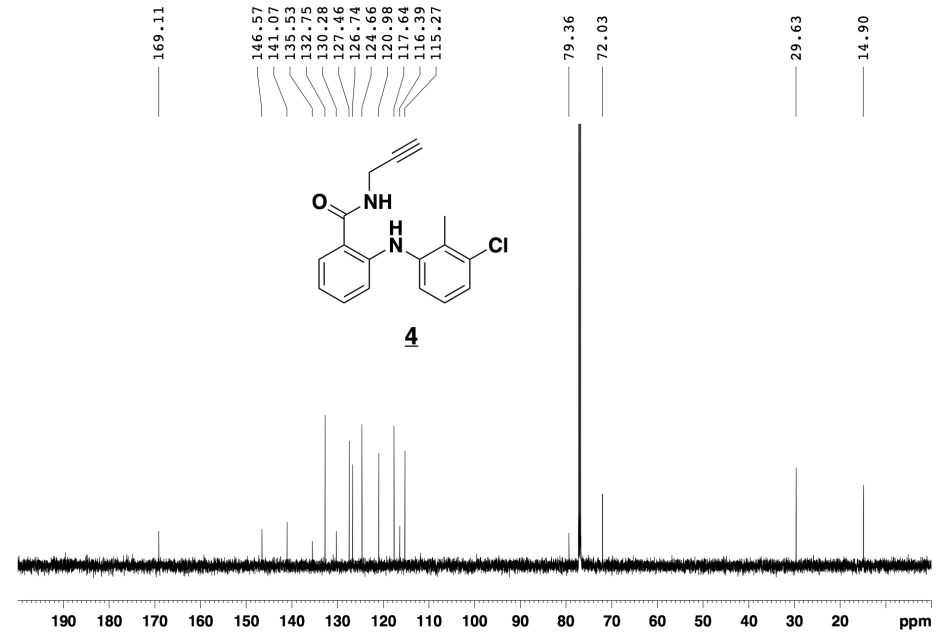
169.11
146.57
141.07
135.53
132.75
130.28
127.46
126.74
124.66
120.98
117.64
116.39
115.27
79.36
72.03
29.63
14.90
O
NH
H
N
Cl
4
190 180 170 160 150 140 130 120 110 100 90 80 70 60 50 40 30 20 ppm

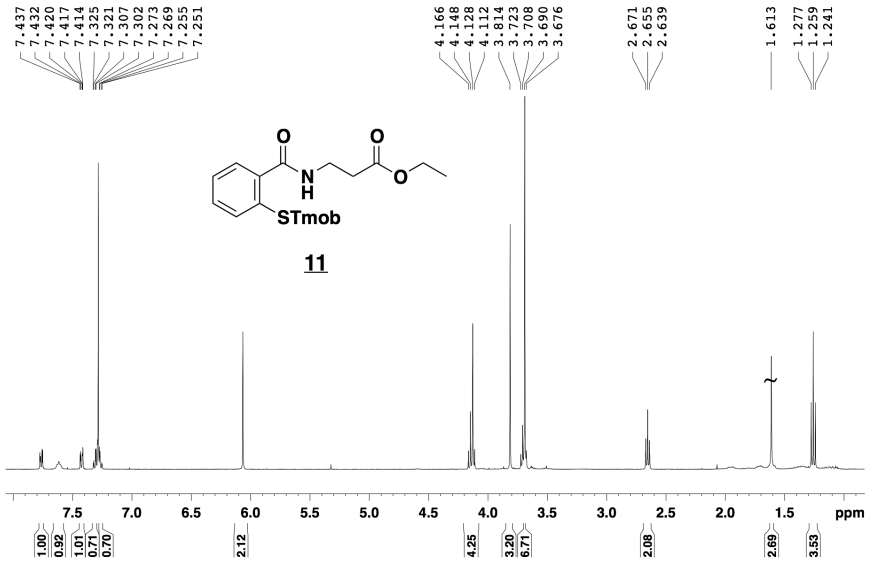
7.437
7.432
7.420
7.417
7.414
7.325
7.321
7.307
7.302
7.273
7.269
7.255
7.251
4.166
4.148
4.128
4.112
3.814
3.723
3.708
3.690
3.676
2.671
2.655
2.639
1.613
1.277
1.259
1.241
O
O
N
H
O
STmob
11
7.5
7.0
6.5
6.0
5.5
5.0
4.5
4.0
3.5
3.0
2.5
2.0
1.5
ppm
1.00
0.92
1.01
0.71
0.70
2.12
4.25
3.20
6.71
2.08
2.69
3.53

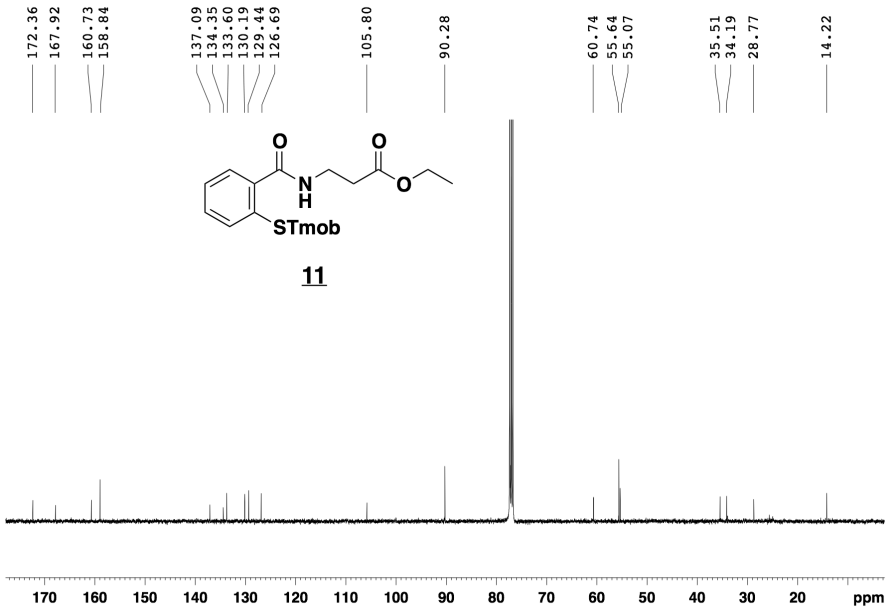
172.36
167.92
160.73
158.84
137.09
134.35
133.60
130.19
129.44
126.69
105.80
90.28
60.74
55.64
55.07
35.51
34.19
28.77
14.22
O
O
N
H
O
STmob
11
170
160
150
140
130
120
110
100
90
80
70
60
50
40
30
20
ppm

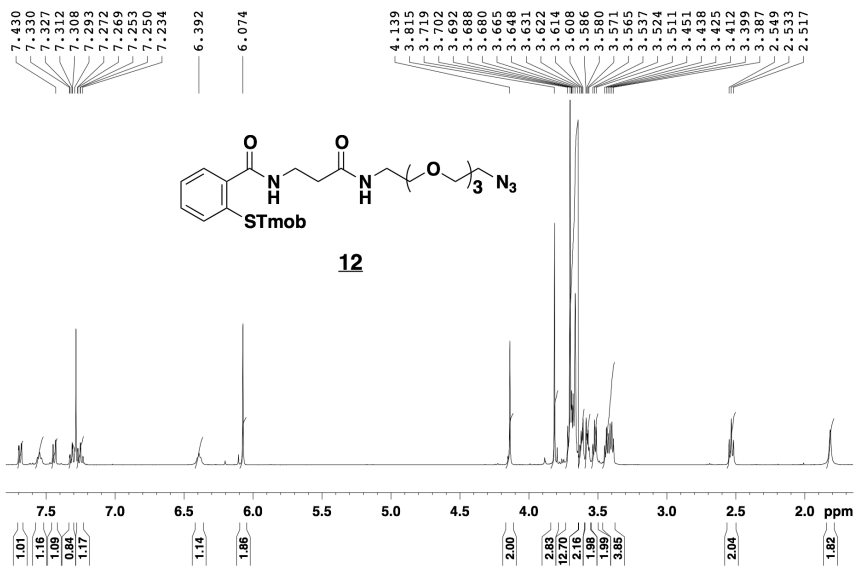
7.430
7.330
7.327
7.312
7.308
7.293
7.272
7.269
7.253
7.250
7.234
6.392
6.074
4.139
3.815
3.719
3.702
3.692
3.688
3.680
3.665
3.648
3.631
3.622
3.614
3.608
3.586
3.580
3.571
3.565
3.537
3.524
3.511
3.451
3.438
3.425
3.412
3.399
3.387
2.549
2.533
2.517
O
O
N
H
N
H
O
3
N3
STmob
12
7.5
7.0
6.5
6.0
5.5
5.0
4.5
4.0
3.5
3.0
2.5
2.0
ppm
1.01
1.16
1.09
0.84
1.17
1.14
1.86
2.00
2.83
12.70
2.16
1.98
1.99
3.85
2.04
1.82

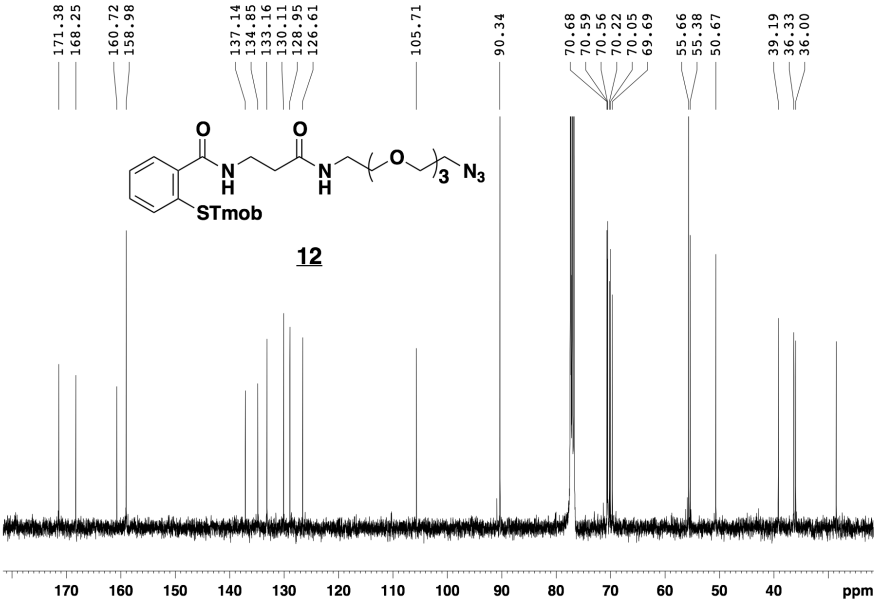
171.38
168.25
160.72
158.98
137.14
134.85
133.16
130.11
128.95
126.61
105.71
90.34
70.68
70.59
70.56
70.22
70.05
69.69
55.66
55.38
50.67
39.19
36.33
36.00
O
O
N
H
N
H
O
3
N3
STmob
12
170
160
150
140
130
120
110
100
90
80
70
60
50
40
ppm

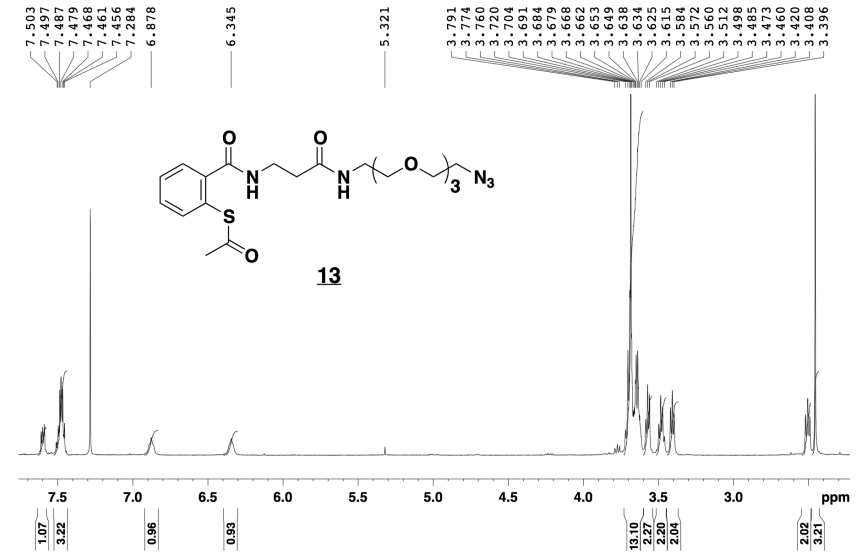
7.503
7.497
7.487
7.479
7.468
7.461
7.456
7.284
6.878
6.345
5.321
3.791
3.774
3.760
3.720
3.704
3.691
3.684
3.679
3.668
3.662
3.653
3.649
3.638
3.634
3.625
3.615
3.584
3.572
3.560
3.512
3.498
3.485
3.473
3.460
3.420
3.408
3.396
13
7.5
7.0
6.5
6.0
5.5
5.0
4.5
4.0
3.5
3.0
ppm
1.07
3.22
0.96
0.93
13.10
2.27
2.20
2.04
2.02
3.21

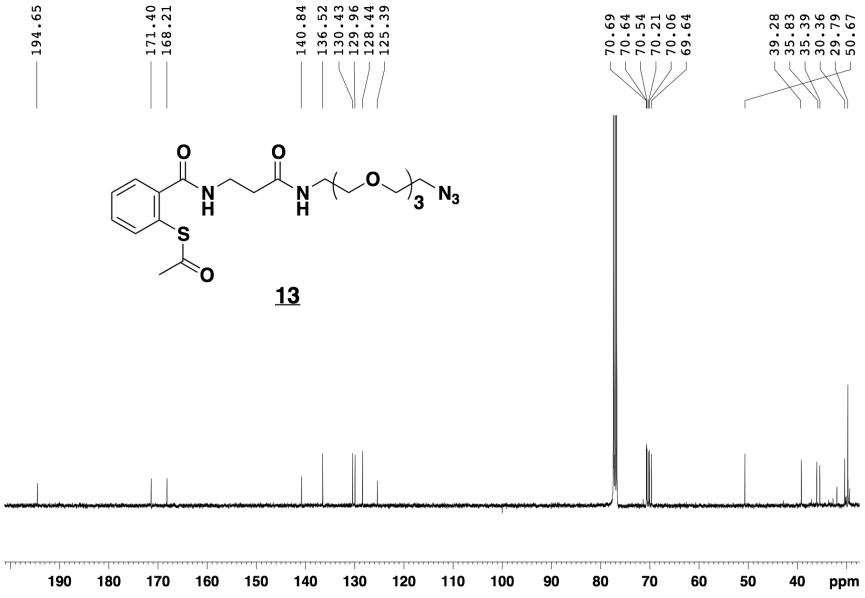
194.65
171.40
168.21
140.84
136.52
130.43
129.96
128.44
125.39
70.69
70.64
70.54
70.21
70.06
69.64
39.28
35.83
35.39
30.36
29.79
50.67
13
190
180
170
160
150
140
130
120
110
100
90
80
70
60
50
40
ppm

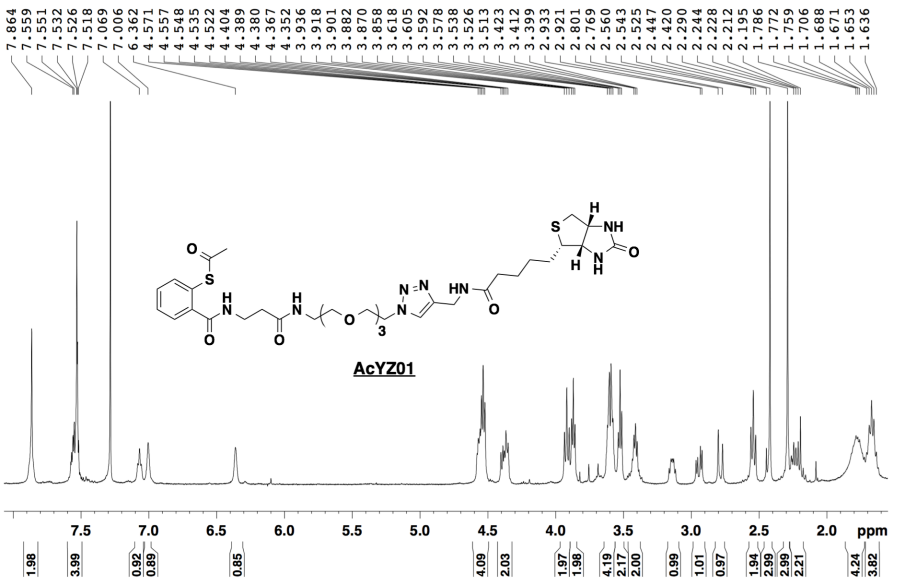
AcYZ01
7.5
7.0
6.5
6.0
5.5
5.0
4.5
4.0
3.5
3.0
2.5
2.0
ppm

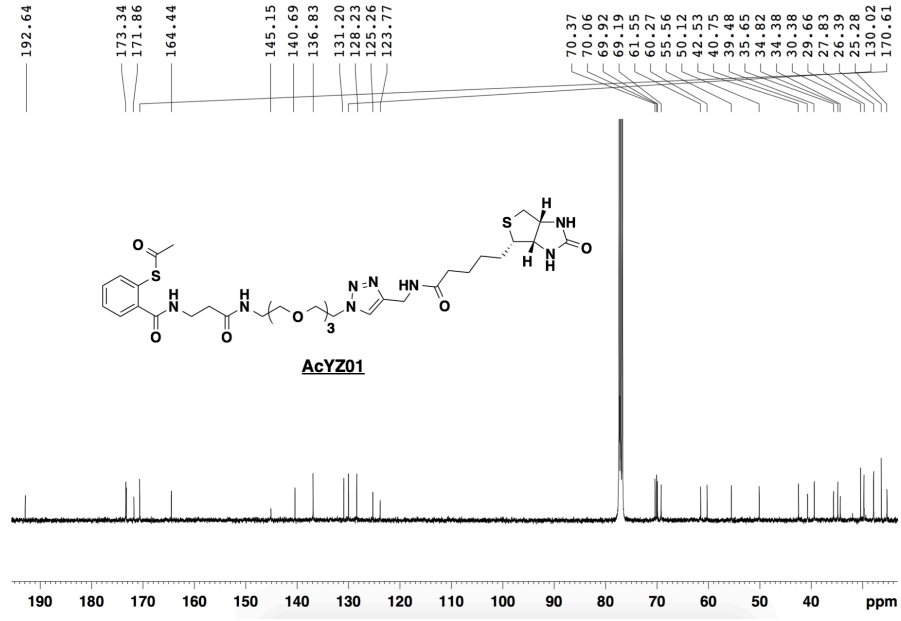
AcYZ01
190
180
170
160
150
140
130
120
110
100
90
80
70
60
50
40
ppm

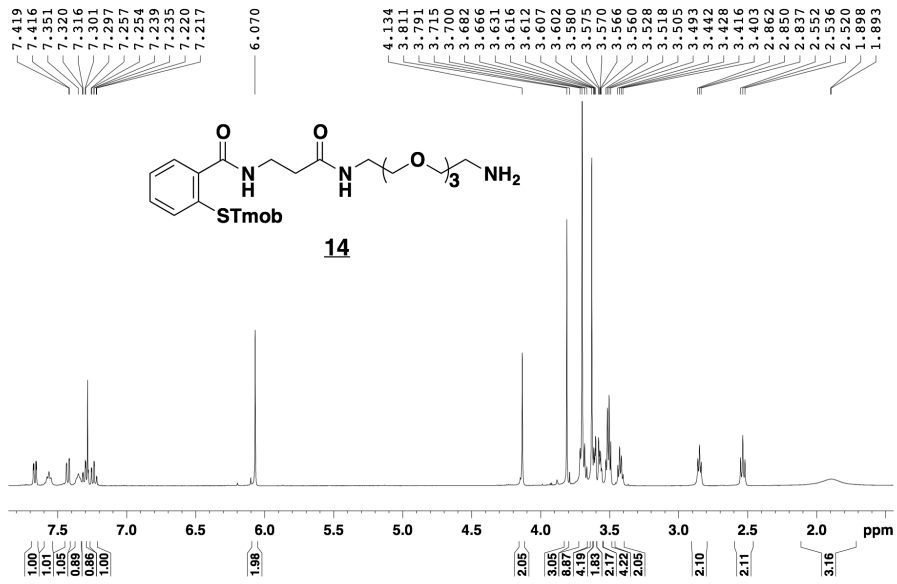
7.419
7.416
7.351
7.320
7.316
7.301
7.297
7.257
7.254
7.239
7.235
7.220
7.217
6.070
4.134
3.811
3.791
3.715
3.700
3.682
3.666
3.631
3.616
3.612
3.607
3.602
3.580
3.575
3.570
3.566
3.560
3.528
3.518
3.505
3.493
3.442
3.428
3.416
3.403
2.862
2.850
2.837
2.552
2.536
2.520
1.898
1.893
O
O
N
H
N
H
O
3
NH2
STmob
14
7.5
7.0
6.5
6.0
5.5
5.0
4.5
4.0
3.5
3.0
2.5
2.0
ppm
1.00
1.01
1.05
0.89
0.86
1.00
1.98
2.05
3.05
8.87
4.19
1.83
2.17
4.22
2.05
2.10
2.11
3.16

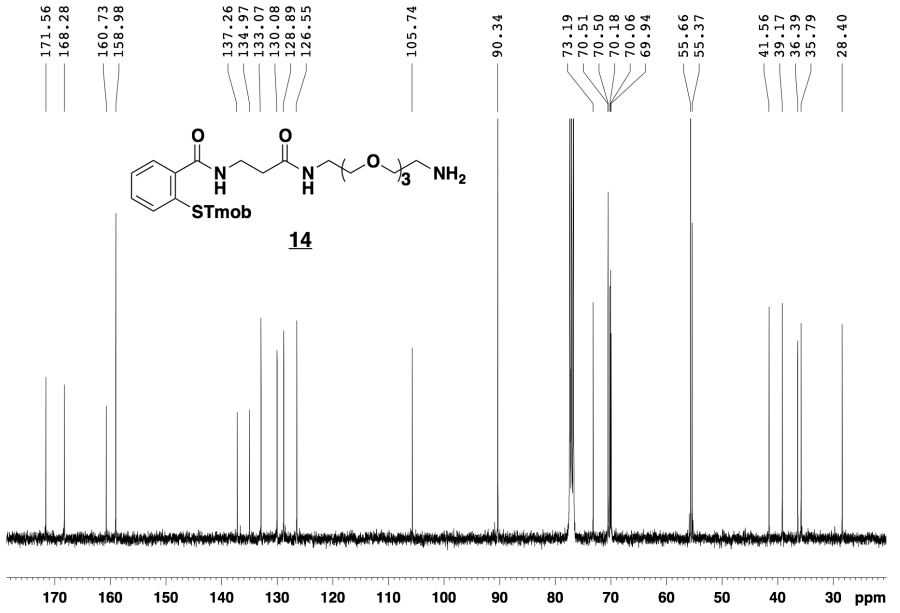
171.56
168.28
160.73
158.98
137.26
134.97
133.07
130.08
128.89
126.55
105.74
90.34
73.19
70.51
70.50
70.18
70.06
69.94
55.66
55.37
41.56
39.17
36.39
35.79
28.40
O
O
N
H
N
H
O
3
NH2
STmob
14
170
160
150
140
130
120
110
100
90
80
70
60
50
40
30
ppm

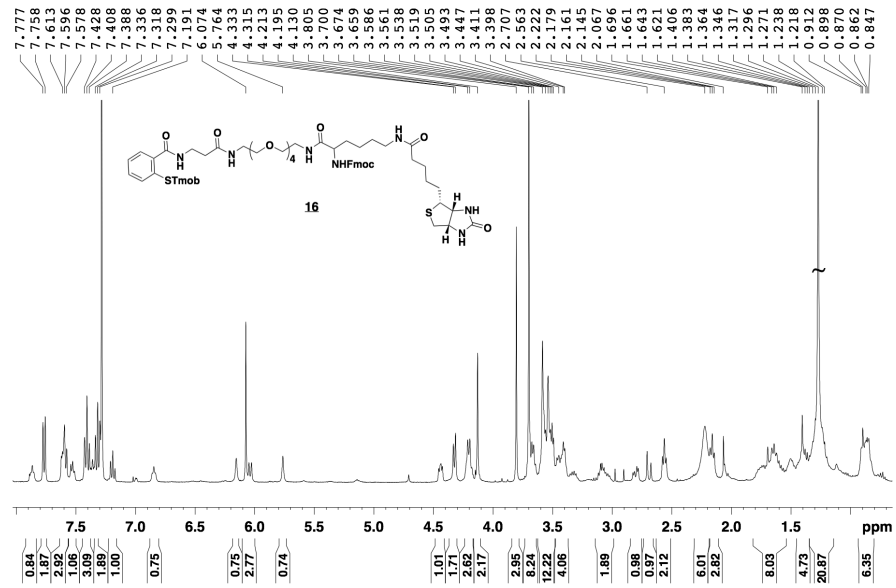
7.777 7.758 7.613 7.596 7.578 7.428 7.408 7.388 7.336 7.318 7.299 7.191 6.074 5.764 4.333 4.315 4.213 4.195 4.130 3.805 3.700 3.674 3.659 3.586 3.561 3.538 3.519 3.505 3.493 3.447 3.411 3.398 2.707 2.563 2.222 2.179 2.161 2.145 2.067 1.696 1.661 1.643 1.621 1.406 1.383 1.364 1.346 1.317 1.296 1.271 1.238 1.218 0.912 0.898 0.870 0.862 0.847
STmob
NHFmoc
16
7.5 7.0 6.5 6.0 5.5 5.0 4.5 4.0 3.5 3.0 2.5 2.0 1.5 ppm
0.84 1.87 2.92 1.06 3.09 1.89 1.00 0.75 0.75 2.77 0.74 1.01 1.71 2.62 2.17 2.95 8.24 12.22 4.06 1.89 0.98 0.97 2.12 6.01 2.82 8.03 4.73 20.87 6.35

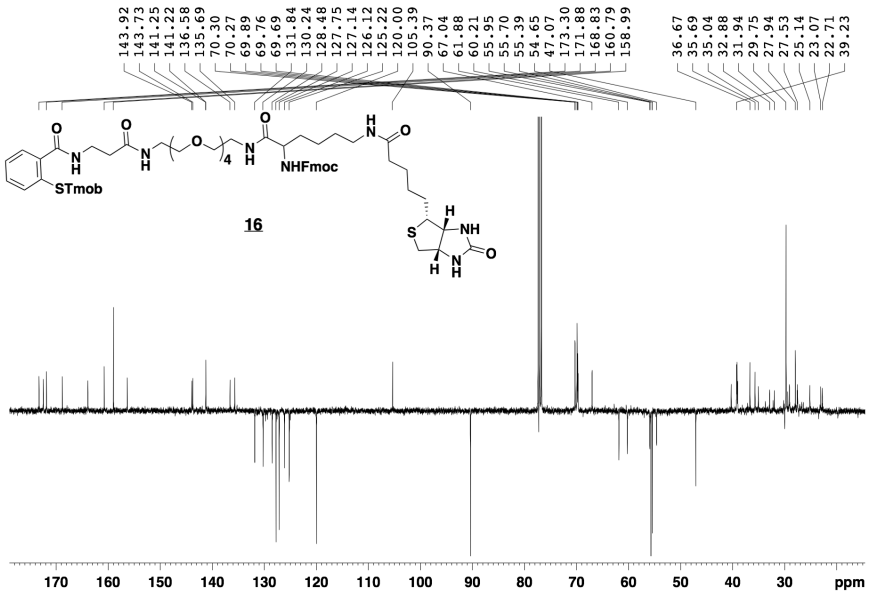
143.92 143.73 141.25 141.22 136.58 135.69 70.30 70.27 69.89 69.76 69.69 131.84 130.24 128.48 127.75 127.14 126.12 125.22 120.00 105.39 90.37 67.04 61.88 60.21 55.95 55.70 55.39 54.65 47.07 173.30 171.88 168.83 160.79 158.99 36.67 35.69 35.04 32.88 31.94 29.75 27.94 27.53 25.14 23.07 22.71 39.23
STmob
NHFmoc
16
170 160 150 140 130 120 110 100 90 80 70 60 50 40 30 ppm

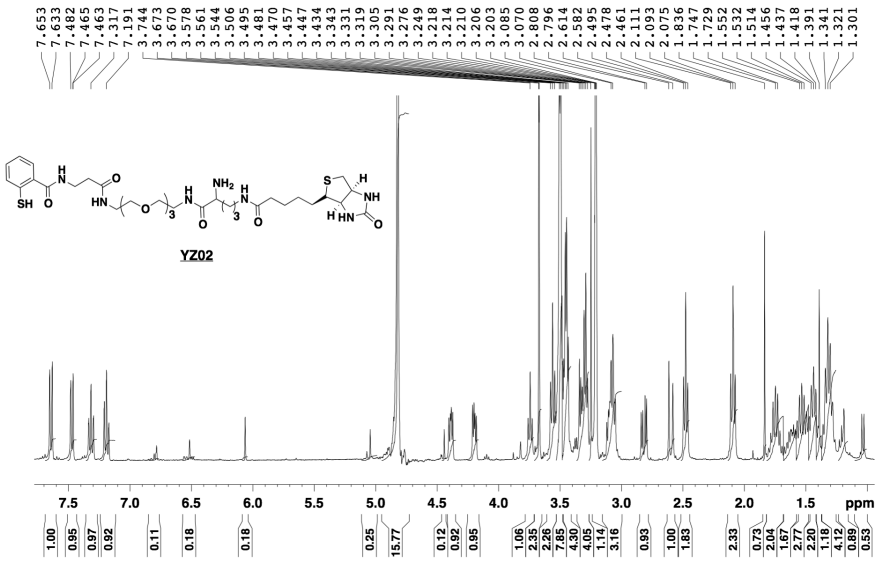
7.653
7.633
7.482
7.465
7.463
7.317
7.191
3.744
3.673
3.670
3.578
3.561
3.544
3.506
3.495
3.481
3.470
3.457
3.447
3.434
3.343
3.331
3.319
3.305
3.291
3.276
3.249
3.218
3.214
3.210
3.206
3.203
3.085
3.070
2.808
2.796
2.614
2.582
2.495
2.478
2.461
2.111
2.093
2.075
1.836
1.747
1.729
1.552
1.532
1.514
1.456
1.437
1.418
1.391
1.341
1.321
1.301
YZ02
7.5
7.0
6.5
6.0
5.5
5.0
4.5
4.0
3.5
3.0
2.5
2.0
1.5
ppm
1.00
0.95
0.97
0.92
0.11
0.18
0.18
0.25
15.77
0.12
0.92
0.95
1.06
2.35
2.26
7.85
4.30
4.05
1.14
3.16
0.83
1.00
1.83
2.33
0.73
2.04
1.67
2.77
2.20
1.18
4.12
0.89
0.53

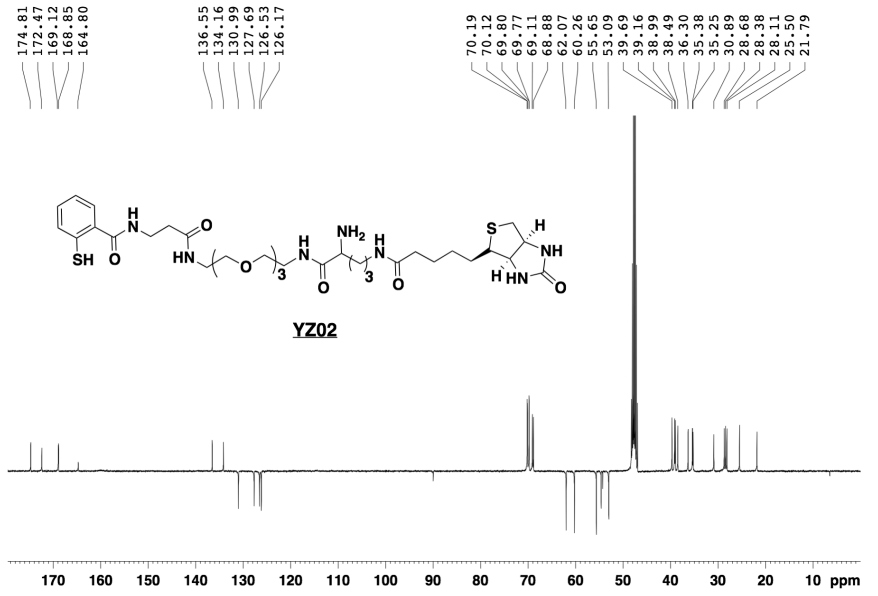
174.81
172.47
169.12
168.85
164.80
136.55
134.16
130.99
127.69
126.53
126.17
70.19
70.12
69.80
69.77
69.11
68.88
62.07
60.26
55.65
53.09
39.69
39.16
38.99
38.49
36.30
35.38
35.25
30.89
28.68
28.38
28.11
25.50
21.79
YZ02
170
160
150
140
130
120
110
100
90
80
70
60
50
40
30
20
10
ppm

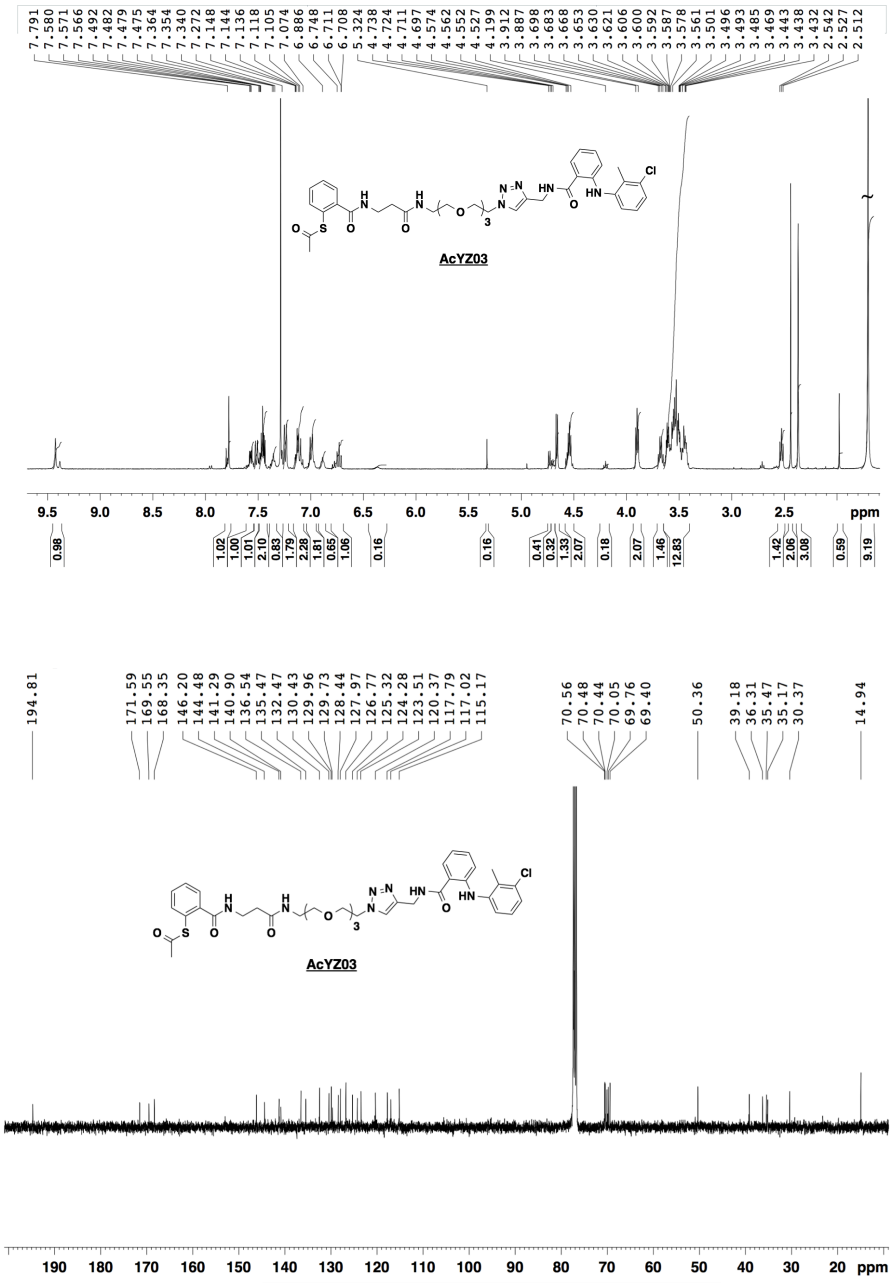
AcYZ03
AcYZ03

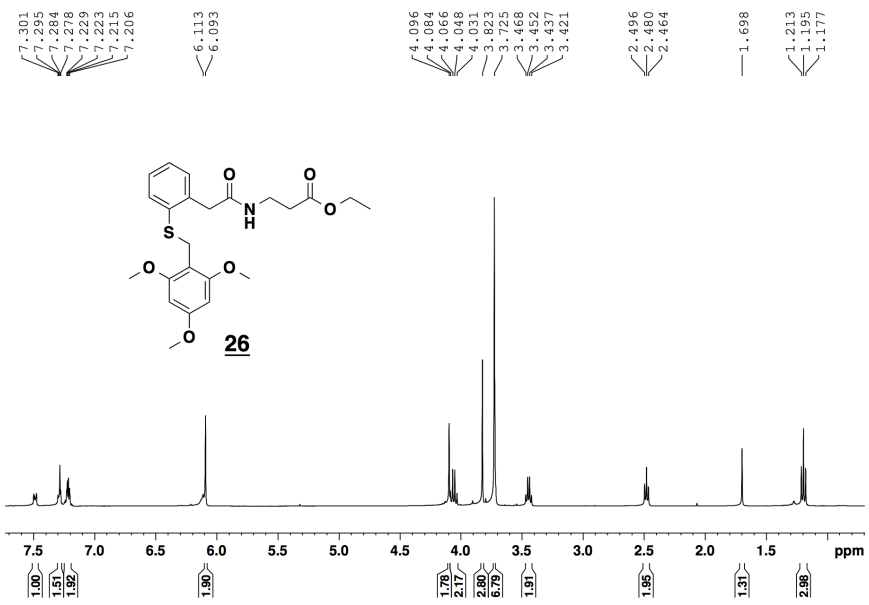
7.301
7.295
7.284
7.278
7.229
7.223
7.215
7.206
6.113
6.093
4.096
4.084
4.066
4.048
4.031
3.823
3.725
3.468
3.452
3.437
3.421
2.496
2.480
2.464
1.698
1.213
1.195
1.177
26
7.5
7.0
6.5
6.0
5.5
5.0
4.5
4.0
3.5
3.0
2.5
2.0
1.5
ppm
1.00
1.51
1.92
1.90
1.78
2.17
2.80
6.79
1.91
1.95
1.31
2.98

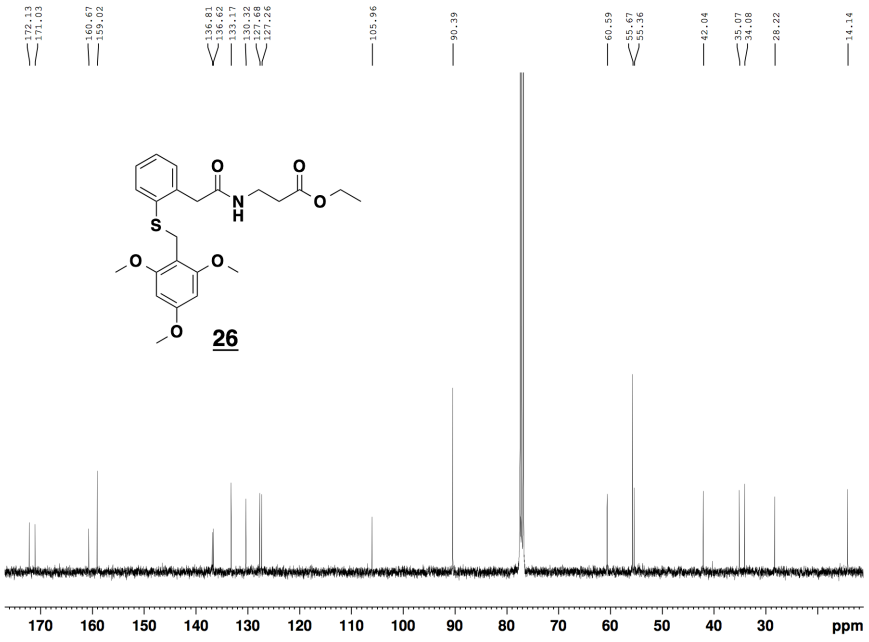
172.13
171.03
160.67
159.02
136.81
136.62
133.17
130.32
127.68
127.26
105.96
90.39
60.59
55.67
55.36
42.04
35.07
34.08
28.22
14.14
26
170
160
150
140
130
120
110
100
90
80
70
60
50
40
30
ppm

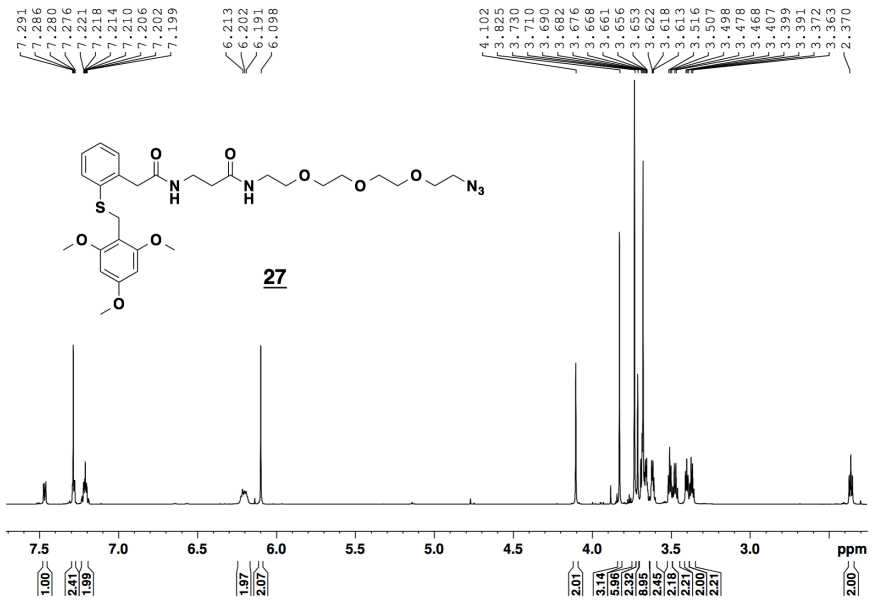
7.291
7.286
7.280
7.276
7.221
7.218
7.214
7.210
7.206
7.202
7.199
6.213
6.202
6.191
6.098
4.102
3.825
3.730
3.710
3.690
3.682
3.676
3.668
3.661
3.656
3.653
3.622
3.618
3.613
3.516
3.507
3.498
3.478
3.468
3.407
3.399
3.391
3.372
3.363
2.370
27
7.5
7.0
6.5
6.0
5.5
5.0
4.5
4.0
3.5
3.0
ppm
1.00
2.41
1.99
1.97
2.07
2.01
3.14
5.96
2.32
8.95
2.45
2.18
2.21
2.00
2.21
2.00

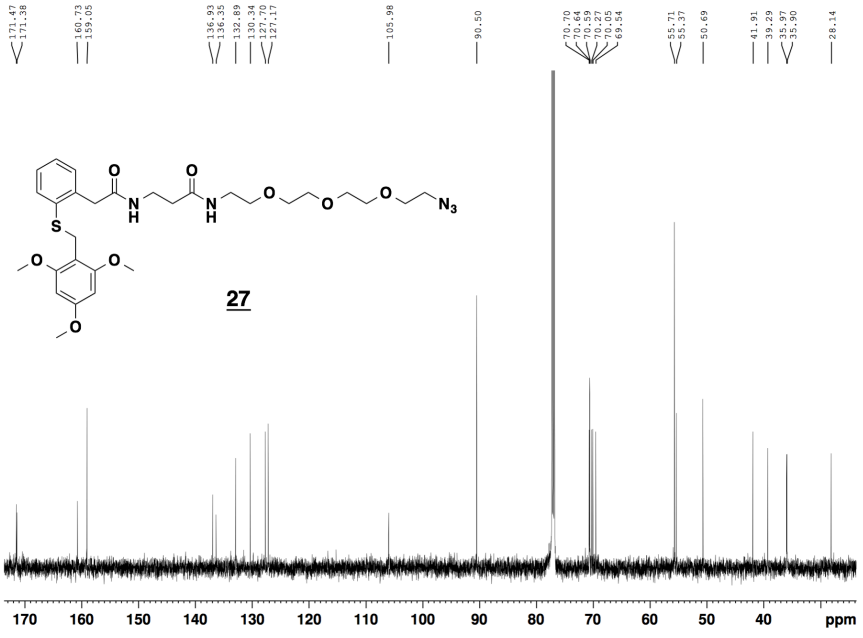
171.47
171.38
160.73
159.05
136.93
136.35
132.89
130.34
127.70
127.17
105.98
90.50
70.70
70.64
70.59
70.27
70.05
69.54
55.71
55.37
50.69
41.91
39.29
35.97
35.90
28.14
27
170
160
150
140
130
120
110
100
90
80
70
60
50
40
ppm

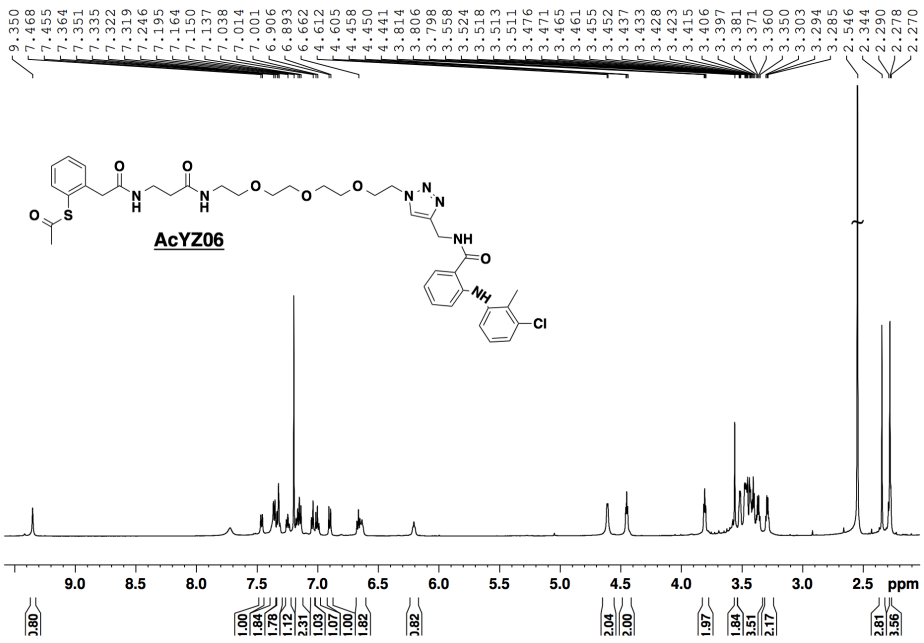
AcYZ06

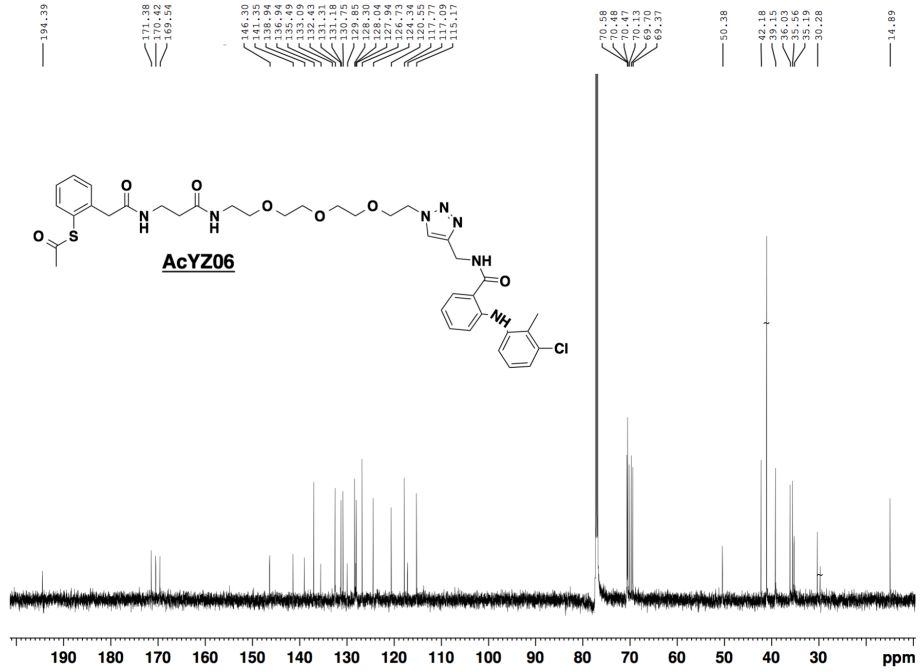
AcYZ06

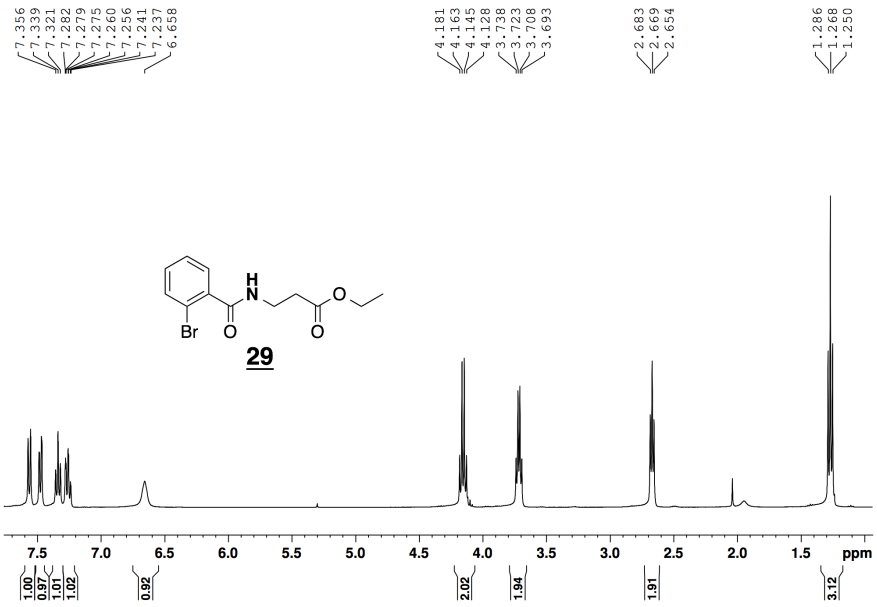
7.356
7.339
7.321
7.282
7.279
7.275
7.260
7.256
7.241
7.237
6.658
4.181
4.163
4.145
4.128
3.738
3.723
3.708
3.693
2.683
2.669
2.654
1.286
1.268
1.250
Br
O
H
N
O
O
29
7.5
7.0
6.5
6.0
5.5
5.0
4.5
4.0
3.5
3.0
2.5
2.0
1.5
ppm
1.00
0.97
1.01
1.02
0.92
2.02
1.94
1.91
3.12

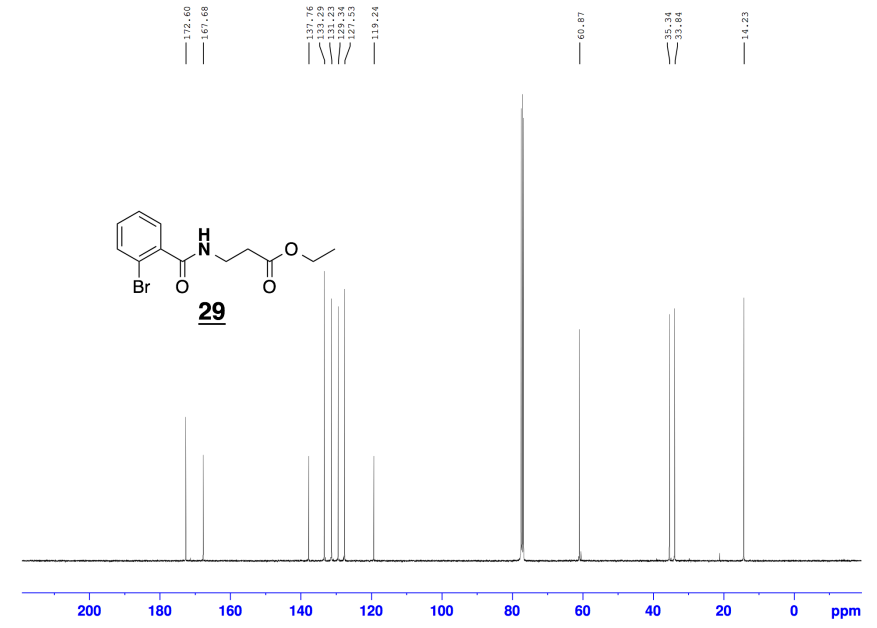
172.60
167.68
137.76
133.29
131.23
129.34
127.53
119.24
60.87
35.34
33.84
14.23
Br
O
H
N
O
O
29
200
180
160
140
120
100
80
60
40
20
0
ppm

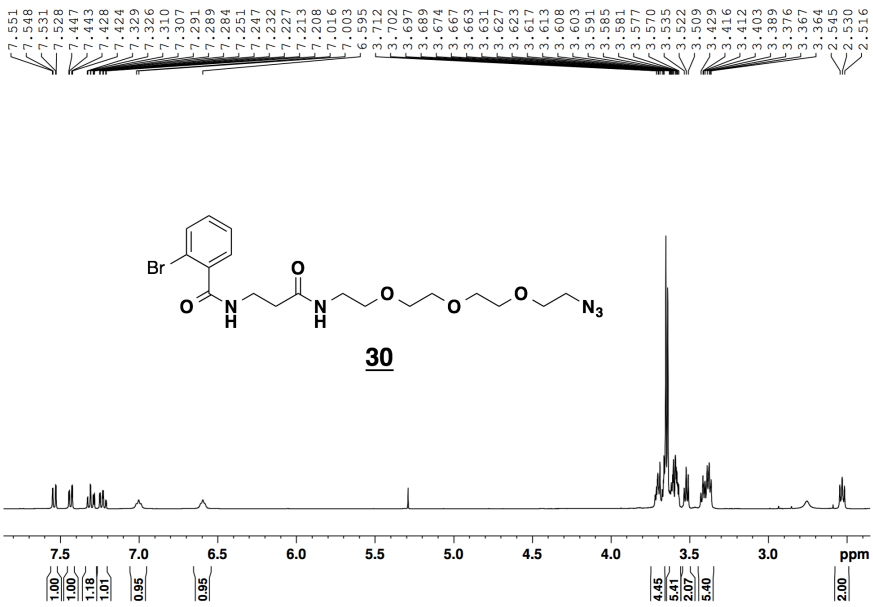
7.551
7.548
7.531
7.528
7.447
7.443
7.428
7.424
7.329
7.326
7.310
7.307
7.291
7.289
7.284
7.251
7.247
7.232
7.227
7.213
7.208
7.016
7.003
6.595
3.712
3.702
3.697
3.689
3.674
3.667
3.663
3.631
3.627
3.623
3.617
3.613
3.608
3.603
3.591
3.585
3.581
3.577
3.570
3.535
3.522
3.509
3.429
3.416
3.412
3.403
3.389
3.376
3.367
3.364
2.545
2.530
2.516
Br
O
N
H
O
N
H
O
O
O
N3
30
7.5
7.0
6.5
6.0
5.5
5.0
4.5
4.0
3.5
3.0
ppm
1.00
1.00
1.18
1.01
0.95
0.95
4.45
5.41
2.07
5.40
2.00

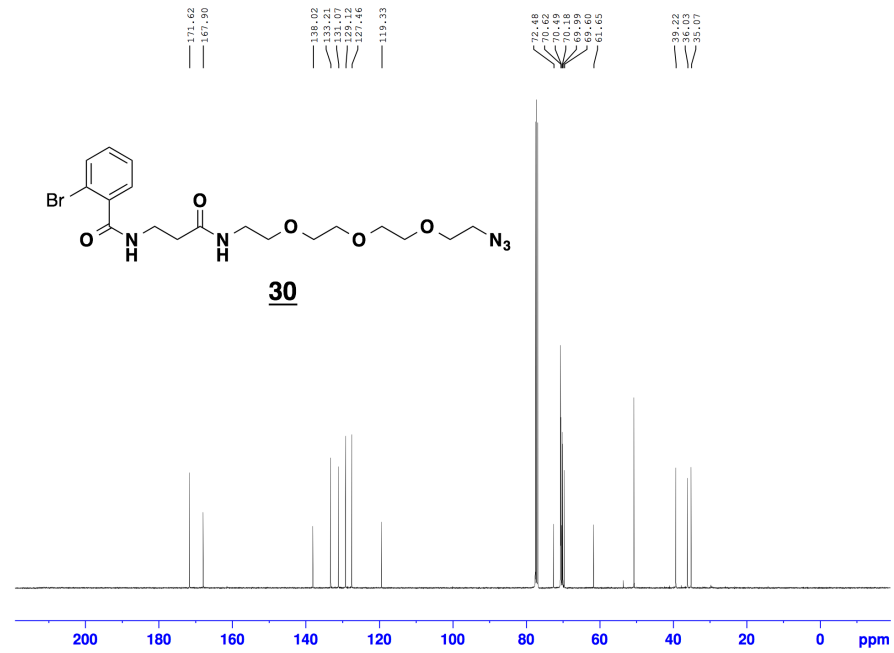
171.62
167.90
138.02
133.21
131.07
129.12
127.46
119.33
72.48
70.62
70.49
70.18
69.99
69.60
61.65
39.22
36.03
35.07
Br
O
N
H
O
N
H
O
O
O
N3
30
200
180
160
140
120
100
80
60
40
20
0
ppm

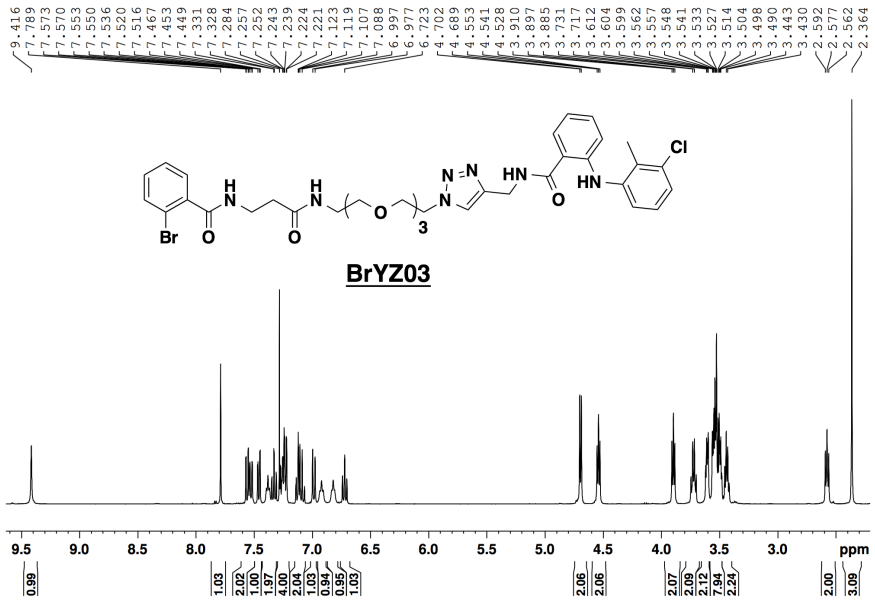
BrYZ03

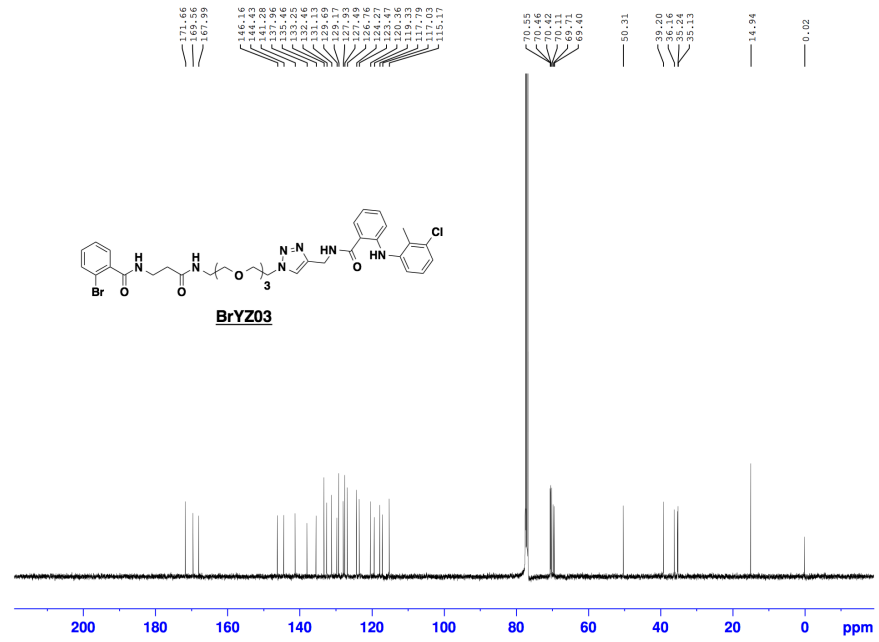
BrYZ03

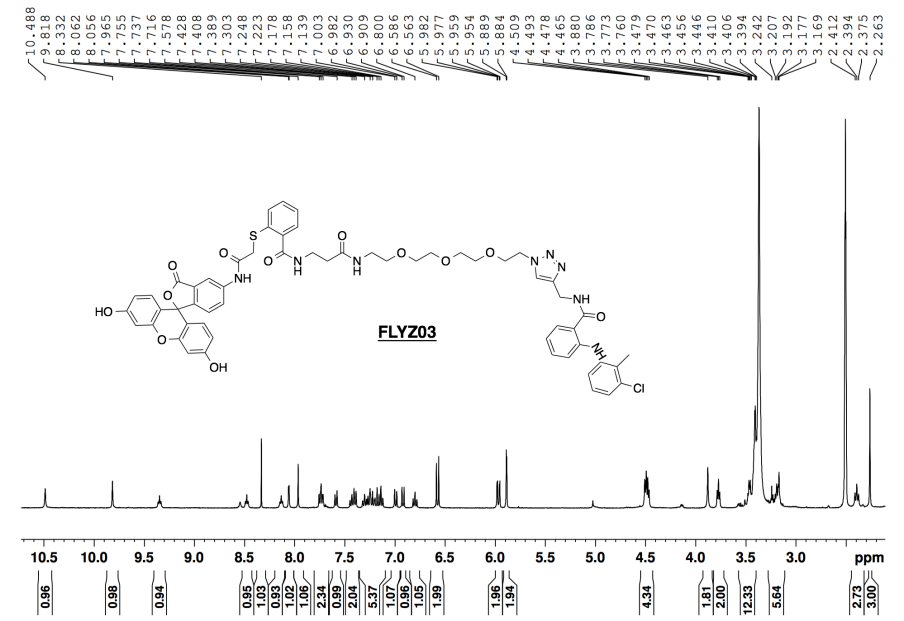
FLYZ03

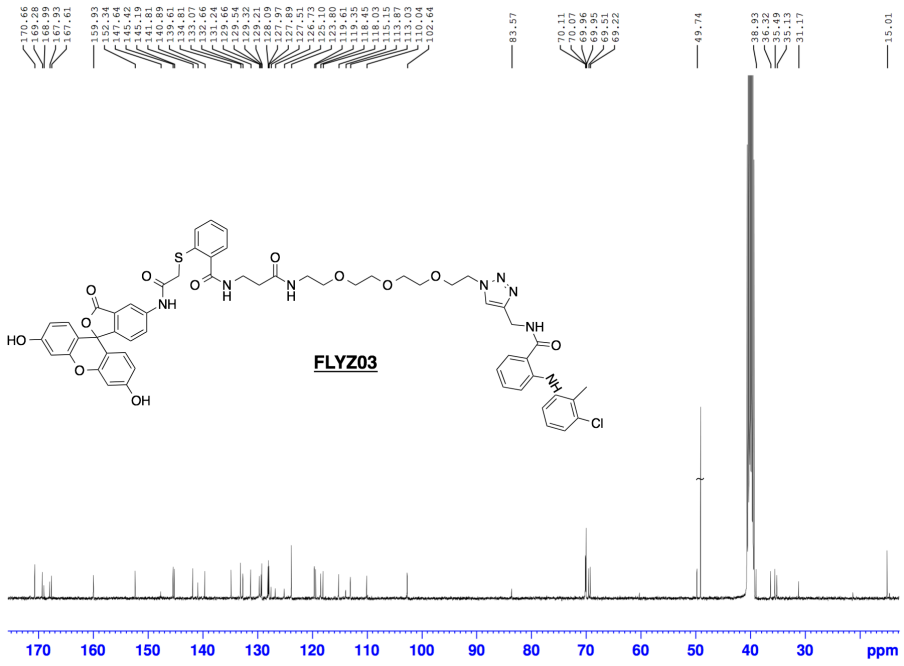
FLYZ03